

**DISASTER PREVENTION RESEARCH INSTITUTE
KYOTO UNIVERSITY**

Peter MOCZO

Geophysical Institute
Slovak Academy of Sciences
Bratislava, Slovak Republic

**INTRODUCTION TO
MODELING SEISMIC WAVE PROPAGATION
BY THE FINITE-DIFFERENCE METHOD**

Lecture Notes

*Lectures given at
Disaster Prevention Research Institute,
Kyoto University
during author's visit from Sep. 7, 1997 to Jan. 9, 1998*

March 1998

Copyright © Peter Moczó 1998

To

Jorge Aguirre, Riki Honda, Hiroe Miyake, Cesar Moya, Nelson Pulido, Haruko Sekiguchi and others *whose attitude and interest in the topic motivated me a lot and made my talks more enjoyable to me.*

Acknowledgments

I wish to express my gratitude to Professor Kojiro Irikura of the Disaster Prevention Research Institute, Kyoto University, who invited me to stay in his lab and give an introductory course on the application of the finite-difference method to seismic wave propagation, and encouraged me to write these lecture notes.

I also thank Professor Ladislav Halada of the Department of Mathematics, Faculty of Engineering, Slovak Technical University, Bratislava, for his critical reading of the manuscript, comments and suggestions.

My thanks also go to Andrej Cipciar, Jozef Kristek, Peter Labák and Desanka Režuchová who helped me with the preparation of the final version of the notes.

PREFACE

I wrote these Lecture Notes on the basis of material I presented during the introductory course on the finite-difference method for the undergraduate and graduate students in the Disaster Prevention Research Institute, Kyoto University, Japan, in October - December 1997.

Lecture Notes include only some selected topics of the application of the finite-difference method to the problems of seismic wave propagation. They are far from being a complete introductory course. No way can they replace a theoretical introduction to the finite-difference method which can be found in the mathematical textbooks; some of them are given in References. A reader is strongly recommended to read more about consistency, convergence, stability and alternative approaches to constructing finite-difference schemes.

I hope the Lecture Notes bring together material that is scattered in various journal articles. Therefore, they could be useful especially to those students and seismologists who are not familiar with the finite-difference method but want to acquire some basic knowledge of how the finite-difference method can be used to study seismic wave propagation.

Contents

PART A : INTRODUCTION	1
1. Solving Partial Differential Equations by the Finite-Difference Method	1
1.1 Introduction to the Finite-Difference Method	1
1.2 Example: Case of the One-Dimensional Wave Equation	5
PART B : APPLICATION OF THE FINITE-DIFFERENCE METHOD TO THE EQUATION OF MOTION IN A PERFECTLY ELASTIC MEDIUM	12
2. Equation of Motion	12
2.1 3D Case	14
2.2 P-SV Case	16
2.3 SH Case	17
2.4 Homogeneous Medium	18
3. Heterogeneous Formulation of the Equation of Motion and Heterogeneous Finite-Difference Schemes	19
4. Finite-Difference Schemes for Interior Points on Regular Grids	23
4.1 Displacement-Stress Scheme on a Staggered Grid	24
4.2 Velocity-Stress Scheme on a Staggered Grid	30
4.3 Displacement Scheme on a Conventional Grid	33
5. Fourth-Order Finite-Difference Schemes for Interior Grid Points	39
5.1 Fourth-Order Finite-Difference Approximations	39
5.2 Displacement-Stress Scheme on a Staggered Grid	41
5.3 Velocity-Stress Scheme on a Staggered Grid	46
6. Finite-Difference Schemes for Interior Points on Irregular Rectangular Grids	48
6.1 Finite-Difference Approximations on an Irregular Grid	48
6.2 Displacement-Stress Scheme on an Irregular Grid	52
7. Finite-Difference Schemes for Interior Points on a Combined Rectangular Grid	54

8. Stability Condition and Dispersion Relations	58
8.1 Stability Condition and Dispersion Relations for the Second-Order Velocity-Stress Scheme for the P-SV Waves	58
8.2 Stability Conditions for the Finite-Difference Schemes	66
9. Approximation of Traction-Free Surface	67
9.1 Traction-Free condition	67
9.2 Approximation of the Free Surface in the Velocity-Stress Formulation	68
9.3 Approximation of the Free Surface in the Displacement Formulation ...	73
10. Simulation of Seismic Source	78
10.1 Simulation of a Point Source with Arbitrary Focal Mechanism Using a Body-Force Term	78
10.2 Decomposition of the Wavefield	85
11. Simulation of Nonreflecting Boundaries	89
11.1 Artificial Damping Zone	89
11.2 Shock Absorber Zone	90
11.3 Approximate Absorbing Boundary Conditions	91
12. Concluding Remarks	94
References	95

PART A : INTRODUCTION

The Earth's interior, mainly its upper part, is laterally inhomogeneous with layers and blocks of irregular shapes. Since analytical methods do not provide solutions of the equation of motion for complex or sufficiently realistic models of the Earth's interior, computation of the seismic wave propagation requires approximate methods. The finite-difference method belongs to those that are most frequently used.

1. SOLVING PARTIAL DIFFERENTIAL EQUATIONS BY THE FINITE-DIFFERENCE METHOD

1.1 INTRODUCTION TO THE FINITE-DIFFERENCE METHOD

Application of the finite-difference method consists of

- a. Construction of a discrete finite-difference model of the problem:
 - coverage of the computational region by a grid,
 - approximation of derivatives by the finite-difference formulae, approximation of functions and approximation of the initial and/or boundary conditions
 - all at the grid points,
 - construction of a system of the finite-difference (i.e., algebraic) equations
- b. Analysis of the finite-difference model:
 - consistency and order of approximation
 - stability
 - convergence
- c. Numerical computations

Grid

Consider domain $D = D^I \cup D^B$ where D^I denotes interior and D^B boundary of the domain. Let the domain D lie in the four-dimensional space of variables (x, y, z, t) . Cover this

space by a **grid** of discrete points

$$(x_i, y_k, z_\ell, t_m)$$

given by

$$x_i = x_0 + i\Delta x, \quad y_k = y_0 + k\Delta y, \quad z_\ell = z_0 + \ell\Delta z, \quad t_m = t_0 + m\Delta t,$$

$$i, k, \ell = 0, \pm 1, \pm 2, \dots,$$

$$m = 0, 1, 2, \dots$$

Here, Δx , Δy and Δz are usually called **grid spacings**, and Δt is called **time step** since t usually represents time. If x , y and z are Cartesian coordinates, the corresponding spatial grid is a rectangular grid.

At the grid points a function $u(x, y, z, t)$ is to be approximated by a grid function $U(x_i, y_k, z_\ell, t_m)$. A value of $u(x_i, y_k, z_\ell, t_m)$ can be denoted by $u_{ik\ell}^m$ while approximation to $u_{ik\ell}^m$ can be denoted by $U_{ik\ell}^m$.

A spatial grid that is the most appropriate for the problem under consideration should be chosen. In many applications the regular rectangular grid with the grid spacings $\Delta x = \Delta y = \Delta z = h$ is a natural and reasonable choice. Other types of grids are used if they better accommodate geometry of the problem (e.g., shapes of material discontinuities) or if they simplify finite-difference approximations of derivatives.

Approximation of Derivatives

Consider function $\Phi(x)$. Taylor's expansion of the function can be used to derive various approximations of the first and higher derivatives of the function.

Taylor's expansions of the function Φ at $x + h$ and $x - h$ (h can denote a grid spacing Δx) are

$$\Phi(x + h) = \Phi(x) + \Phi'(x)h + \frac{1}{2}\Phi''(x)h^2 + \frac{1}{6}\Phi'''(x)h^3 + \dots, \quad (1.1.1a)$$

$$\Phi(x - h) = \Phi(x) - \Phi'(x)h + \frac{1}{2}\Phi''(x)h^2 - \frac{1}{6}\Phi'''(x)h^3 + \dots \quad (1.1.1b)$$

From expansion (1.1.1a) we get

$$\Phi(x + h) - \Phi(x) = \Phi'(x)h + \frac{1}{2}\Phi''(x)h^2 + \frac{1}{6}\Phi'''(x)h^3 + \dots,$$

$$\Phi'(x) = \frac{1}{h} [\Phi(x + h) - \Phi(x)] - O(h)$$

and the so-called **forward-difference formula**

$$\Phi'(x) \doteq \frac{1}{h} [\Phi(x + h) - \Phi(x)]. \quad (1.1.2)$$

Similarly, from expansion (1.1.1b) we get

$$\begin{aligned}\Phi(x) - \Phi(x-h) &= \Phi'(x)h - \frac{1}{2}\Phi''(x)h^2 + \frac{1}{6}\Phi'''(x)h^3 - \dots, \\ \Phi'(x) &= \frac{1}{h} [\Phi(x) - \Phi(x-h)] + O(h)\end{aligned}$$

and the so-called **backward-difference formula**

$$\Phi'(x) \doteq \frac{1}{h} [\Phi(x) - \Phi(x-h)]. \quad (1.1.3)$$

Both approximations are of the first order since the leading term of the approximation error is proportional to h .

Subtracting expansion (1.1.1a) from (1.1.1b) gives

$$\begin{aligned}\Phi(x+h) - \Phi(x-h) &= 2\Phi'(x)h + \frac{2}{6}\Phi'''(x)h^3 + \dots, \\ \Phi'(x) &= \frac{1}{2h} [\Phi(x+h) - \Phi(x-h)] - O(h^2)\end{aligned}$$

and the so-called **central-difference formula**

$$\Phi'(x) \doteq \frac{1}{2h} [\Phi(x+h) - \Phi(x-h)] \quad (1.1.4)$$

which is the second-order accurate approximation of the first derivative.

Summing up expansions (1.1.1a) and (1.1.1b) gives the second-order accurate approximation of the second derivative

$$\Phi''(x) \doteq \frac{1}{h^2} [\Phi(x+h) - 2\Phi(x) + \Phi(x-h)]. \quad (1.1.5)$$

Higher-order approximations on a regular grid and approximations on a grid with varying grid spacings will be given later.

Finite-Difference Scheme

Let $f(P)$ be a function defined on D^I . Let $L(u)$ be a differential operator. Then

$$L(u(P)) = f(P); \quad P \in D^I \quad (1.1.6a)$$

represents a partial differential equation for unknown $u(P)$.

The initial/boundary conditions can be represented by equation

$$B(u(P)) = g(P); \quad P \in D^B. \quad (1.1.6b)$$

Consider problems for which a unique, smooth and bounded solution u exists for any data in some class of smooth functions $\{f, g\}$.

Denote D_{Δ}^I grid points interior to D and D_{Δ}^B boundary grid points. Let U be a solution of the system of the **finite-difference equations** (or the **finite-difference scheme**)

$$L_{\Delta}(U) = f(P) ; \quad P \in D_{\Delta}^I , \quad (1.1.7a)$$

$$B_{\Delta}(U) = g(P) ; \quad P \in D_{\Delta}^B . \quad (1.1.7b)$$

Consider the scheme (1.1.7) to be a finite-difference approximation to equations (1.1.6) and U a finite-difference approximation to u .

It is reasonable to require that U be a close approximation to the solution u at the corresponding grid points for all data that are sufficiently smooth and that U be uniquely defined by the scheme (1.1.7).

A finite-difference scheme has to be consistent, convergent and stable in order to give a reasonable approximation to the solution of the partial differential equation and adjoined initial/boundary condition.

Properties of a Finite-Difference Scheme

Let $\Phi(P)$ be any smooth function in D . For each such a function a **local truncation error** can be defined:

$$\tau \{ \Phi(P) \} \equiv L(\Phi(P)) - L_{\Delta}(\Phi(P)) ; \quad P \in D_{\Delta}^I \quad (1.1.8a)$$

and

$$\beta \{ \Phi(P) \} \equiv B(\Phi(P)) - B_{\Delta}(\Phi(P)) ; \quad P \in D_{\Delta}^B . \quad (1.1.8b)$$

Then the difference problem (1.1.7) is **consistent** with the problem (1.1.6) if

$$\| \tau \{ \Phi \} \| \rightarrow 0 \quad (1.1.9a)$$

and

$$\| \beta \{ \Phi \} \| \rightarrow 0 \quad (1.1.9b)$$

for $\Delta x \rightarrow 0, \dots, \Delta t \rightarrow 0,$

where $\| \|$ stand for appropriate norms.

The difference problem (1.1.7) is said to be a **conditionally consistent** with the problem (1.1.6), if relations (1.1.9) are satisfied only when certain relationship among $\Delta x, \dots, \Delta t$ is satisfied.

The difference **solution U is convergent** to the exact solution u if

$$\| u(P) - U(P) \| \rightarrow 0 ; \quad P \in D$$

for $\Delta x \rightarrow 0, \dots, \Delta t \rightarrow 0.$

If the difference solution is convergent for all data in some class of smooth functions $\{f, g\}$, the corresponding finite-difference **scheme is convergent**.

A scheme determined by linear difference operators L_Δ and B_Δ is **stable** if there a finite positive quantity K exists, independent of the grid spacings, such that

$$\| U \| \leq K \left(\| L_\Delta(U) \| + \| B_\Delta(U) \| \right) \quad (1.1.10)$$

for all grid functions U on D .

If (1.1.10) is valid for all grid spacings the linear finite-difference scheme is **unconditionally stable**. If (1.1.10) is valid only for some restricted family of grid spacings in which Δx , ..., Δt may all be made arbitrarily small, the scheme is **conditionally stable**.

Let us stress that the stability of the finite-difference scheme is a property independent of any differential-equation problem.

Finally, we conclude this short review with a very important theorem connecting consistency, stability and convergence of the finite-difference schemes:

Let L_Δ and B_Δ be linear difference operators which are stable and consistent with L and B on some family of grids in which Δx , ..., Δt may be arbitrarily small. Then the difference solution U of (1.1.7) is convergent to the solution u of (1.1.6).

We recommend much more reading on the theory of the finite-difference method that can be found in the mathematical textbooks, e.g., Forsythe & Wasow (1960), Isaacson & Keller (1966), Richtmyer & Morton (1967), Mitchell & Griffith (1980) and Morton & Mayers (1994).

1.2 EXAMPLE : CASE OF THE ONE-DIMENSIONAL WAVE EQUATION

Consider a medium described by density $\rho(x)$ and Lamé's coefficients $\mu(x)$ and $\lambda(x)$. Furthermore, consider a plane wave propagating in the x -direction. The equation

$$\rho d_{tt} = (E d_x)_x \quad (1.2.1)$$

describes either propagation of P-wave if $E = \lambda + 2\mu$ or S-wave if $E = \mu$ and d is a corresponding displacement. We used notation

$$d_{tt} = \frac{\partial^2 d}{\partial t^2} \quad \text{and} \quad (E d_x)_x = \frac{\partial}{\partial x} \left(E \frac{\partial d}{\partial x} \right).$$

We will follow the example of constructing and investigating the finite-difference scheme given by Aki & Richards (1980).

Instead of equation (1.2.1) we can write equivalently two first-order equations

$$v_t = \frac{1}{\rho} \tau_x, \quad \tau_t = E v_x \quad (1.2.2)$$

where $v = d_t$ is a particle velocity and $\tau = E d_x$ stress.

Denote $\rho_i = \rho(i \Delta x)$, $E_i = E(i \Delta x)$ and V_i^m and T_i^m the finite-difference approximations to $v_i^m = v(i \Delta x, m \Delta t)$ and $\tau_i^m = \tau(i \Delta x, m \Delta t)$. Approximating $v_t(i \Delta x, m \Delta t)$ and $\tau_t(i \Delta x, m \Delta t)$ by the forward-difference formula and $v_x(i \Delta x, m \Delta t)$ and $\tau_x(i \Delta x, m \Delta t)$ by the central-difference formula in equations (1.2.2) we get the following finite-difference equations:

$$\frac{1}{\Delta t} (V_i^{m+1} - V_i^m) = \frac{1}{\rho_i} \frac{1}{2 \Delta x} (T_{i+1}^m - T_{i-1}^m), \quad (1.2.3a)$$

$$\frac{1}{\Delta t} (T_i^{m+1} - T_i^m) = E_i \frac{1}{2 \Delta x} (V_{i+1}^m - V_{i-1}^m). \quad (1.2.3b)$$

It is easy to check consistency of the scheme (1.2.3) in the homogeneous medium. Check, for example, equation (1.2.3a):

$$L_\Delta = \frac{1}{\Delta t} (v_i^{m+1} - v_i^m) - \frac{1}{\rho_i} \frac{1}{2 \Delta x} (\tau_{i+1}^m - \tau_{i-1}^m),$$

$$L = v_t(i \Delta x, m \Delta t) - \frac{1}{\rho_i} \tau_x(i \Delta x, m \Delta t).$$

Substituting Taylor's expansions instead of v_i^{m+1} , v_i^m , τ_{i+1}^m and τ_{i-1}^m about $(i \Delta x, m \Delta t)$ in L_Δ we get

$$L_\Delta = v_t(i \Delta x, m \Delta t) - \frac{1}{\rho_i} \tau_x(i \Delta x, m \Delta t) + O(\Delta t) + O(\Delta^2 x)$$

and

$$L - L_\Delta = -O(\Delta t) - O(\Delta^2 x) \rightarrow 0 \quad \text{when} \quad \Delta x, \Delta t \rightarrow 0.$$

Similarly we could check consistency of equation (1.2.3b).

The finite-difference scheme given by equations (1.2.3) is consistent with differential equations (1.2.2). The scheme is 1st-order accurate in time and 2nd-order accurate in space.

Let us check now stability of the scheme. Assume **initial errors** in V and T and investigate their propagation in the grid.

Let the errors in $x = i\Delta x$ and $t = m\Delta t$ be

$$\begin{aligned}\mathcal{E}(T_i^m) &= A \exp(-i\omega m\Delta t + i k i \Delta x) , \\ \mathcal{E}(V_i^m) &= B \exp(-i\omega m\Delta t + i k i \Delta x) .\end{aligned}\tag{1.2.4}$$

Since the errors satisfy the same equations as the solution itself substitute (1.2.4) into the finite-difference equations (1.2.3):

$$\begin{aligned}B [\exp(-i\omega \Delta t) - 1] &= \frac{\Delta t}{2\rho_i \Delta x} A 2i \sin k \Delta x , \\ A [\exp(-i\omega \Delta t) - 1] &= \frac{E_i \Delta t}{2 \Delta x} B 2i \sin k \Delta x .\end{aligned}$$

Eliminating B and A gives

$$\begin{aligned}[\exp(-i\omega \Delta t) - 1]^2 &= - \frac{E_i}{\rho_i} \left(\frac{\Delta t}{\Delta x} \right)^2 (\sin k \Delta x)^2 , \\ \exp(-i\omega \Delta t) &= 1 \pm i \left(\frac{E_i}{\rho_i} \right)^{1/2} \frac{\Delta t}{\Delta x} \sin k \Delta x , \\ |\exp(-i\omega \Delta t)| &= \left| 1 \pm i \left(\frac{E_i}{\rho_i} \right)^{1/2} \frac{\Delta t}{\Delta x} \sin k \Delta x \right| > 1 .\end{aligned}$$

It follows from the inequality that ω is complex. This means that the errors grow exponentially with time. The scheme given by equations (1.2.3) is unstable.

Let us try now to approximate v_t and τ_t in (1.2.2) by the central-difference formula. We obtain

$$\begin{aligned}\frac{1}{2\Delta t} (V_i^{m+1} - V_i^{m-1}) &= \frac{1}{\rho_i} \frac{1}{2\Delta x} (T_{i+1}^m - T_{i-1}^m) , \\ \frac{1}{2\Delta t} (T_i^{m+1} - T_i^{m-1}) &= E_i \frac{1}{2\Delta x} (V_{i+1}^m - V_{i-1}^m) .\end{aligned}\tag{1.2.5}$$

Substitute the errors (1.2.4) into (1.2.5):

$$\begin{aligned}-i2B \sin \omega \Delta t &= \frac{\Delta t}{\rho_i \Delta x} A 2i \sin k \Delta x , \\ -i2A \sin \omega \Delta t &= \frac{E_i \Delta t}{\Delta x} B 2i \sin k \Delta x , \\ (\sin \omega \Delta t)^2 &= \frac{E_i}{\rho_i} \left(\frac{\Delta t}{\Delta x} \right)^2 (\sin k \Delta x)^2 , \\ \sin \omega \Delta t &= \pm \left(\frac{E_i}{\rho_i} \right)^{1/2} \frac{\Delta t}{\Delta x} \sin k \Delta x .\end{aligned}$$

Assume now that

$$\left(\frac{E_i}{\rho_i} \right)^{1/2} \frac{\Delta t}{\Delta x} \leq 1.$$

Then

$$|\sin \omega \Delta t| \leq 1$$

and consequently ω is real. This means that the errors (1.2.4) do not grow with time. The scheme given by equations (1.2.5) is stable under condition

$$\Delta t \leq \frac{\Delta x}{c_i} \quad (1.2.6)$$

where

$$c_i = \left(\frac{E_i}{\rho_i} \right)^{1/2}.$$

Condition (1.2.6) is called a **stability condition**.

Try now to use the central-difference formula over smaller grid distances - Δx and Δt instead of $2\Delta x$ and $2\Delta t$, respectively. We get first

$$\frac{1}{\Delta t} \left(V_i^{m+1/2} - V_i^{m-1/2} \right) = \frac{1}{\rho_i} \frac{1}{\Delta x} \left(T_{i+1/2}^m - T_{i-1/2}^m \right). \quad (1.2.7a)$$

The approximation leads to the so-called **staggered grid**: the grid for T is shifted with respect to that for V by $\Delta x/2$ in space and by $\Delta t/2$ in time.

Then equation (1.2.7a) implies

$$\frac{1}{\Delta t} \left(T_{i+1/2}^{m+1} - T_{i+1/2}^m \right) = E_{i+1/2} \frac{1}{\Delta x} \left(V_{i+1}^{m+1/2} - V_i^{m+1/2} \right). \quad (1.2.7b)$$

$E_{i+1/2}$ refers to $E((i+1/2)\Delta x)$. (We want to note here that considering local values ρ_i and E_i is usual. It does not follow, however, from the derivation of the scheme itself and should be justified a posteriori. Taking local values may be appropriate in sufficiently smooth media.)

Differencing over twice smaller grid distances implies that the leading term of the approximation error is now four times smaller than that in the scheme given by equations (1.2.5).

In this case stability analysis gives the relation

$$\sin \frac{\omega \Delta t}{2} = \left(\frac{E_{i+1/2}}{\rho_i} \right)^{1/2} \frac{\Delta t}{\Delta x} \sin \frac{k \Delta x}{2}. \quad (1.2.8)$$

This means that the stability condition is the same as for the scheme given by equations (1.2.5). The physical meaning of the stability condition (1.2.6) is clear: The time step cannot be larger than the time necessary for any disturbance to propagate over the distance Δx .

Let us now investigate equation (1.2.8) since it gives the relation between ω and k (frequency and wavenumber). Assume Δt and Δx small enough for the approximations

$$\sin \frac{\omega \Delta t}{2} \doteq \frac{\omega \Delta t}{2} \quad , \quad \sin \frac{k \Delta x}{2} \doteq \frac{k \Delta x}{2} .$$

Then it follows from (1.2.8) that

$$\frac{\omega}{k} = \left(\frac{E_{i+1/2}}{\rho_i} \right)^{1/2} = c_0 . \quad (1.2.9)$$

This means that for small Δt and Δx equation (1.2.8) determines a correct local value of the phase velocity. The question is how small Δx should be in order to justify the approximate relation (1.2.9). Obviously Δx has to be related to a wavelength for which approximation (1.2.9) should be valid.

Using $k = 2\pi/\lambda$ we get from (1.2.8) relations for the actual **grid phase** and **group velocities**:

$$c^{\text{grid}} = \frac{\omega}{k} = \frac{\Delta x}{\pi \Delta t} \frac{\lambda}{\Delta x} \arcsin \left(c_0 \frac{\Delta t}{\Delta x} \sin \frac{\pi \Delta x}{\lambda} \right) ,$$

$$v_g^{\text{grid}} = \frac{\partial \omega}{\partial k} = \frac{c_0 \cos \frac{\pi \Delta x}{\lambda}}{\left[1 - \left(c_0 \frac{\Delta t}{\Delta x} \sin \frac{\pi \Delta x}{\lambda} \right)^2 \right]^{1/2}} .$$

Assuming a homogeneous medium with phase velocity c_0 , it is easy to see the dependence of c^{grid} and v_g^{grid} on a spatial sampling ratio $\Delta x/\lambda$ and stability ratio $c_0 \Delta t/\Delta x$, i. e., the so-called **grid dispersion**, by plotting both velocities normalized by c_0 as it is illustrated in Fig. 1.2.1.

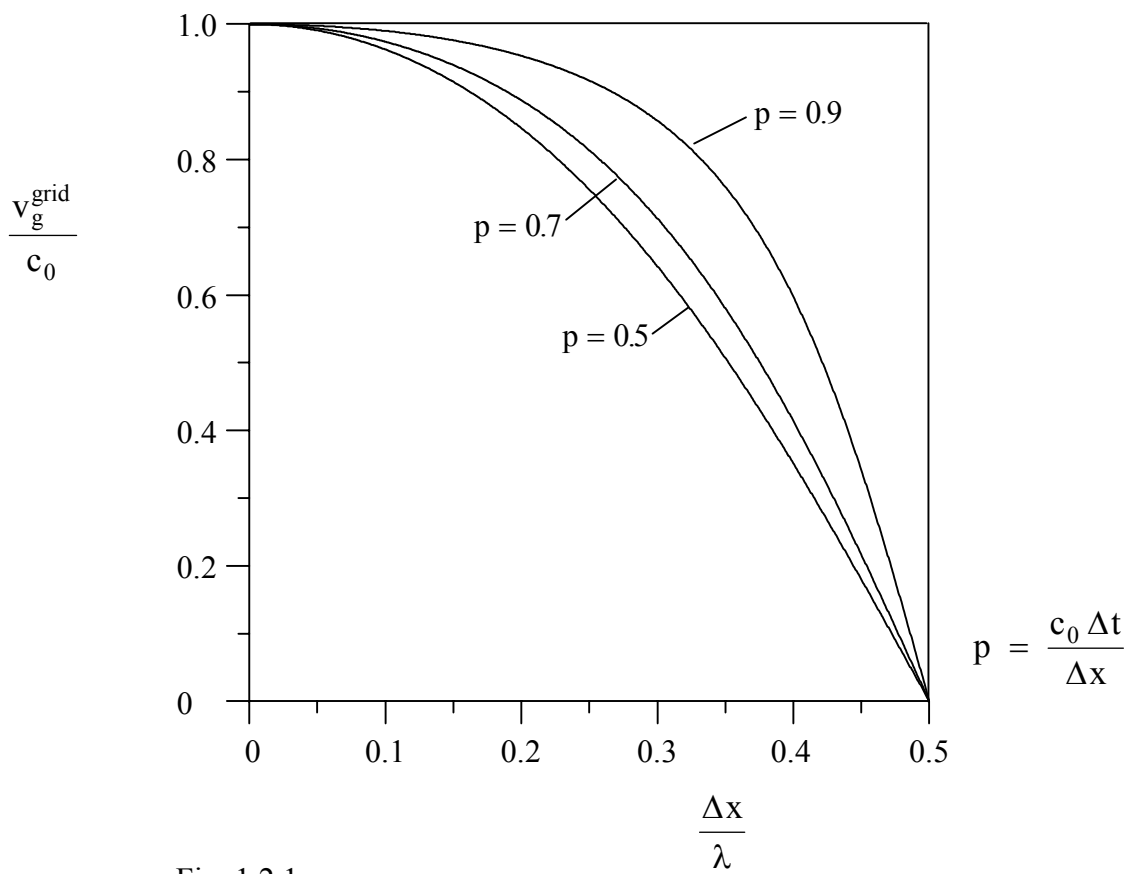
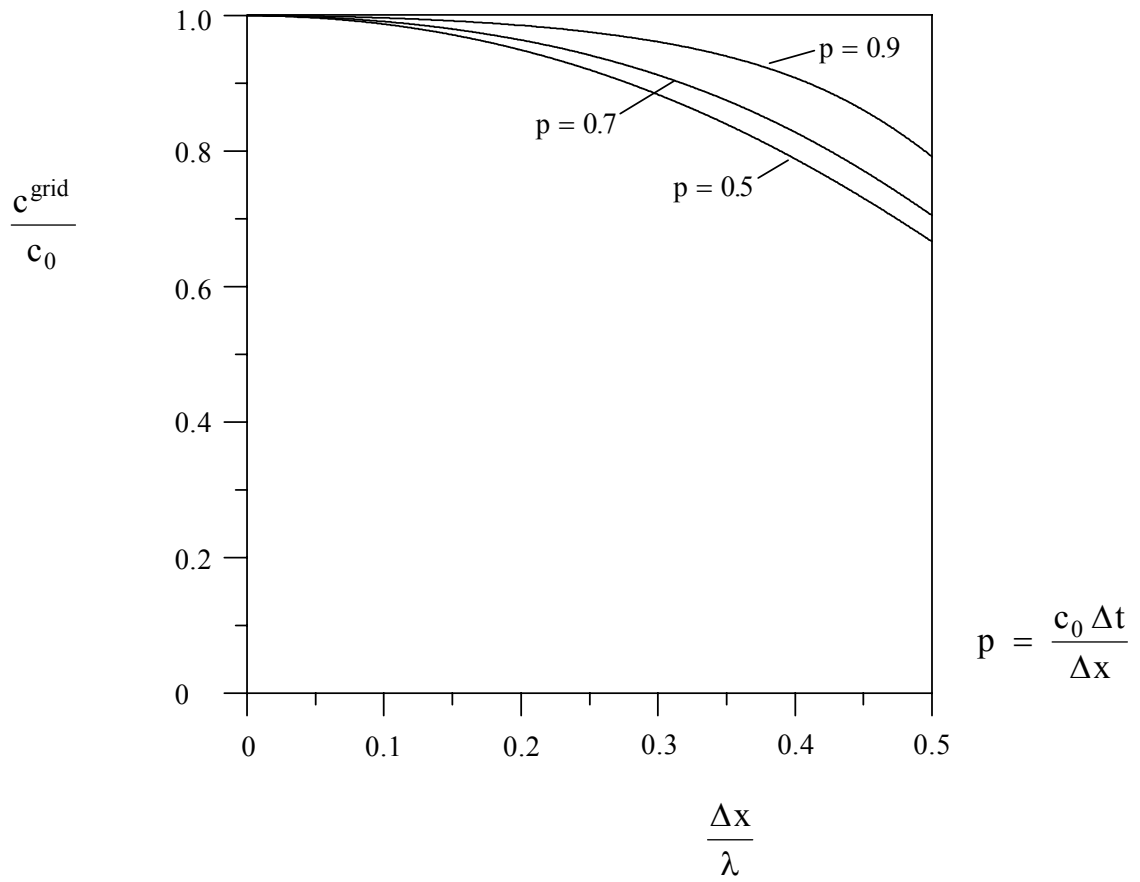


Fig. 1.2.1
Grid-dispersion curves for the finite-difference scheme (1.2.7)

It is clear from the figures that c^{grid} and v_g^{grid} are close to the real phase and group velocities if $\Delta x/\lambda < 0.1$. This means that at least 10 grid spacings Δx should be used to sample the wavelength λ in order to avoid the grid dispersion of the phase and group velocities for the wavelength λ . Relation

$$\Delta x < \frac{\lambda}{10}$$

can be called a **sampling criterion**. Let v_{min} be a minimum velocity in a medium. Then, if we want to have our finite-difference computation "accurate" up to the frequency f_{ac} , the grid spacing has to satisfy the sampling criterion

$$\Delta x < \frac{v_{\text{min}}}{10 f_{\text{ac}}}. \quad (1.2.10)$$

PART B : APPLICATION OF THE FINITE-DIFFERENCE METHOD TO THE EQUATION OF MOTION IN A PERFECTLY ELASTIC MEDIUM

2. EQUATION OF MOTION

Consider a Cartesian coordinate system (x_1, x_2, x_3) . Denote $\rho(\bar{x})$ **density**, $\bar{u}(\bar{x}, t)$ **displacement vector**, $\bar{f}(\bar{x}, t)$ **body force** per unit volume, and $\tau_{ij}(\bar{x}, t)$; $i, j = 1, 2, 3$ **stress-tensor**, \bar{x} meaning position and t time.

Then the **equation of motion** reads

$$\rho u_{i,tt} = \tau_{ij,j} + f_i \quad ; \quad i, j \in \{1, 2, 3\} \quad (2.0.1)$$

where

$$u_{i,tt} = \frac{\partial^2 u_i}{\partial t^2} \quad \text{and} \quad \tau_{ij,j} = \frac{\partial \tau_{ij}}{\partial x_j}$$

and summation convention for repeated subscripts i and j is assumed.

In the isotropic medium the stress-tensor is given by **Hooke's law**

$$\tau_{ij} = \lambda u_{k,k} \delta_{ij} + \mu (u_{i,j} + u_{j,i}) \quad ; \quad i, j \in \{1, 2, 3\} \quad (2.0.2)$$

where $\lambda(\bar{x})$ and $\mu(\bar{x})$ are **Lamé's elastic coefficients** and

$$u_{i,j} = \frac{\partial u_i}{\partial x_j} .$$

As it is clear from equation (2.0.2), the stress-tensor is symmetric:

$$\tau_{ij} = \tau_{ji} .$$

A **particle velocity** $\bar{u}(\bar{x}, t)$ is given by

$$\bar{u} = \frac{\partial \bar{u}}{\partial t} . \quad (2.0.3)$$

Using equations (2.0.1)-(2.0.3) we can consider three formulations of the equation of motion:

Displacement-stress formulation

$$\begin{aligned}\rho u_{i,tt} &= \tau_{ij,j} + f_i \\ \tau_{ij} &= \lambda u_{k,k} \delta_{ij} + \mu (u_{i,j} + u_{j,i})\end{aligned}\quad (2.0.4)$$

Velocity-stress formulation

$$\begin{aligned}\rho u_{i,t} &= \tau_{ij,j} + f_i \\ \tau_{ij,t} &= \lambda u_{k,k} \delta_{ij} + \mu (u_{i,j} + u_{j,i})\end{aligned}\quad (2.0.5)$$

Displacement formulation

$$\rho u_{i,tt} = (\lambda u_{k,k})_{,i} + (\mu u_{i,j})_{,j} + (\mu u_{j,i})_{,j} + f_i \quad (2.0.6)$$

Instead of a concise subscript notation used in equations (2.0.4)-(2.0.6) it may be useful to use an alternative notation:

$$\begin{aligned}x &= x_1 & , & & y &= x_2 & , & & z &= x_3 & , \\ u &= u_1 & , & & v &= u_2 & , & & w &= u_3 & , \\ \tau_{xx} &= \tau_{11} & , & & \tau_{yy} &= \tau_{22} & , & & \tau_{zz} &= \tau_{33} & , \\ \tau_{xy} &= \tau_{12} & , & & \tau_{xz} &= \tau_{13} & , & & \tau_{yz} &= \tau_{23} & , \\ f_x &= f_1 & , & & f_y &= f_2 & , & & f_z &= f_3 & , \\ u &= u_1 & , & & v &= u_2 & , & & w &= u_3 & ,\end{aligned}$$

and

$$\begin{aligned}u_x &= u_{1,1} & , & & u_y &= u_{1,2} & , & & u_z &= u_{1,3} & , \\ v_x &= u_{2,1} & , & & v_y &= u_{2,2} & , & & v_z &= u_{2,3} & , \\ w_x &= u_{3,1} & , & & w_y &= u_{3,2} & , & & w_z &= u_{3,3}\end{aligned}$$

and analogously for derivatives of the stress-tensor components (e.g., $\tau_{xy,x} = \tau_{12,1}$).

Then we can write equation of motion in the three formulations in the 3D, P-SV and SH cases as follows.

2.1 3D CASE

$$\begin{aligned} \vec{u} & (u(x,y,z,t), v(x,y,z,t), w(x,y,z,t)) \\ \tau_{\xi\eta} & (x,y,z,t) ; \quad \xi, \eta \in \{x,y,z\} \\ \vec{f} & (f_x(x,y,z,t), f_y(x,y,z,t), f_z(x,y,z,t)) \\ \rho & (x,y,z) , \quad \lambda (x,y,z) , \quad \mu (x,y,z) \\ \vec{u} & (u(x,y,z,t), v(x,y,z,t), w(x,y,z,t)) \end{aligned}$$

Displacement-Stress Formulation

$$\begin{aligned} \rho u_{tt} &= \tau_{xx,x} + \tau_{xy,y} + \tau_{xz,z} + f_x \\ \rho v_{tt} &= \tau_{xy,x} + \tau_{yy,y} + \tau_{yz,z} + f_y \\ \rho w_{tt} &= \tau_{xz,x} + \tau_{yz,y} + \tau_{zz,z} + f_z \end{aligned} \tag{2.1.1a}$$

$$\begin{aligned} \tau_{xx} &= [\lambda + 2\mu] u_x + \lambda v_y + \lambda w_z \\ \tau_{yy} &= \lambda u_x + [\lambda + 2\mu] v_y + \lambda w_z \\ \tau_{zz} &= \lambda u_x + \lambda v_y + [\lambda + 2\mu] w_z \\ \tau_{xy} &= \mu (u_y + v_x) \\ \tau_{xz} &= \mu (u_z + w_x) \\ \tau_{yz} &= \mu (v_z + w_y) \end{aligned} \tag{2.1.1b}$$

Displacement Formulation

$$\begin{array}{l}
 \rho u_{tt} = \\
 ([\lambda + 2\mu] u_x)_x \\
 + (\mu u_y)_y \\
 + (\mu u_z)_z \\
 + (\lambda v_y)_x \\
 + (\lambda w_z)_x \\
 + (\mu v_x)_y \\
 + (\mu w_x)_z \\
 + f_x \\
 \rho v_{tt} = \\
 (\mu v_x)_x \\
 + ([\lambda + 2\mu] v_y)_y \\
 + (\mu v_z)_z \\
 + (\mu u_y)_x \\
 + (\lambda u_x)_y \\
 + (\lambda w_z)_y \\
 + (\mu w_y)_z \\
 + f_y \\
 \rho w_{tt} = \\
 (\mu w_x)_x \\
 + (\mu w_y)_y \\
 + ([\lambda + 2\mu] w_z)_z \\
 + (\mu u_z)_x \\
 + (\mu v_z)_y \\
 + (\lambda u_x)_z \\
 + (\lambda v_y)_z \\
 + f_z
 \end{array} \quad (2.1.2)$$

Velocity-Stress Formulation

$$\begin{aligned}
 \rho u_t &= \tau_{xx,x} + \tau_{xy,y} + \tau_{xz,z} + f_x \\
 \rho v_t &= \tau_{xy,x} + \tau_{yy,y} + \tau_{yz,z} + f_y \\
 \rho w_t &= \tau_{xz,x} + \tau_{yz,y} + \tau_{zz,z} + f_z
 \end{aligned} \quad (2.1.3a)$$

$$\begin{aligned}
 \tau_{xx,t} &= [\lambda + 2\mu] u_x + \lambda v_y + \lambda w_z \\
 \tau_{yy,t} &= \lambda u_x + [\lambda + 2\mu] v_y + \lambda w_z \\
 \tau_{zz,t} &= \lambda u_x + \lambda v_y + [\lambda + 2\mu] w_z \\
 \tau_{xy,t} &= \mu (u_y + v_x) \\
 \tau_{xz,t} &= \mu (u_z + w_x) \\
 \tau_{yz,t} &= \mu (v_z + w_y)
 \end{aligned} \quad (2.1.3b)$$

2.2 P-SV CASE

$$\begin{aligned} \bar{u} & (u(x,z,t), 0, w(x,z,t)) \\ \tau_{\xi\eta} & (x,z,t) \quad ; \quad \xi, \eta \in \{x,z\} \\ \bar{f} & (f_x(x,z,t), 0, f_z(x,z,t)) \\ \rho & (x,z) \quad , \quad \lambda (x,z) \quad , \quad \mu (x,z) \\ \bar{u} & (u(x,z,t), 0, w(x,z,t)) \end{aligned}$$

Displacement-Stress Formulation

$$\begin{aligned} \rho u_{tt} &= \tau_{xx,x} + \tau_{xz,z} + f_x \\ \rho w_{tt} &= \tau_{xz,x} + \tau_{zz,z} + f_z \end{aligned} \tag{2.2.1a}$$

$$\begin{aligned} \tau_{xx} &= [\lambda + 2\mu] u_x + \lambda w_z \\ \tau_{zz} &= \lambda u_x + [\lambda + 2\mu] w_z \\ \tau_{xz} &= \mu (u_z + w_x) \end{aligned} \tag{2.2.1b}$$

Displacement Formulation

$$\begin{aligned} \rho u_{tt} &= ([\lambda + 2\mu] u_x)_x + (\mu u_z)_z + (\lambda w_z)_x + (\mu w_x)_z + f_x \\ \rho w_{tt} &= (\mu w_x)_x + ([\lambda + 2\mu] w_z)_z + (\mu u_z)_x + (\lambda u_x)_z + f_z \end{aligned} \tag{2.2.2}$$

Velocity-Stress Formulation

$$\begin{aligned} \rho u_t &= \tau_{xx,x} + \tau_{xz,z} + f_x \\ \rho w_t &= \tau_{xz,x} + \tau_{zz,z} + f_z \end{aligned} \tag{2.2.3a}$$

$$\begin{aligned} \tau_{xx,t} &= [\lambda + 2\mu] u_x + \lambda w_z \\ \tau_{zz,t} &= \lambda u_x + [\lambda + 2\mu] w_z \\ \tau_{xz,t} &= \mu (u_z + w_x) \end{aligned} \tag{2.2.3b}$$

2.3 SH CASE

$$\begin{aligned} & \bar{u} (0, v(x, z, t), 0) \\ & \tau_{xy} (x, z, t) \ ; \ \tau_{yz} (x, z, t) \\ & \tau_{xx} = \tau_{yy} = \tau_{zz} = \tau_{xz} = 0 \\ & \bar{f} (0, f_y(x, z, t), 0) \\ & \rho (x, z) \ , \ \lambda (x, z) \ , \ \mu (x, z) \\ & \bar{u} (0, v(x, z, t), 0) \end{aligned}$$

Displacement-Stress Formulation

$$\rho v_{tt} = \tau_{xy,x} + \tau_{yz,z} + f_y \quad (2.3.1a)$$

$$\begin{aligned} \tau_{xy} &= \mu v_x \\ \tau_{yz} &= \mu v_z \end{aligned} \quad (2.3.1b)$$

Displacement Formulation

$$\rho v_{tt} = (\mu v_x)_x + (\mu v_z)_z + f_y \quad (2.3.2)$$

Velocity-Stress Formulation

$$\rho v_t = \tau_{xy,x} + \tau_{yz,z} + f_y \quad (2.3.3a)$$

$$\begin{aligned} \tau_{xy,t} &= \mu v_x \\ \tau_{yz,t} &= \mu v_z \end{aligned} \quad (2.3.3b)$$

2.4 HOMOGENEOUS MEDIUM

In the homogeneous medium density ρ and Lamé's coefficients are spatial constants. Equations (2.1.1), (2.2.1) and (2.3.1) in the displacement-stress formulation do not change except that ρ , λ and μ in those equations are spatial constants. The same is true about equations (2.1.3), (2.2.3) and (2.3.3) in the velocity-stress formulation.

Equations (2.1.2), (2.2.2) and (2.3.2) in the displacement formulation can be simplified:

3D Case

$$\begin{array}{l}
 \rho u_{tt} = \\
 [\lambda + 2\mu] u_{xx} \\
 + \mu u_{yy} \\
 + \mu u_{zz} \\
 + \lambda v_{yx} \\
 + \lambda w_{zx} \\
 + \mu v_{xy} \\
 + \mu w_{xz} \\
 + f_x
 \end{array}
 \left|
 \begin{array}{l}
 \rho v_{tt} = \\
 \mu v_{xx} \\
 + [\lambda + 2\mu] v_{yy} \\
 + \mu v_{zz} \\
 + \mu u_{yx} \\
 + \lambda u_{xy} \\
 + \lambda w_{zy} \\
 + \mu w_{yz} \\
 + f_y
 \end{array}
 \right|
 \begin{array}{l}
 \rho w_{tt} = \\
 \mu w_{xx} \\
 + \mu w_{yy} \\
 + [\lambda + 2\mu] w_{zz} \\
 + \mu u_{zx} \\
 + \mu v_{zy} \\
 + \lambda u_{xz} \\
 + \lambda v_{yz} \\
 + f_z
 \end{array}
 \quad (2.4.1)$$

P-SV Case

$$\begin{aligned}
 \rho u_{tt} &= [\lambda + 2\mu] u_{xx} + \mu u_{zz} + \lambda w_{zx} + \mu w_{xz} + f_x, \\
 \rho w_{tt} &= \mu w_{xx} + [\lambda + 2\mu] w_{zz} + \mu u_{zx} + \lambda u_{xz} + f_z,
 \end{aligned}
 \quad (2.4.2)$$

SH Case

$$\rho v_{tt} = \mu v_{xx} + \mu v_{zz} + f_y, \quad (2.4.3)$$

where $u_{xx} = \frac{\partial^2 u}{\partial x^2}$, $u_{xy} = \frac{\partial^2 u}{\partial x \partial y}$, \dots

3. HETEROGENEOUS FORMULATION OF THE EQUATION OF MOTION AND HETEROGENEOUS FINITE-DIFFERENCE SCHEMES

It is relatively easy to replace equations of motion for a homogeneous medium, i.e., equations (2.4.1)-(2.4.3) by the finite-difference schemes.

Finding appropriate schemes becomes more difficult if material parameters are functions of the spatial coordinates.

In a smooth inhomogeneous medium the finite-difference approximations of derivatives in the case of the displacement-stress and velocity-stress formulations remain the same as those in the homogeneous medium. What, however, is not obvious from the scheme construction itself is a proper material factorization, i.e., determination of the grid material parameters. Local (point) values of material parameters or some effective material parameters may be used. A particular choice for a problem under consideration (i. e., medium-wavefield configuration) should be examined.

In the case of the displacement formulation it is necessary to find proper finite-difference approximations for terms as, e.g.,

$$(\mu w_x)_x, (\lambda u_y)_x,$$

i.e., non-mixed and mixed derivatives in which μ and λ are functions of the spatial coordinates. There are several possible finite-difference schemes. However, they are not equally accurate.

If the medium contains material discontinuities we can follow either the so-called homogeneous or heterogeneous formulation.

In the **homogeneous formulation** we apply the equation of motion inside blocks and boundary condition (usually continuity of displacement and continuity of traction) at the discontinuities separating blocks. Such an approach is traditional and usual generally in physics. Equation of motion and boundary condition are replaced by the finite-difference schemes.

In the seismological practice we need to consider material discontinuities of complicated shapes. Then the homogeneous approach can be complicated and tedious, in other words, impractical.

Therefore, the **heterogeneous formulation** is preferred. In the heterogeneous approach no explicit condition is specified. Material discontinuities are accounted for only by spatial variations of the material parameters in the equation of motion.

The equation of motion is replaced by the finite-difference scheme. It is not so obvious, however, whether

1. the equation of motion can be used without explicitly specified boundary condition,
2. a heterogeneous finite-difference scheme satisfies boundary condition.

In order to answer the second question it is necessary to check consistency of a particular finite-difference scheme at material discontinuities; see Zahradník et al. (1993). The

first question was recently addressed by Zahradník & Priolo (1995). Here we present a simple case of a horizontal discontinuity.

Let horizontal discontinuity separate two homogeneous halfspaces as it is illustrated in Fig. 3.1.

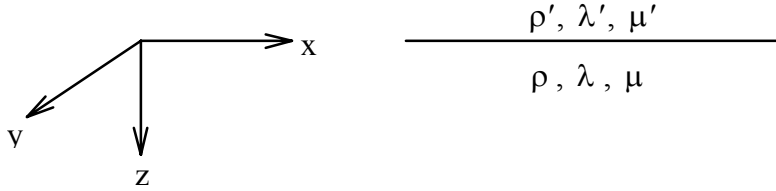


Fig. 3.1

Density ρ and Lamé's coefficients λ and μ are functions of the z -coordinate:

$$\begin{aligned}\rho(z) &= \rho H(z) + \rho' H(-z) , \\ \lambda(z) &= \lambda H(z) + \lambda' H(-z) , \\ \mu(z) &= \mu H(z) + \mu' H(-z) ,\end{aligned}\tag{3.1}$$

where $H(z)$ is a unit step function.

Consider first the displacement-stress formulation (2.1.1). Due to relations (3.1) and (2.1.1b) we distinguish stress-components in the upper and lower halfspaces,

$$\begin{aligned}\rho u_{tt} H(z) + \rho' u'_{tt} H(-z) &= (\tau_{xx} H(z) + \tau'_{xx} H(-z))_x \\ &+ (\tau_{xy} H(z) + \tau'_{xy} H(-z))_y \\ &+ (\tau_{xz} H(z) + \tau'_{xz} H(-z))_z ,\end{aligned}\tag{3.2}$$

and similarly for the v and w components. Differentiating expressions in the parentheses in the equation (3.2) we obtain

$$\begin{aligned}\rho u_{tt} H(z) + \rho' u'_{tt} H(-z) &= \tau_{xx,x} H(z) + \tau'_{xx,x} H(-z) \\ &+ \tau_{xy,y} H(z) + \tau'_{xy,y} H(-z) \\ &+ \tau_{xz,z} H(z) + \tau'_{xz,z} H(-z) \\ &+ \tau_{xz} \delta(z) - \tau'_{xz} \delta(z) .\end{aligned}$$

Rewriting the equation we finally arrive in

$$\begin{aligned}
& (-\rho u_{tt} + \tau_{xx,x} + \tau_{xy,y} + \tau_{xz,z}) H(z) \\
& + \\
& (-\rho u'_{tt} + \tau'_{xx,x} + \tau'_{xy,y} + \tau'_{xz,z}) H(-z) \\
& + \\
& \{ \tau_{xz} - \tau'_{xz} \} \delta(z) = 0 .
\end{aligned} \tag{3.3}$$

Equation (3.3) can be symbolically written as

$$E H(z) + E' H(-z) + C \delta(z) = 0 \tag{3.4}$$

where

E represents equation of motion for the u component in the lower halfspace,

E' represents equation of motion for the u component in the upper halfspace

and

C represents the continuity of the x -component of the traction at the discontinuity.

Analogous results can be obtained for the v and w components of the displacement vector and, respectively, for the y - and z -components of the traction:

$$\begin{aligned}
& (-\rho v_{tt} + \tau_{xy,x} + \tau_{yy,y} + \tau_{yz,z}) H(z) \\
& + \\
& (-\rho v'_{tt} + \tau'_{xy,x} + \tau'_{yy,y} + \tau'_{yz,z}) H(-z) \\
& + \\
& \{ \tau_{yz} - \tau'_{yz} \} \delta(z) = 0 ,
\end{aligned}$$

$$\begin{aligned}
& (-\rho w_{tt} + \tau_{xz,x} + \tau_{yz,y} + \tau_{zz,z}) H(z) \\
& + \\
& (-\rho w'_{tt} + \tau'_{xz,x} + \tau'_{yz,y} + \tau'_{zz,z}) H(-z) \\
& + \\
& \{ \tau_{zz} - \tau'_{zz} \} \delta(z) = 0 .
\end{aligned}$$

The conclusion is that equations (2.1.1) can be – at least in the considered medium – used in the heterogeneous formulation: they can fully account for the boundary condition if the material parameters are treated properly. No explicitly formulated adjointed boundary condition is needed.

Consider now the displacement formulation (2.1.2). Due to (3.1) we can rewrite, e.g.,

equation for the u-component as

$$\begin{aligned}
& \rho u_{tt} H(z) + \rho' u'_{tt} H(-z) = \\
& ([\lambda + 2\mu] u_x H(z) + [\lambda' + 2\mu'] u'_x H(-z))_x \\
& + (\mu u_y H(z) + \mu' u'_y H(-z))_y \\
& + (\mu u_z H(z) + \mu' u'_z H(-z))_z \\
& + (\lambda v_y H(z) + \lambda' v'_y H(-z))_x \\
& + (\lambda w_z H(z) + \lambda' w'_z H(-z))_x \\
& + (\mu v_x H(z) + \mu' v'_x H(-z))_y \\
& + (\mu w_x H(z) + \mu' w'_x H(-z))_z .
\end{aligned} \tag{3.5}$$

Differentiating expressions in the parentheses gives

$$\begin{aligned}
& \rho u_{tt} H(z) + \rho' u'_{tt} H(-z) = \\
& [\lambda + 2\mu] u_{xx} H(z) + [\lambda' + 2\mu'] u'_{xx} H(-z) \\
& + \mu u_{yy} H(z) + \mu' u'_{yy} H(-z) \\
& + \mu u_{zz} H(z) + \mu u_z \delta(z) + \mu' u'_{zz} H(-z) - \mu' u'_z \delta(z) \\
& + \lambda v_{yx} H(z) + \lambda' v'_{yx} H(-z) \\
& + \lambda w_{zx} H(z) + \lambda' w'_{zx} H(-z) \\
& + \mu v_{xy} H(z) + \mu' v'_{xy} H(-z) \\
& + \mu w_{xz} H(z) + \mu w_x \delta(z) + \mu' w'_{xz} H(-z) - \mu' w'_x \delta(z).
\end{aligned}$$

Rearranging the equation we obtain

$$\begin{aligned}
& ([\lambda + 2\mu] u_{xx} + \mu u_{yy} + \mu u_{zz} \\
& \quad + \lambda v_{yx} + \lambda w_{zx} + \mu v_{xy} + \mu w_{xz} - \rho u_{tt}) H(z) \\
& + \\
& ([\lambda' + 2\mu'] u'_{xx} + \mu' u'_{yy} + \mu' u'_{zz} \\
& \quad + \lambda' v'_{yx} + \lambda' w'_{zx} + \mu' v'_{xy} + \mu' w'_{xz} - \rho' u'_{tt}) H(-z) \\
& + \\
& \{ \mu (u_z + w_x) - \mu' (u'_z + w'_x) \} \delta(z) = 0
\end{aligned} \tag{3.6}$$

which can be symbolically written in the form of equation (3.4). Analogous equations can be obtained for the v and w components of the displacement vector and, respectively, for the y- and z-components of the traction.

4. FINITE-DIFFERENCE SCHEMES FOR INTERIOR POINTS ON REGULAR GRIDS

In order to explain construction of various finite-difference schemes we will use the P-SV case which is simpler than the 3D case. However, at the end of the next sections we will present also finite-difference schemes for the 3D case.

Consider the x-z plane and cover it by a regular rectangular grid with the spacings $\Delta x = \Delta z = h$. We can use either a **conventional grid** or a **staggered grid**.

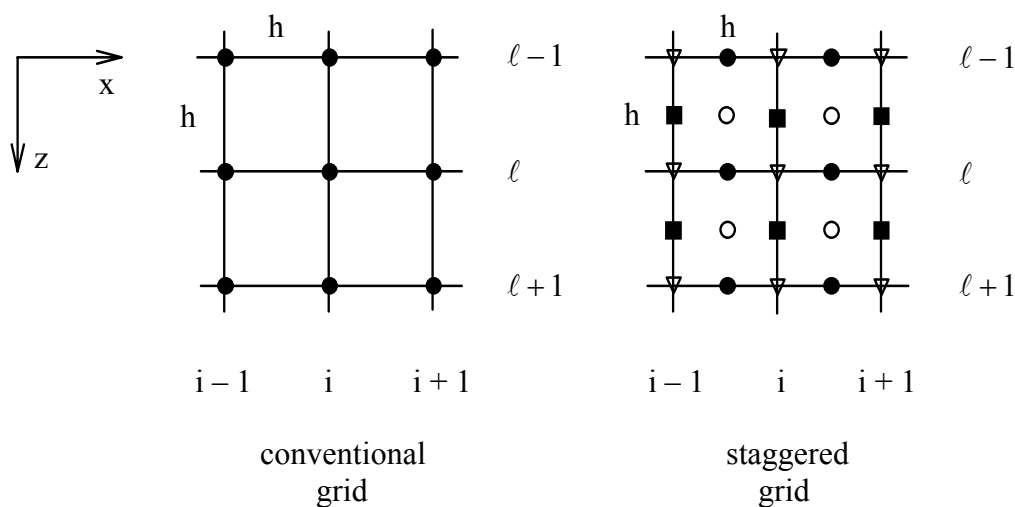


Fig. 4.1
Two types of a spatial grid

A conventional grid is usual in the displacement formulation while a staggered grid is used in the displacement-stress and velocity-stress formulations. In a conventional grid all displacement components and material parameters are defined at each grid point. In a staggered grid, different displacement/particle-velocity components, stress-tensor components, and material parameters are defined in different grid positions.

Displacement finite-difference schemes on a conventional grid have been used for modeling seismic wave propagation since the end of the sixties, e.g. Alterman & Karal (1968), Kelly et al. (1976). Madariaga (1976) suggested a velocity-stress finite-difference scheme on a staggered grid. The scheme was adapted for modeling the SH and P-SV waves by Virieux (1984, 1986). Levander (1988) developed a fourth-order velocity-stress finite-difference scheme on a staggered grid for the P-SV waves. Luo & Schuster (1990) suggested a parsimonious staggered-grid finite-difference scheme for the P-SV waves based on the displacement-stress formulation. While mathematically equivalent to the velocity-stress scheme it requires less computer memory (in the 3D case only 75% of that required by the velocity-stress scheme) since the stress-tensor components are not stored. Zahradnik (1995b) developed a new and accurate second-order displacement scheme on a conventional grid for the P-SV waves (easily applicable also to the 3D case). Graves (1996) presented fourth-order velocity-stress scheme for the 3D case. Ohminato & Chouet (1997) presented a

second-order displacement-stress scheme for the 3D case which also includes 3D topography of the free surface.

4.1 DISPLACEMENT-STRESS SCHEME ON A STAGGERED GRID

Recall equations of motion (2.2.1) :

$$\begin{aligned}\rho u_{tt} &= \tau_{xx,x} + \tau_{xz,z} + f_x \\ \rho w_{tt} &= \tau_{xz,x} + \tau_{zz,z} + f_z \\ \tau_{xx} &= [\lambda + 2\mu] u_x + \lambda w_z \\ \tau_{zz} &= \lambda u_x + [\lambda + 2\mu] w_z \\ \tau_{xz} &= \mu (u_z + w_x)\end{aligned}$$

Let us approximate the first spatial derivatives using the central-difference formula applied over one grid spacing. We should start with equations for the diagonal stress-tensor components. Both equations contain terms proportional to u_x and w_z . Therefore, we should localize T^{xx} and T^{zz} , the discrete approximations to τ_{xx} and τ_{zz} , in the same grid position, say $i+1/2 \ell+1/2$; see Fig. 4.1.1. Then we obtain for the time level m

$$\begin{aligned}T_{i+1/2 \ell+1/2}^{xx,m} &= [\lambda + 2\mu]_{i+1/2 \ell+1/2} \frac{1}{h} \left(U_{i+1 \ell+1/2}^m - U_{i \ell+1/2}^m \right) \\ &+ \lambda_{i+1/2 \ell+1/2} \frac{1}{h} \left(W_{i+1/2 \ell+1}^m - W_{i+1/2 \ell}^m \right)\end{aligned}$$

and

$$\begin{aligned}T_{i+1/2 \ell+1/2}^{zz,m} &= \lambda_{i+1/2 \ell+1/2} \frac{1}{h} \left(U_{i+1 \ell+1/2}^m - U_{i \ell+1/2}^m \right) \\ &+ [\lambda + 2\mu]_{i+1/2 \ell+1/2} \frac{1}{h} \left(W_{i+1/2 \ell+1}^m - W_{i+1/2 \ell}^m \right),\end{aligned}$$

where U and W stand for discrete approximations to u and w , respectively.

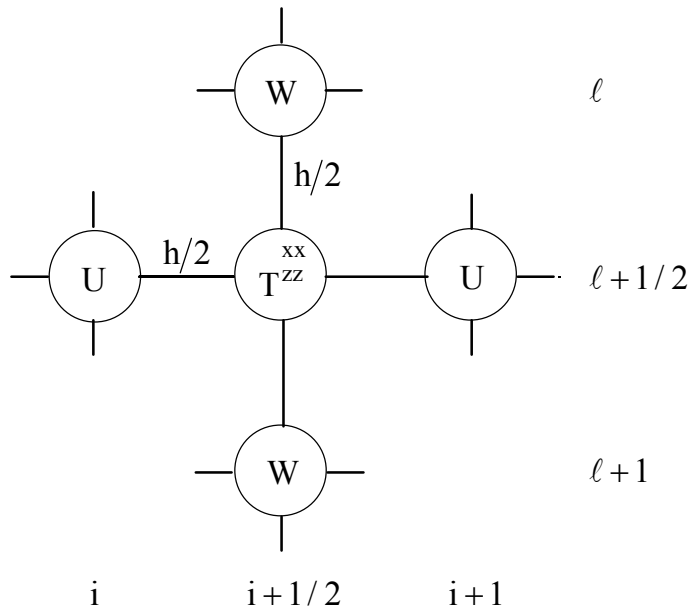


Fig. 4.1.1
Illustration of approximating U_x and W_z

If we now localize T^{xz} , a discrete approximation to τ_{xz} , at the grid position $i\ell$, see Fig. 4.1.2, we obtain the finite-difference approximation of the equation for τ_{xz} at the time level m :

$$T_{i\ell}^{xz,m} = \mu_{i\ell} \frac{1}{h} \left(U_{i\ell+1/2}^m - U_{i\ell-1/2}^m + W_{i+1/2\ell}^m - W_{i-1/2\ell}^m \right).$$

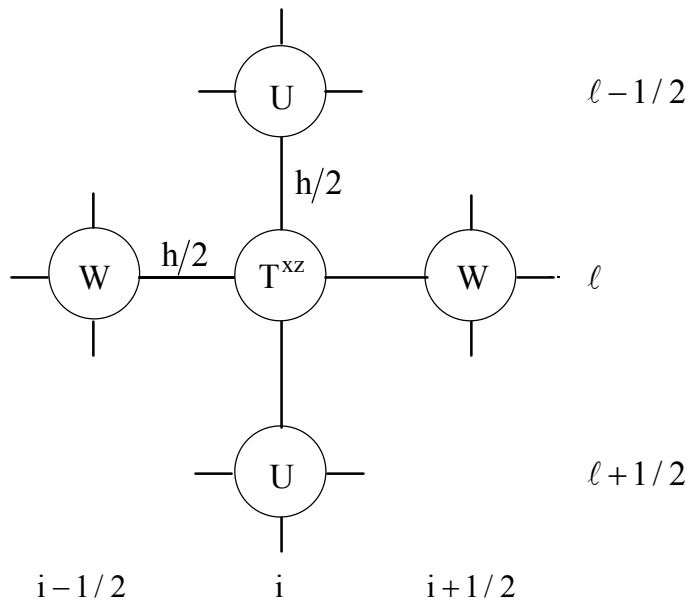


Fig. 4.1.2
Illustration of approximating W_x and U_z

The second time derivative, e.g., of the u -component, at the time level m and position $i \ell+1/2$ can be approximated by

$$\frac{1}{\Delta^2 t} \left(u_{i \ell+1/2}^{m+1} - 2u_{i \ell+1/2}^m + u_{i \ell+1/2}^{m-1} \right).$$

Then the finite-difference approximation of the equation for the u -component at the time level m and position $i \ell+1/2$ is

$$\begin{aligned} \rho_{i \ell+1/2} \frac{1}{\Delta^2 t} \left(U_{i \ell+1/2}^{m+1} - 2U_{i \ell+1/2}^m + U_{i \ell+1/2}^{m-1} \right) \\ = \frac{1}{h} \left(T_{i+1/2 \ell+1/2}^{xx,m} - T_{i-1/2 \ell+1/2}^{xx,m} + T_{i \ell+1}^{xz,m} - T_{i \ell}^{xz,m} \right) + F_{i \ell+1/2}^x, \end{aligned}$$

where $F_{i \ell+1/2}^x$ is a discrete approximation to $f_x(x_i, z_{\ell+1/2}, t_m)$.

Now we can write a complete **displacement-stress finite-difference scheme for the P-SV waves**:

$$\begin{aligned} U_{i \ell+1/2}^{m+1} &= 2U_{i \ell+1/2}^m - U_{i \ell+1/2}^{m-1} + (\Delta^2 t / \rho_{i \ell+1/2}) F_{i \ell+1/2}^{x,m} \\ &\quad + \frac{\Delta^2 t}{h} \frac{1}{\rho_{i \ell+1/2}} \left(T_{i+1/2 \ell+1/2}^{xx,m} - T_{i-1/2 \ell+1/2}^{xx,m} + T_{i \ell+1}^{xz,m} - T_{i \ell}^{xz,m} \right), \\ W_{i+1/2 \ell}^{m+1} &= 2W_{i+1/2 \ell}^m - W_{i+1/2 \ell}^{m-1} + (\Delta^2 t / \rho_{i+1/2 \ell}) F_{i+1/2 \ell}^{z,m} \\ &\quad + \frac{\Delta^2 t}{h} \frac{1}{\rho_{i+1/2 \ell}} \left(T_{i+1/2 \ell+1/2}^{zz,m} - T_{i+1/2 \ell-1/2}^{zz,m} + T_{i+1 \ell}^{xz,m} - T_{i \ell}^{xz,m} \right), \end{aligned} \tag{4.1.1}$$

$$\begin{aligned} T_{i+1/2 \ell+1/2}^{xx,m} &= \frac{1}{h} \left\{ [\lambda + 2\mu]_{i+1/2 \ell+1/2} \left(U_{i+1 \ell+1/2}^m - U_{i \ell+1/2}^m \right) \right. \\ &\quad \left. + \lambda_{i+1/2 \ell+1/2} \left(W_{i+1/2 \ell+1}^m - W_{i+1/2 \ell}^m \right) \right\}, \\ T_{i+1/2 \ell+1/2}^{zz,m} &= \frac{1}{h} \left\{ \lambda_{i+1/2 \ell+1/2} \left(U_{i+1 \ell+1/2}^m - U_{i \ell+1/2}^m \right) \right. \\ &\quad \left. + [\lambda + 2\mu]_{i+1/2 \ell+1/2} \left(W_{i+1/2 \ell+1}^m - W_{i+1/2 \ell}^m \right) \right\}, \\ T_{i \ell}^{xz,m} &= \frac{1}{h} \mu_{i \ell} \left(U_{i \ell+1/2}^m - U_{i \ell-1/2}^m + W_{i+1/2 \ell}^m - W_{i-1/2 \ell}^m \right). \end{aligned}$$

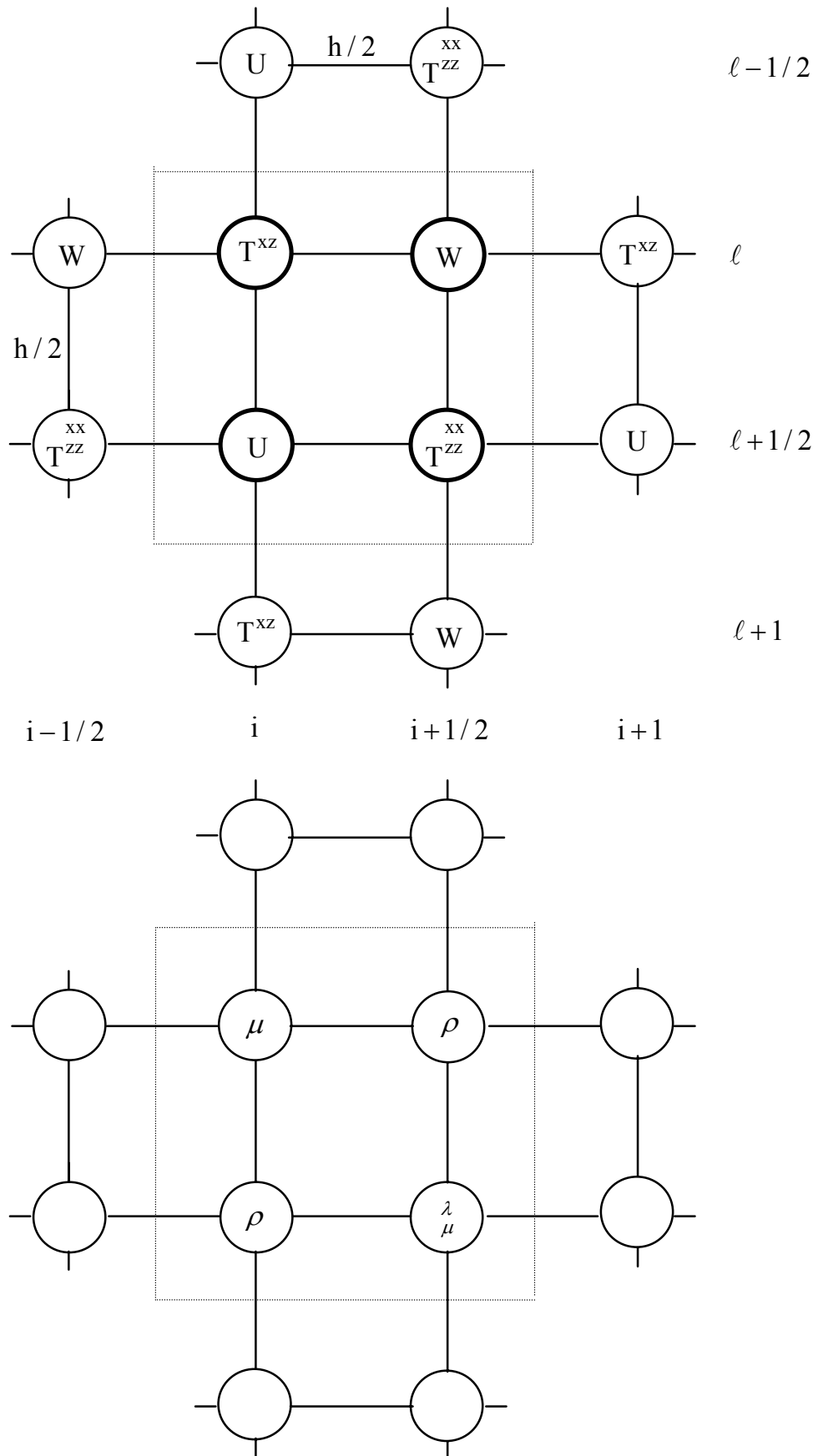


Fig. 4.1.3
 Field variables and material parameters entering the displacement-stress finite-difference scheme (4.1.1). A dashed line indicates a finite-difference cell $i\ell$.

Assuming medium in an equilibrium, i. e.,

$$\begin{aligned} \mathbf{u}(\mathbf{x}, z, t = 0) &= 0 & , & & \mathbf{u}_t(\mathbf{x}, z, t = 0) &= 0 & , \\ \mathbf{w}(\mathbf{x}, z, t = 0) &= 0 & , & & \mathbf{w}_t(\mathbf{x}, z, t = 0) &= 0 & , \end{aligned}$$

we can compute the first time level putting $U_{i\ell+1/2}^0 = W_{i+1/2\ell}^0 = 0$ and, formally, $U_{i\ell+1/2}^{-1} = W_{i+1/2\ell}^{-1} = 0$, in the scheme (4.1.1). We also assume $F_{i\ell+1/2}^{x,0} = 0$ and $F_{i+1/2\ell}^{y,0} = 0$.

In a computer code it is reasonable to consider integer values of grid indices. Let $\{ T_{i\ell}^{xz,m}, T_{i+1/2\ell+1/2}^{xx,m}, T_{i+1/2\ell+1/2}^{zz,m}, U_{i\ell+1/2}^m, W_{i+1/2\ell}^m \}$ be a **finite-difference cell** $i\ell$. Then we can rewrite the finite-difference scheme (4.1.1) with indices showing the actual grid position by the finite-difference scheme with the finite-difference cell indices. A rule for re-indexing is simple: 1. index having an integer value does not change, 2. $1/2$ has to be subtracted from an index which does not have an integer value.

$$\begin{aligned} U_{i\ell}^{m+1} &= 2U_{i\ell}^m - U_{i\ell}^{m-1} + (\Delta^2 t / \rho_{i\ell}) F_{i\ell}^{x,m} \\ &+ \frac{\Delta^2 t}{h} \frac{1}{\rho_{i\ell}} \left(T_{i\ell}^{xx,m} - T_{i-1\ell}^{xx,m} + T_{i\ell+1}^{xz,m} - T_{i\ell}^{xz,m} \right) , \\ W_{i\ell}^{m+1} &= 2W_{i\ell}^m - U_{i\ell}^{m-1} + (\Delta^2 t / \rho_{i\ell}) F_{i\ell}^{z,m} \\ &+ \frac{\Delta^2 t}{h} \frac{1}{\rho_{i\ell}} \left(T_{i\ell}^{zz,m} - T_{i\ell-1}^{zz,m} + T_{i+1\ell}^{xz,m} - T_{i\ell}^{xz,m} \right) , \end{aligned} \tag{4.1.2}$$

$$\begin{aligned} T_{i\ell}^{xx,m} &= \frac{1}{h} \{ [\lambda + 2\mu]_{i\ell} \left(U_{i+1\ell}^m - U_{i\ell}^m \right) \\ &+ \lambda_{i\ell} \left(W_{i\ell+1}^m - W_{i\ell}^m \right) \} , \end{aligned}$$

$$\begin{aligned} T_{i\ell}^{zz,m} &= \frac{1}{h} \{ \lambda_{i\ell} \left(U_{i+1\ell}^m - U_{i\ell}^m \right) \\ &+ [\lambda + 2\mu]_{i\ell} \left(W_{i\ell+1}^m - W_{i\ell}^m \right) \} , \end{aligned}$$

$$T_{i\ell}^{xz,m} = \frac{1}{h} \mu_{i\ell} \left(U_{i\ell}^m - U_{i\ell-1}^m + W_{i\ell}^m - W_{i-1\ell}^m \right) .$$

In the scheme we assumed a homogeneous medium inside the finite-difference cell. Scheme (4.1.2) is now ready for programming.

A **displacement-stress finite-difference scheme for the 3D case** with integer indices corresponding to the finite-difference cells is

$$\begin{aligned}
U_{i k \ell}^{m+1} &= 2U_{i k \ell}^m - U_{i k \ell}^{m-1} + (\Delta^2 t / \rho_{i k \ell}) F_{i k \ell}^{x,m} \\
&+ \frac{\Delta^2 t}{h} \frac{1}{\rho_{i k \ell}} \left(T_{i k \ell}^{xx,m} - T_{i-1 k \ell}^{xx,m} + T_{i k+1 \ell}^{xy,m} - T_{i k \ell}^{xy,m} + T_{i k \ell+1}^{xz,m} - T_{i k \ell}^{xz,m} \right) \\
V_{i k \ell}^{m+1} &= 2V_{i k \ell}^m - V_{i k \ell}^{m-1} + (\Delta^2 t / \rho_{i k \ell}) F_{i k \ell}^{y,m} \\
&+ \frac{\Delta^2 t}{h} \frac{1}{\rho_{i k \ell}} \left(T_{i+1 k \ell}^{xy,m} - T_{i k \ell}^{xy,m} + T_{i k \ell}^{yy,m} - T_{i k-1 \ell}^{yy,m} + T_{i k \ell+1}^{yz,m} - T_{i k \ell}^{yz,m} \right) \\
W_{i k \ell}^{m+1} &= 2W_{i k \ell}^m - W_{i k \ell}^{m-1} + (\Delta^2 t / \rho_{i k \ell}) F_{i k \ell}^{z,m} \\
&+ \frac{\Delta^2 t}{h} \frac{1}{\rho_{i k \ell}} \left(T_{i+1 k \ell}^{xz,m} - T_{i k \ell}^{xz,m} + T_{i k+1 \ell}^{yz,m} - T_{i k \ell}^{yz,m} + T_{i k \ell}^{zz,m} - T_{i k \ell-1}^{zz,m} \right)
\end{aligned} \tag{4.1.3}$$

$$\begin{aligned}
T_{i k \ell}^{xx,m} &= \\
&\frac{1}{h} \left[(\lambda + 2\mu)_{i k \ell} \left(U_{i+1 k \ell}^m - U_{i k \ell}^m \right) \right. \\
&\quad \left. + \lambda_{i k \ell} \left(V_{i k+1 \ell}^m - V_{i k \ell}^m + W_{i k \ell+1}^m - W_{i k \ell}^m \right) \right]
\end{aligned}$$

$$\begin{aligned}
T_{i k \ell}^{yy,m} &= \\
&\frac{1}{h} \left[\lambda_{i k \ell} \left(U_{i+1 k \ell}^m - U_{i k \ell}^m \right) \right. \\
&\quad + (\lambda + 2\mu)_{i k \ell} \left(V_{i k+1 \ell}^m - V_{i k \ell}^m \right) \\
&\quad \left. + \lambda_{i k \ell} \left(W_{i k \ell+1}^m - W_{i k \ell}^m \right) \right]
\end{aligned}$$

$$\begin{aligned}
T_{i k \ell}^{zz,m} &= \\
&\frac{1}{h} \left[\lambda_{i k \ell} \left(U_{i+1 k \ell}^m - U_{i k \ell}^m + V_{i k+1 \ell}^m - V_{i k \ell}^m \right) \right. \\
&\quad \left. + (\lambda + 2\mu)_{i k \ell} \left(W_{i k \ell+1}^m - W_{i k \ell}^m \right) \right]
\end{aligned}$$

$$T_{i k \ell}^{xy,m} = \frac{1}{h} \mu_{i k \ell} \left(U_{i k \ell}^m - U_{i k-1 \ell}^m + V_{i k \ell}^m - V_{i-1 k \ell}^m \right)$$

$$T_{i k \ell}^{xz,m} = \frac{1}{h} \mu_{i k \ell} \left(U_{i k \ell}^m - U_{i k \ell-1}^m + W_{i k \ell}^m - W_{i-1 k \ell}^m \right)$$

$$T_{i k \ell}^{yz,m} = \frac{1}{h} \mu_{i k \ell} \left(V_{i k \ell}^m - V_{i k \ell-1}^m + W_{i k \ell}^m - W_{i k-1 \ell}^m \right)$$

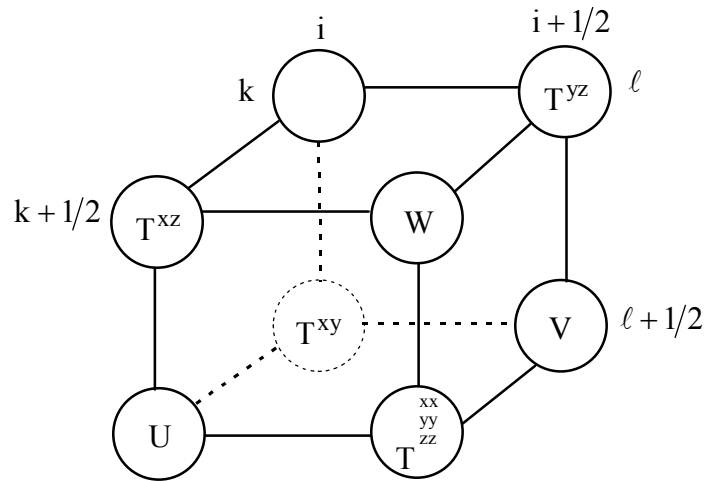


Fig. 4.1.4
Finite-difference cell corresponding to the finite-difference scheme (4.1.3).

More on the displacement-stress schemes can be found in Luo & Schuster (1990) and Ohminato & Chouet (1997).

4.2 VELOCITY-STRESS SCHEME ON A STAGGERED GRID

Recall equations (2.2.3)

$$\rho u_t = \tau_{xx,x} + \tau_{xz,z} + f_x$$

$$\rho w_t = \tau_{xz,x} + \tau_{zz,z} + f_z$$

$$\begin{aligned}
\tau_{xx,t} &= [\lambda + 2\mu] u_x + \lambda w_z \\
\tau_{zz,t} &= \lambda u_x + [\lambda + 2\mu] w_z \\
\tau_{xz,t} &= \mu (u_z + w_x)
\end{aligned}$$

As it is clear from the right-hand sides of the equations, the approximation of the first spatial derivatives may be the same as in the case of the displacement-stress formulation. The only difference comes from using particle velocity instead of displacement. Here we present, however, the finite-difference scheme assuming the alternative positions of the stress-tensor and particle-velocity components, see Fig. 4.2.1, which is consistent with the scheme presented recently by Graves (1996).

If we approximate time derivatives of the particle velocity at the time level m by a central-difference formula applied over the time step Δt , we have to approximate the time derivative of the stress-tensor at the time level $m + 1/2$. We obtain the following **velocity-stress finite-difference scheme for the P-SV waves**:

$$\begin{aligned}
U_{i+1/2 \ell}^{m+1/2} &= U_{i+1/2 \ell}^{m-1/2} + (\Delta t / \rho_{i+1/2 \ell}) F_{i+1/2 \ell}^{x,m} \\
&\quad + \frac{\Delta t}{h} \frac{1}{\rho_{i+1/2 \ell}} \left(T_{i+1 \ell}^{xx,m} - T_{i \ell}^{xx,m} + T_{i+1/2 \ell+1/2}^{xz,m} - T_{i+1/2 \ell-1/2}^{xz,m} \right), \\
W_{i \ell+1/2}^{m+1/2} &= W_{i \ell+1/2}^{m-1/2} + (\Delta t / \rho_{i \ell+1/2}) F_{i \ell+1/2}^{z,m} \\
&\quad + \frac{\Delta t}{h} \frac{1}{\rho_{i \ell+1/2}} \left(T_{i \ell+1}^{zz,m} - T_{i \ell}^{zz,m} + T_{i+1/2 \ell+1/2}^{xz,m} - T_{i-1/2 \ell+1/2}^{xz,m} \right),
\end{aligned} \tag{4.2.1}$$

$$\begin{aligned}
T_{i \ell}^{xx,m+1} &= T_{i \ell}^{xx,m} + \frac{\Delta t}{h} \left\{ [\lambda + 2\mu]_{i \ell} \left(U_{i+1/2 \ell}^{m+1/2} - U_{i-1/2 \ell}^{m+1/2} \right) \right. \\
&\quad \left. + \lambda_{i \ell} \left(W_{i \ell+1/2}^{m+1/2} - W_{i \ell-1/2}^{m+1/2} \right) \right\},
\end{aligned}$$

$$\begin{aligned}
T_{i \ell}^{zz,m+1} &= T_{i \ell}^{zz,m} + \frac{\Delta t}{h} \left\{ \lambda_{i \ell} \left(U_{i+1/2 \ell}^{m+1/2} - U_{i-1/2 \ell}^{m+1/2} \right) \right. \\
&\quad \left. + [\lambda + 2\mu]_{i \ell} \left(W_{i \ell+1/2}^{m+1/2} - W_{i \ell-1/2}^{m+1/2} \right) \right\},
\end{aligned}$$

$$\begin{aligned}
T_{i+1/2 \ell+1/2}^{xz,m+1} &= T_{i+1/2 \ell+1/2}^{xz,m} + \frac{\Delta t}{h} \mu_{i+1/2 \ell+1/2} \left\{ U_{i+1/2 \ell+1}^{m+1/2} - U_{i+1/2 \ell}^{m+1/2} \right. \\
&\quad \left. + W_{i+1 \ell+1/2}^{m+1/2} - W_{i \ell+1/2}^{m+1/2} \right\}.
\end{aligned}$$

U and W stand for discrete approximations of the x- and z-components of the particle velocity, i. e., u and w , respectively.

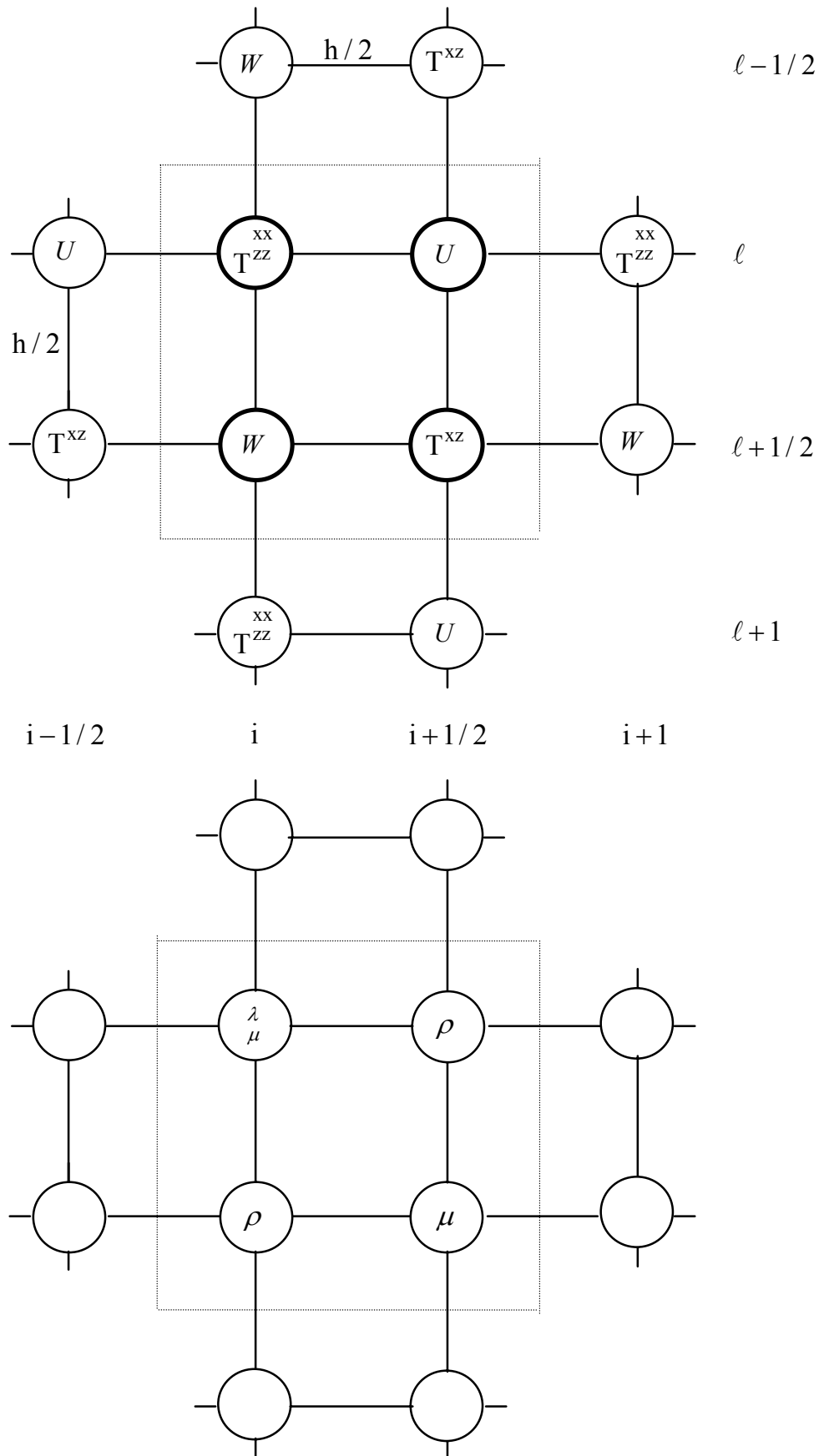


Fig. 4.2.1
Field variables and material parameters entering the velocity-stress finite-difference scheme (4.2.1). A dashed line indicates a finite difference cell i^l .

Scheme (4.2.1) can be rewritten by replacing indices corresponding to the actual grid positions with indices corresponding to the finite-difference cells. We can use the same rule to determine spatial indices as in the case of the displacement-stress scheme. In order to determine the time index we add 1/2 to those indices which are non-integer in the scheme (4.2.1).

$$\begin{aligned}
U_{i\ell}^{m+1} &= U_{i\ell}^m + (\Delta t/\rho_{i\ell}) F_{i\ell}^{x,m} \\
&\quad + \frac{\Delta t}{h} \frac{1}{\rho_{i\ell}} \left(T_{i+1\ell}^{xx,m} - T_{i\ell}^{xx,m} + T_{i\ell}^{xz,m} - T_{i-1\ell}^{xz,m} \right), \\
W_{i\ell}^{m+1} &= W_{i\ell}^m + (\Delta t/\rho_{i\ell}) F_{i\ell}^{z,m} \\
&\quad + \frac{\Delta t}{h} \frac{1}{\rho_{i\ell}} \left(T_{i\ell+1}^{zz,m} - T_{i\ell}^{zz,m} + T_{i\ell}^{xz,m} - T_{i-1\ell}^{xz,m} \right),
\end{aligned} \tag{4.2.2}$$

$$\begin{aligned}
T_{i\ell}^{xx,m+1} &= T_{i\ell}^{xx,m} + \frac{\Delta t}{h} \left\{ [\lambda + 2\mu]_{i\ell} \left(U_{i\ell}^{m+1} - U_{i-1\ell}^{m+1} \right) \right. \\
&\quad \left. + \lambda_{i\ell} \left(W_{i\ell}^{m+1} - W_{i-1\ell}^{m+1} \right) \right\},
\end{aligned}$$

$$\begin{aligned}
T_{i\ell}^{zz,m+1} &= T_{i\ell}^{zz,m} + \frac{\Delta t}{h} \left\{ \lambda_{i\ell} \left(U_{i\ell}^{m+1} - U_{i-1\ell}^{m+1} \right) \right. \\
&\quad \left. + [\lambda + 2\mu]_{i\ell} \left(W_{i\ell}^{m+1} - W_{i-1\ell}^{m+1} \right) \right\},
\end{aligned}$$

$$\begin{aligned}
T_{i\ell}^{xz,m+1} &= T_{i\ell}^{xz,m} + \frac{\Delta t}{h} \mu_{i\ell} \left\{ U_{i\ell+1}^{m+1} - U_{i\ell}^{m+1} \right. \\
&\quad \left. + W_{i+1\ell}^{m+1} - W_{i\ell}^{m+1} \right\}.
\end{aligned}$$

Properties of the velocity-stress scheme and results of the numerical tests can be found in the paper by Virieux (1986).

4.3 DISPLACEMENT SCHEME ON A CONVENTIONAL GRID

Recall equations (2.2.2):

$$\begin{aligned}
\rho u_{tt} &= \\
& \left([\lambda + 2\mu] u_x \right)_x + \left(\mu u_z \right)_z + \left(\lambda w_z \right)_x + \left(\mu w_x \right)_z + f_x,
\end{aligned}$$

$$\begin{aligned}
\rho w_{tt} &= \\
& \left(\mu w_x \right)_x + \left([\lambda + 2\mu] w_z \right)_z + \left(\mu u_z \right)_x + \left(\lambda u_x \right)_z + f_z.
\end{aligned}$$

We have to find a finite-difference approximation of the mixed and nonmixed second spatial derivatives, e. g.,

$$(a \Psi_x)_x = \frac{\partial}{\partial x} \left(a(x, z) \frac{\partial \Psi(x, z)}{\partial x} \right)$$

and

$$(a \Psi_x)_z = \frac{\partial}{\partial z} \left(a(x, z) \frac{\partial \Psi(x, z)}{\partial x} \right) .$$

First, let us derive an approximation of the nonmixed derivative. Define an auxiliary function Φ :

$$\Phi = a \Psi_x \quad , \quad \Phi_x = (a \Psi_x)_x . \quad (4.3.1)$$

Approximate Φ_x at the point $i\ell$:

$$\Phi_x|_{i\ell} \doteq \frac{1}{h} (\Phi_{i+1/2\ell} - \Phi_{i-1/2\ell}) . \quad (4.3.2)$$

Find now approximations of $\Phi_{i+1/2\ell}$ and $\Phi_{i-1/2\ell}$. From equation (4.3.1) we have

$$\frac{\Phi}{a} = \Psi_x . \quad (4.3.3)$$

Integrate equation (4.3.3) along the grid leg between the points $i\ell$ and $i+1\ell$:

$$\int_{x_i}^{x_{i+1}} \frac{\Phi(x, z_\ell)}{a(x, z_\ell)} dx = \int_{x_i}^{x_{i+1}} \Psi_x(x, z_\ell) dx .$$

Denoting the left- and right-hand side of the equation by L and R, respectively, we can obtain

$$\begin{aligned} R &= \Psi_{i+1\ell} - \Psi_{i\ell} , \\ L &\doteq \Phi_{i+1/2\ell} \int_{x_i}^{x_{i+1}} \frac{dx}{a(x, z_\ell)} . \end{aligned}$$

In the approximation of the left-hand side we assumed that the mean value is in the position $x_{i+1/2\ell}$. Define a so-called **effective medium parameter**

$$a_{i\ell}^x = h \left[\int_{x_i}^{x_{i+1}} \frac{dx}{a(x, z_\ell)} \right]^{-1} . \quad (4.3.4)$$

Then

$$L \doteq \frac{h}{a_{i\ell}^x} \Phi_{i+1/2\ell}$$

and

$$\Phi_{i+1/2\ell} \doteq \frac{1}{h} a_{i\ell}^x (\Psi_{i+1\ell} - \Psi_{i\ell}) . \quad (4.3.5a)$$

Similarly,

$$\Phi_{i-1/2\ell} \doteq \frac{1}{h} a_{i-1\ell}^x (\Psi_{i\ell} - \Psi_{i-1\ell}) . \quad (4.3.5b)$$

Substituting approximations (4.3.5) and (4.3.2) into (4.3.1) we get

$$(a\Psi_x)_x|_{i\ell} \doteq \frac{1}{h^2} \{ a_{i\ell}^x (\Psi_{i+1\ell} - \Psi_{i\ell}) - a_{i-1\ell}^x (\Psi_{i\ell} - \Psi_{i-1\ell}) \} . \quad (4.3.6a)$$

Analogously we can obtain

$$(a\Psi_z)_z|_{i\ell} \doteq \frac{1}{h^2} \{ a_{i\ell}^z (\Psi_{i\ell+1} - \Psi_{i\ell}) - a_{i\ell-1}^z (\Psi_{i\ell} - \Psi_{i\ell-1}) \} . \quad (4.3.6b)$$

where

$$a_{i\ell}^z = h \left[\int_{z_\ell}^{z_{\ell+1}} \frac{dz}{a(x_i, z)} \right]^{-1} . \quad (4.3.7)$$

Let us derive now an approximation of the mixed derivative. We will follow the derivation suggested by Zahradník (1995b). Define again an auxiliary function Φ

$$\Phi = a\Psi_x \quad , \quad \Phi_z = (a\Psi_x)_z . \quad (4.3.8)$$

Then

$$\Phi_z|_{i\ell} \doteq \frac{1}{h} (\Phi_{i\ell+1/2} - \Phi_{i\ell-1/2}) . \quad (4.3.9)$$

Find approximations of $\Phi_{i\ell+1/2}$ and $\Phi_{i\ell-1/2}$. From equation (4.3.8) we have

$$\frac{\Phi}{a} = \Psi_x . \quad (4.3.10)$$

Integrate equation (4.3.10) along the grid leg between the points $i\ell$ and $i\ell+1$:

$$\int_{z_\ell}^{z_{\ell+1}} \frac{\Phi(x_i, z)}{a(x_i, z)} dz = \int_{z_\ell}^{z_{\ell+1}} \Psi_x(x_i, z) dz .$$

$$L \doteq \frac{h}{a_{i\ell}^z} \Phi_{i\ell+1/2} \quad , \quad R \doteq h\Psi_x|_{i\ell+1/2} ,$$

$$\begin{aligned}
\Psi_x|_{i \ell+1/2} &\doteq \frac{1}{2h} (\Psi_{i+1 \ell+1/2} - \Psi_{i-1 \ell+1/2}), \\
\Psi_{i+1 \ell+1/2} &\doteq \frac{1}{2} (\Psi_{i+1 \ell+1} + \Psi_{i+1 \ell}), \\
\Psi_{i-1 \ell+1/2} &\doteq \frac{1}{2} (\Psi_{i-1 \ell+1} + \Psi_{i-1 \ell}), \\
R &\doteq \frac{1}{4} (\Psi_{i+1 \ell+1} - \Psi_{i-1 \ell+1} + \Psi_{i+1 \ell} - \Psi_{i-1 \ell}), \\
\Phi_{i \ell+1/2} &\doteq \frac{1}{4h} a_{i \ell}^z (\Psi_{i+1 \ell+1} - \Psi_{i-1 \ell+1} + \Psi_{i+1 \ell} - \Psi_{i-1 \ell}). \quad (4.3.11a)
\end{aligned}$$

Similarly we can obtain

$$\Phi_{i \ell-1/2} \doteq \frac{1}{4h} a_{i \ell-1}^z (\Psi_{i+1 \ell} - \Psi_{i-1 \ell} + \Psi_{i+1 \ell-1} - \Psi_{i-1 \ell-1}). \quad (4.3.11b)$$

Substituting approximations (4.3.11) and (4.3.9) into (4.3.8) we obtain

$$\begin{aligned}
(a \Psi_x)_z|_{i \ell} &\doteq \frac{1}{4h^2} \{ a_{i \ell}^z (\Psi_{i+1 \ell+1} - \Psi_{i-1 \ell+1} + \Psi_{i+1 \ell} - \Psi_{i-1 \ell}) \\
&\quad - a_{i \ell-1}^z (\Psi_{i+1 \ell} - \Psi_{i-1 \ell} + \Psi_{i+1 \ell-1} - \Psi_{i-1 \ell-1}) \}. \quad (4.3.12a)
\end{aligned}$$

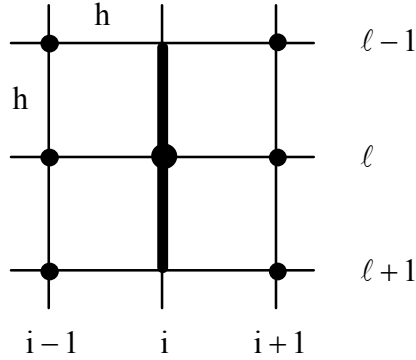


Fig. 4.3.1

Illustration of approximation (4.3.12a). Full circles indicate values of Ψ entering the finite-difference formula. Two heavy grid legs indicate effective media parameters.

Applying the $z \rightarrow x$, $x \rightarrow z$, $i \rightarrow \ell$, $\ell \rightarrow i$ substitutions in the equation (4.3.12a) we get

$$\begin{aligned}
(a \Psi_z)_x|_{i \ell} &\doteq \frac{1}{4h^2} \{ a_{i \ell}^x (\Psi_{i+1 \ell+1} - \Psi_{i+1 \ell-1} + \Psi_{i \ell+1} - \Psi_{i \ell-1}) \\
&\quad - a_{i-1 \ell}^x (\Psi_{i \ell+1} - \Psi_{i \ell-1} + \Psi_{i-1 \ell+1} - \Psi_{i-1 \ell-1}) \}. \quad (4.3.12b)
\end{aligned}$$

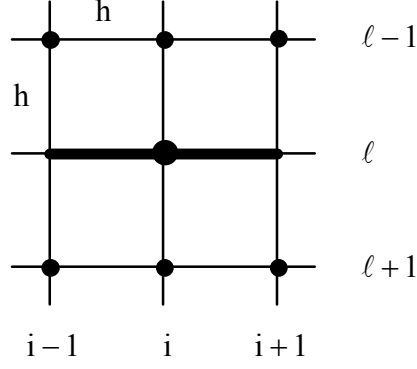


Fig. 4.3.2
Illustration of approximation (4.3.12b). The meaning of symbols is the same as in Fig. 4.3.1.

Applying approximations (4.3.6) and (4.3.12) to the nonmixed and mixed spatial derivatives in the equations of motion (2.2.2) and applying the same approximation of the second time derivative as in the displacement-stress scheme we obtain the following **displacement finite-difference scheme for the P-SV waves**:

$$\begin{aligned}
 U_{i\ell}^{m+1} &= 2U_{i\ell}^m - U_{i\ell}^{m-1} + (\Delta^2 t / \rho_{i\ell}) F_{i\ell}^{x,m} \\
 &+ \frac{\Delta^2 t}{\rho_{i\ell}} \{ L_{xx}(\lambda + 2\mu, U) + L_{zz}(\mu, U) + L_{zx}(\lambda, W) + L_{xz}(\mu, W) \}, \\
 W_{i\ell}^{m+1} &= 2W_{i\ell}^m - W_{i\ell}^{m-1} + (\Delta^2 t / \rho_{i\ell}) F_{i\ell}^{z,m} \\
 &+ \frac{\Delta^2 t}{\rho_{i\ell}} \{ L_{xx}(\mu, W) + L_{zz}(\lambda + 2\mu, W) + L_{zx}(\mu, U) + L_{xz}(\lambda, U) \},
 \end{aligned} \tag{4.3.13}$$

$$L_{xx}(a, \Psi) = \frac{1}{h^2} \{ a_{i\ell}^x (\Psi_{i+1\ell}^m - \Psi_{i\ell}^m) - a_{i-1\ell}^x (\Psi_{i\ell}^m - \Psi_{i-1\ell}^m) \},$$

$$L_{zz}(a, \Psi) = \frac{1}{h^2} \{ a_{i\ell}^z (\Psi_{i\ell+1}^m - \Psi_{i\ell}^m) - a_{i\ell-1}^z (\Psi_{i\ell}^m - \Psi_{i\ell-1}^m) \},$$

$$\begin{aligned}
 L_{zx}(a, \Psi) &= \frac{1}{4h^2} \{ a_{i\ell}^x (\Psi_{i+1\ell+1}^m - \Psi_{i+1\ell-1}^m + \Psi_{i\ell+1}^m - \Psi_{i\ell-1}^m) \\
 &- a_{i-1\ell}^x (\Psi_{i\ell+1}^m - \Psi_{i\ell-1}^m + \Psi_{i-1\ell+1}^m - \Psi_{i-1\ell-1}^m) \},
 \end{aligned}$$

$$\begin{aligned}
 L_{xz}(a, \Psi) &= \frac{1}{4h^2} \{ a_{i\ell}^z (\Psi_{i+1\ell+1}^m - \Psi_{i-1\ell+1}^m + \Psi_{i+1\ell}^m - \Psi_{i-1\ell}^m) \\
 &- a_{i\ell-1}^z (\Psi_{i+1\ell}^m - \Psi_{i-1\ell}^m + \Psi_{i+1\ell-1}^m - \Psi_{i-1\ell-1}^m) \},
 \end{aligned}$$

$$a_{i\ell}^x = h \left[\int_{x_i}^{x_{i+1}} \frac{dx}{a(x, z_\ell)} \right]^{-1}, \quad a_{i\ell}^z = h \left[\int_{z_\ell}^{z_{\ell+1}} \frac{dz}{a(x_i, z)} \right]^{-1}.$$

The theoretical investigation of consistency at the material discontinuities, including the flat free surface, (Zahradník, 1995b and Zahradník & Priolo, 1995) and numerical tests (the two above papers and Moczo et al., 1997) suggest that the scheme (4.3.13) is one of the most accurate finite-difference schemes.

5. FOURTH-ORDER FINITE-DIFFERENCE SCHEMES FOR INTERIOR GRID POINTS

While in Chapter 4 we only used the second-order approximation of the spatial derivatives, here we will make use of more accurate fourth-order approximation. Its approximation error (local truncation error) is considerably smaller than that of the second-order since it is proportional to the h^4 . Consequently, the fourth-order finite-difference schemes allow to reduce a spatial sampling of the wavelength which is to be propagated without grid dispersion. While the second-order schemes require at least 10 samples per wavelength, the fourth-order schemes only require 5 samples.

5.1 FOURTH-ORDER FINITE-DIFFERENCE APPROXIMATIONS

Let us find a fourth-order approximation of the derivative Ψ_x . Taylor's expansions for $\Psi(x+h/2)$ and $\Psi(x-h/2)$ are

$$\Psi(x + \frac{1}{2}h) = \Psi(x) + \frac{1}{2}h\Psi'(x) + \frac{1}{8}h^2\Psi''(x) + \frac{1}{48}h^3\Psi'''(x) + \dots, \quad (5.1.1)$$

and

$$\Psi(x - \frac{1}{2}h) = \Psi(x) - \frac{1}{2}h\Psi'(x) + \frac{1}{8}h^2\Psi''(x) - \frac{1}{48}h^3\Psi'''(x) + \dots. \quad (5.1.2)$$

Subtracting expansion (5.1.2) from (5.1.1) we get

$$\Psi(x + \frac{1}{2}h) - \Psi(x - \frac{1}{2}h) = h\Psi'(x) + \frac{1}{24}h^3\Psi'''(x) + O(h^5). \quad (5.1.3)$$

In order to remove the Ψ''' -term we need an independent approximation of Ψ' which includes the Ψ''' -term. This can be obtained from Taylor's expansions for, e.g., $\Psi(x+3h/2)$ and $\Psi(x-3h/2)$,

$$\Psi(x + \frac{3}{2}h) = \Psi(x) + \frac{3}{2}h\Psi'(x) + \frac{9}{8}h^2\Psi''(x) + \frac{9}{16}h^3\Psi'''(x) + \dots \quad (5.1.4)$$

and

$$\Psi(x - \frac{3}{2}h) = \Psi(x) - \frac{3}{2}h\Psi'(x) + \frac{9}{8}h^2\Psi''(x) - \frac{9}{16}h^3\Psi'''(x) + \dots. \quad (5.1.5)$$

Subtracting expansion (5.1.5) from (5.1.4) we get

$$\Psi\left(x + \frac{3}{2}h\right) - \Psi\left(x - \frac{3}{2}h\right) = 3h\Psi'(x) + \frac{9}{8}h^3\Psi'''(x) + O(h^5). \quad (5.1.6)$$

Multiplying equation (5.1.3) by $9/8$ and subtracting equation (5.1.6) multiplied by $1/24$ we obtain

$$\Psi'(x) = \frac{1}{h} \left\{ -\frac{1}{24} \left[\Psi\left(x + \frac{3}{2}h\right) - \Psi\left(x - \frac{3}{2}h\right) \right] + \frac{9}{8} \left[\Psi\left(x + \frac{1}{2}h\right) - \Psi\left(x - \frac{1}{2}h\right) \right] \right\} + O(h^4). \quad (5.1.7)$$

Let $x = x_i$. Then $x + \frac{3}{2}h = x_{i+3/2}$, $x - \frac{3}{2}h = x_{i-3/2}$,
 $x + \frac{1}{2}h = x_{i+1/2}$, $x - \frac{1}{2}h = x_{i-1/2}$.

Then the approximation (5.1.7) can be written as

$$\Psi_x|_i \doteq \frac{1}{h} \left\{ -\frac{1}{24} [\Psi_{i+3/2} - \Psi_{i-3/2}] + \frac{9}{8} [\Psi_{i+1/2} - \Psi_{i-1/2}] \right\}. \quad (5.1.8)$$

Let $x = x_{i+1/2}$. Then $x + \frac{3}{2}h = x_{i+2}$, $x - \frac{3}{2}h = x_{i-1}$,
 $x + \frac{1}{2}h = x_{i+1}$, $x - \frac{1}{2}h = x_i$.

Then the approximation (5.1.7) can be written as

$$\Psi_x|_{i+1/2} \doteq \frac{1}{h} \left\{ -\frac{1}{24} [\Psi_{i+2} - \Psi_{i-1}] + \frac{9}{8} [\Psi_{i+1} - \Psi_i] \right\}. \quad (5.1.9)$$

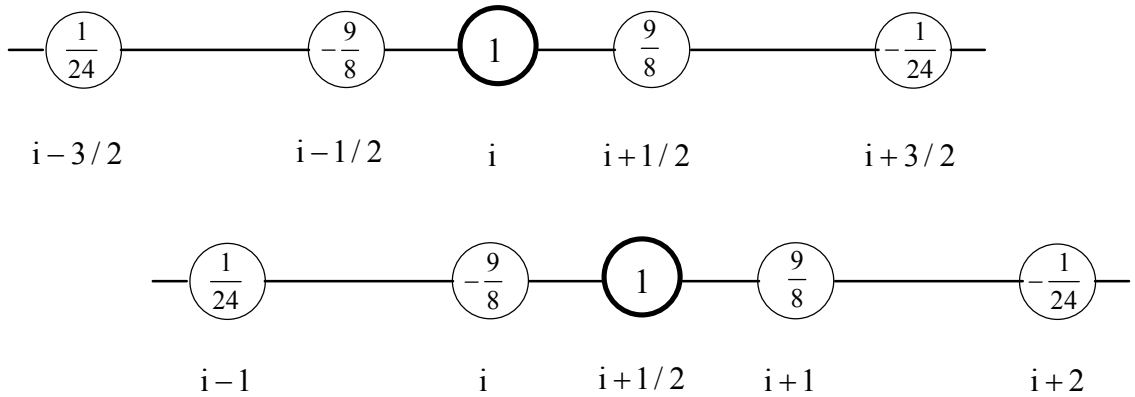


Fig. 5.1.1
 Illustration of approximations (5.1.8) and (5.1.9)

5.2 DISPLACEMENT-STRESS SCHEME ON A STAGGERED GRID

Approximations (5.1.8) and (5.1.9) can be used to construct a fourth-order finite-difference scheme on a staggered grid to solve equations (2.2.1). Keeping a second-order approximation of the time derivative we get a **fourth-order displacement-stress finite-difference scheme for the P-SV waves**:

$$\begin{aligned}
 U_{i\ell+1/2}^{m+1} &= 2U_{i\ell+1/2}^m - U_{i\ell+1/2}^{m-1} + (\Delta^2 t / \rho_{i\ell+1/2}) F_{i\ell+1/2}^{x,m} \\
 &+ \frac{\Delta^2 t}{h} \frac{1}{\rho_{i\ell+1/2}} \left\{ A \left(T_{i+3/2\ell+1/2}^{xx,m} - T_{i-3/2\ell+1/2}^{xx,m} + T_{i\ell+2}^{xz,m} - T_{i\ell-1}^{xz,m} \right) \right. \\
 &\quad \left. + B \left(T_{i+1/2\ell+1/2}^{xx,m} - T_{i-1/2\ell+1/2}^{xx,m} + T_{i\ell+1}^{xz,m} - T_{i\ell}^{xz,m} \right) \right\} \\
 W_{i+1/2\ell}^{m+1} &= 2W_{i+1/2\ell}^m - W_{i+1/2\ell}^{m-1} + (\Delta^2 t / \rho_{i+1/2\ell}) F_{i+1/2\ell}^{z,m} \\
 &+ \frac{\Delta^2 t}{h} \frac{1}{\rho_{i+1/2\ell}} \left\{ A \left(T_{i+1/2\ell+3/2}^{zz,m} - T_{i+1/2\ell-3/2}^{zz,m} + T_{i+2\ell}^{xz,m} - T_{i-1\ell}^{xz,m} \right) \right. \\
 &\quad \left. + B \left(T_{i+1/2\ell+1/2}^{zz,m} - T_{i+1/2\ell-1/2}^{zz,m} + T_{i+1\ell}^{xz,m} - T_{i\ell}^{xz,m} \right) \right\}
 \end{aligned} \tag{5.2.1}$$

$$\begin{aligned}
 T_{i+1/2\ell+1/2}^{xx,m} &= \frac{1}{h} \left\{ (\lambda + 2\mu)_{i+1/2\ell+1/2} \left[A \left(U_{i+2\ell+1/2}^m - U_{i-1\ell+1/2}^m \right) \right. \right. \\
 &\quad \left. \left. + B \left(U_{i+1\ell+1/2}^m - U_{i\ell+1/2}^m \right) \right] \right. \\
 &+ \lambda_{i+1/2\ell+1/2} \left[A \left(W_{i+1/2\ell+2}^m - W_{i+1/2\ell-1}^m \right) \right. \\
 &\quad \left. \left. + B \left(W_{i+1/2\ell+1}^m - W_{i+1/2\ell}^m \right) \right] \right\}
 \end{aligned}$$

$$\begin{aligned}
 T_{i+1/2\ell+1/2}^{zz,m} &= \frac{1}{h} \left\{ \lambda_{i+1/2\ell+1/2} \left[A \left(U_{i+2\ell+1/2}^m - U_{i-1\ell+1/2}^m \right) \right. \right. \\
 &\quad \left. \left. + B \left(U_{i+1\ell+1/2}^m - U_{i\ell+1/2}^m \right) \right] \right. \\
 &+ (\lambda + 2\mu)_{i+1/2\ell+1/2} \left[A \left(W_{i+1/2\ell+2}^m - W_{i+1/2\ell-1}^m \right) \right. \\
 &\quad \left. \left. + B \left(W_{i+1/2\ell+1}^m - W_{i+1/2\ell}^m \right) \right] \right\}
 \end{aligned}$$

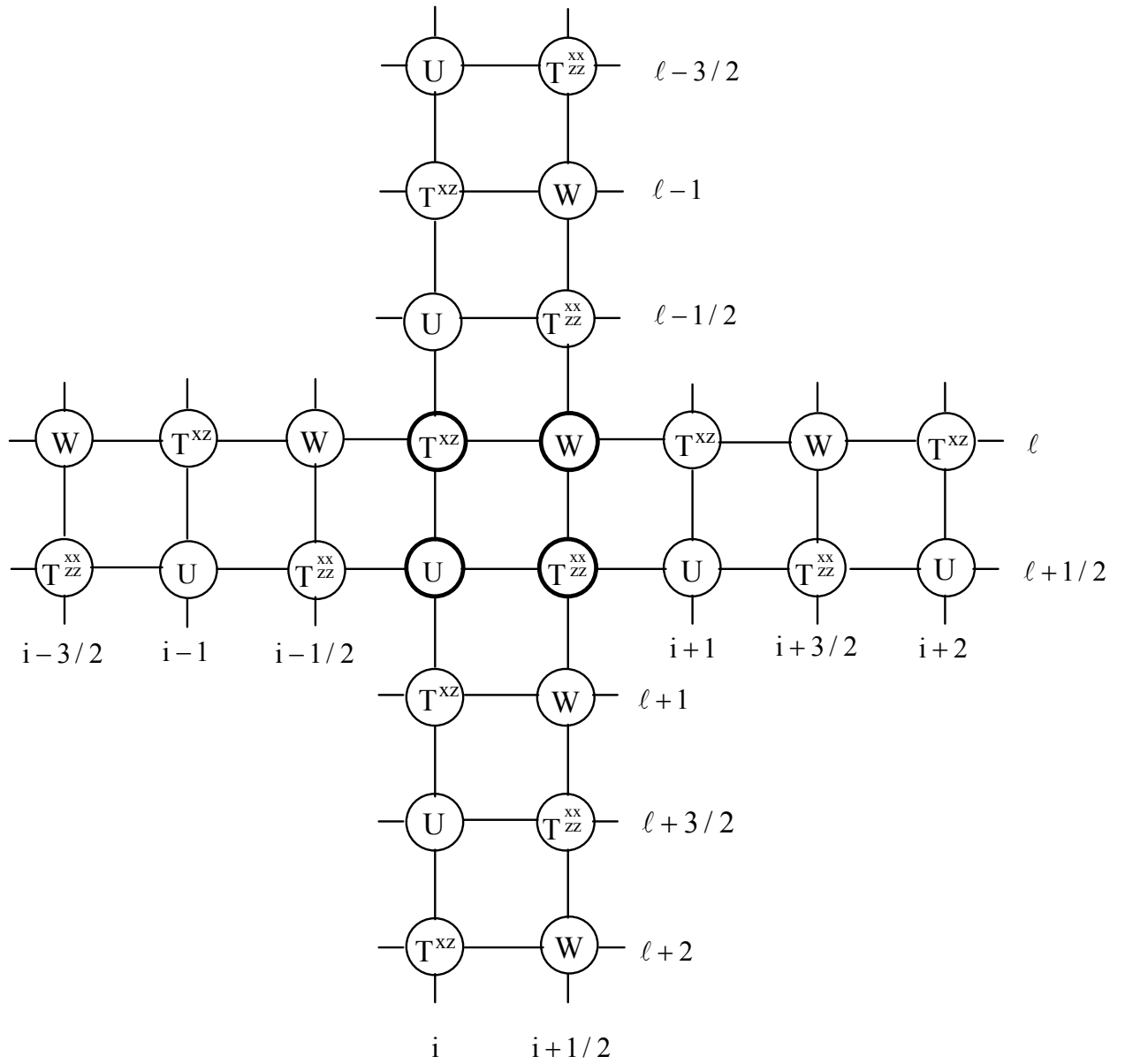


Fig. 5.2.1
Field variables entering the fourth-order displacement-stress finite-difference scheme (5.2.1)

$$\begin{aligned} T_{i\ell}^{xz,m} &= \frac{1}{h} \mu_{i\ell} \left\{ A \left(U_{i\ell+3/2}^m - U_{i\ell-3/2}^m + W_{i+3/2\ell}^m - W_{i-3/2\ell}^m \right) \right. \\ &\quad \left. + B \left(U_{i\ell+1/2}^m - U_{i\ell-1/2}^m + W_{i+1/2\ell}^m - W_{i-1/2\ell}^m \right) \right\} \end{aligned}$$

$$A = -\frac{1}{24}, \quad B = \frac{9}{8}$$

It is easy to obtain a **fourth-order displacement-stress finite-difference scheme for the 3D case**. Here is a scheme with integer indices corresponding to the finite-difference cells (similarly as in schemes 4.1.2 and 4.1.3).

$$\begin{aligned} U_{ik\ell}^{m+1} &= 2U_{ik\ell}^m - U_{ik\ell}^{m-1} + (\Delta^2 t / \rho_{ik\ell}^u) F_{ik\ell}^{x,m} \\ &\quad + \frac{\Delta^2 t}{h} \frac{1}{\rho_{ik\ell}^u} \left[A \left(T_{i+1k\ell}^{xx,m} - T_{i-2k\ell}^{xx,m} \right) + B \left(T_{ik\ell}^{xx,m} - T_{i-1k\ell}^{xx,m} \right) \right. \\ &\quad \left. + A \left(T_{ik+2\ell}^{xy,m} - T_{ik-1\ell}^{xy,m} \right) + B \left(T_{ik+1\ell}^{xy,m} - T_{ik\ell}^{xy,m} \right) \right. \\ &\quad \left. + A \left(T_{ik\ell+2}^{xz,m} - T_{ik\ell-1}^{xz,m} \right) + B \left(T_{ik\ell+1}^{xz,m} - T_{ik\ell}^{xz,m} \right) \right] \end{aligned}$$

$$\begin{aligned} V_{ik\ell}^{m+1} &= 2V_{ik\ell}^m - V_{ik\ell}^{m-1} + (\Delta^2 t / \rho_{ik\ell}^v) F_{ik\ell}^{y,m} \\ &\quad + \frac{\Delta^2 t}{h} \frac{1}{\rho_{ik\ell}^v} \left[A \left(T_{i+2k\ell}^{xy,m} - T_{i-1k\ell}^{xy,m} \right) + B \left(T_{i+1k\ell}^{xy,m} - T_{ik\ell}^{xy,m} \right) \right. \\ &\quad \left. + A \left(T_{ik+1\ell}^{yy,m} - T_{ik-2\ell}^{yy,m} \right) + B \left(T_{ik\ell}^{yy,m} - T_{i-1k\ell}^{yy,m} \right) \right. \\ &\quad \left. + A \left(T_{ik\ell+2}^{yz,m} - T_{ik\ell-1}^{yz,m} \right) + B \left(T_{ik\ell+1}^{yz,m} - T_{ik\ell}^{yz,m} \right) \right] \end{aligned}$$

(5.2.2)

$$\begin{aligned} W_{ik\ell}^{m+1} &= 2W_{ik\ell}^m - W_{ik\ell}^{m-1} + (\Delta^2 t / \rho_{ik\ell}^w) F_{ik\ell}^{z,m} \\ &\quad + \frac{\Delta^2 t}{h} \frac{1}{\rho_{ik\ell}^w} \left[A \left(T_{i+2k\ell}^{xz,m} - T_{i-1k\ell}^{xz,m} \right) + B \left(T_{i+1k\ell}^{xz,m} - T_{ik\ell}^{xz,m} \right) \right. \\ &\quad \left. + A \left(T_{ik+2\ell}^{yz,m} - T_{ik-1\ell}^{yz,m} \right) + B \left(T_{ik+1\ell}^{yz,m} - T_{ik\ell}^{yz,m} \right) \right. \\ &\quad \left. + A \left(T_{ik\ell+1}^{zz,m} - T_{ik\ell-2}^{zz,m} \right) + B \left(T_{ik\ell}^{zz,m} - T_{ik\ell-1}^{zz,m} \right) \right] \end{aligned}$$

$$\begin{aligned}
T_{i k \ell}^{xx,m} = & \\
& \frac{1}{h} \{ (\lambda + 2\mu)_{i k \ell} [A (U_{i+2 k \ell}^m - U_{i-1 k \ell}^m) + B (U_{i+1 k \ell}^m - U_{i k \ell}^m)] \\
& + \lambda_{i k \ell} [A (V_{i k+2 \ell}^m - V_{i k-1 \ell}^m) + B (V_{i k+1 \ell}^m - V_{i k \ell}^m) \\
& + A (W_{i k \ell+2}^m - W_{i k \ell-1}^m) + B (W_{i k \ell+1}^m - W_{i k \ell}^m)] \}
\end{aligned}$$

$$\begin{aligned}
T_{i k \ell}^{yy,m} = & \\
& \frac{1}{h} \{ \lambda_{i k \ell} [A (U_{i+2 k \ell}^m - U_{i-1 k \ell}^m) + B (U_{i+1 k \ell}^m - U_{i k \ell}^m)] \\
& + (\lambda + 2\mu)_{i k \ell} [A (V_{i k+2 \ell}^m - V_{i k-1 \ell}^m) + B (V_{i k+1 \ell}^m - V_{i k \ell}^m)] \\
& + \lambda_{i k \ell} [A (W_{i k \ell+2}^m - W_{i k \ell-1}^m) + B (W_{i k \ell+1}^m - W_{i k \ell}^m)] \}
\end{aligned}$$

$$\begin{aligned}
T_{i k \ell}^{zz,m} = & \\
& \frac{1}{h} \{ \lambda_{i k \ell} [A (U_{i+2 k \ell}^m - U_{i-1 k \ell}^m) + B (U_{i+1 k \ell}^m - U_{i k \ell}^m) \\
& + A (V_{i k+2 \ell}^m - V_{i k-1 \ell}^m) + B (V_{i k+1 \ell}^m - V_{i k \ell}^m)] \\
& + (\lambda + 2\mu)_{i k \ell} [A (W_{i k \ell+2}^m - W_{i k \ell-1}^m) + B (W_{i k \ell+1}^m - W_{i k \ell}^m)] \}
\end{aligned}$$

$$\begin{aligned}
T_{i k \ell}^{xy,m} = & \\
& \frac{1}{h} \mu_{i k \ell}^{xy} [A (U_{i k+1 \ell}^m - U_{i k-2 \ell}^m) + B (U_{i k \ell}^m - U_{i k-1 \ell}^m) \\
& + A (V_{i+1 k \ell}^m - V_{i-2 k \ell}^m) + B (V_{i k \ell}^m - V_{i-1 k \ell}^m)]
\end{aligned}$$

$$\begin{aligned}
T_{i k \ell}^{xz,m} = & \\
& \frac{1}{h} \mu_{i k \ell}^{xz} [A (U_{i k \ell+1}^m - U_{i k \ell-2}^m) + B (U_{i k \ell}^m - U_{i k \ell-1}^m) \\
& + A (W_{i+1 k \ell}^m - W_{i-2 k \ell}^m) + B (W_{i k \ell}^m - W_{i-1 k \ell}^m)]
\end{aligned}$$

$$\begin{aligned}
T_{ik\ell}^{yz,m} &= \\
\frac{1}{h} \mu_{ik\ell}^{yz} &[A (V_{ik\ell+1}^m - V_{ik\ell-2}^m) + B (V_{ik\ell}^m - V_{ik\ell-1}^m) \\
&+ A (W_{ik+1\ell}^m - W_{ik-2\ell}^m) + B (W_{ik\ell}^m - W_{ik-1\ell}^m)] \\
A &= -\frac{1}{24} , \quad B = \frac{9}{8} .
\end{aligned}$$

5.3 VELOCITY-STRESS SCHEME ON A STAGGERED GRID

We also easily obtain the **fourth-order velocity-stress finite-difference scheme for the P-SV waves**. Again, as in the case of the second-order velocity-stress scheme, the positions of the field variables are different from those in the displacement-stress scheme (5.2.1).

$$\begin{aligned}
U_{i+1/2 \ell}^{m+1/2} &= U_{i+1/2 \ell}^{m-1/2} + (\Delta t / \rho_{i+1/2 \ell}) F_{i+1/2 \ell}^{x,m} \\
&+ \frac{\Delta t}{h} \frac{1}{\rho_{i+1/2 \ell}} \left\{ A \left(T_{i+2 \ell}^{xx,m} - T_{i-1 \ell}^{xx,m} + T_{i+1/2 \ell+3/2}^{xz,m} - T_{i+1/2 \ell-3/2}^{xz,m} \right) \right. \\
&\quad \left. + B \left(T_{i+1 \ell}^{xx,m} - T_{i \ell}^{xx,m} + T_{i+1/2 \ell+1/2}^{xz,m} - T_{i+1/2 \ell-1/2}^{xz,m} \right) \right\} \\
W_{i \ell+1/2}^{m+1/2} &= W_{i \ell+1/2}^{m-1/2} + (\Delta t / \rho_{i \ell+1/2}) F_{i \ell+1/2}^{z,m} \\
&+ \frac{\Delta t}{h} \frac{1}{\rho_{i \ell+1/2}} \left\{ A \left(T_{i \ell+2}^{zz,m} - T_{i \ell-1}^{zz,m} + T_{i+3/2 \ell+1/2}^{xz,m} - T_{i-3/2 \ell+1/2}^{xz,m} \right) \right. \\
&\quad \left. + B \left(T_{i \ell+1}^{zz,m} - T_{i \ell}^{zz,m} + T_{i+1/2 \ell+1/2}^{xz,m} - T_{i-1/2 \ell+1/2}^{xz,m} \right) \right\}
\end{aligned} \tag{5.3.1}$$

$$\begin{aligned}
T_{i \ell}^{xx,m+1} &= T_{i \ell}^{xx,m} \\
&+ \frac{\Delta t}{h} \left\{ (\lambda + 2\mu)_{i \ell} \left[A \left(U_{i+3/2 \ell}^{m+1/2} - U_{i-3/2 \ell}^{m+1/2} \right) + B \left(U_{i+1/2 \ell}^{m+1/2} - U_{i-1/2 \ell}^{m+1/2} \right) \right] \right. \\
&\quad \left. + \lambda_{i \ell} \left[A \left(W_{i \ell+3/2}^{m+1/2} - W_{i \ell-3/2}^{m+1/2} \right) + B \left(W_{i \ell+1/2}^{m+1/2} - W_{i \ell-1/2}^{m+1/2} \right) \right] \right\}
\end{aligned}$$

$$\begin{aligned}
T_{i \ell}^{zz,m+1} &= T_{i \ell}^{zz,m} \\
&+ \frac{\Delta t}{h} \left\{ \lambda_{i \ell} \left[A \left(U_{i+3/2 \ell}^{m+1/2} - U_{i-3/2 \ell}^{m+1/2} \right) + B \left(U_{i+1/2 \ell}^{m+1/2} - U_{i-1/2 \ell}^{m+1/2} \right) \right] \right. \\
&\quad \left. + (\lambda + 2\mu)_{i \ell} \left[A \left(W_{i \ell+3/2}^{m+1/2} - W_{i \ell-3/2}^{m+1/2} \right) + B \left(W_{i \ell+1/2}^{m+1/2} - W_{i \ell-1/2}^{m+1/2} \right) \right] \right\}
\end{aligned}$$

$$\begin{aligned}
T_{i+1/2 \ell+1/2}^{xz,m+1} &= T_{i+1/2 \ell+1/2}^{xz,m} \\
&+ \frac{\Delta t}{h} \mu_{i+1/2 \ell+1/2} \left\{ A \left(U_{i+1/2 \ell+2}^{m+1/2} - U_{i+1/2 \ell-1}^{m+1/2} + W_{i+2 \ell+1/2}^{m+1/2} - W_{i-1 \ell+1/2}^{m+1/2} \right) \right. \\
&\quad \left. + B \left(U_{i+1/2 \ell+1}^{m+1/2} - U_{i+1/2 \ell}^{m+1/2} + W_{i+1 \ell+1/2}^{m+1/2} - W_{i \ell+1/2}^{m+1/2} \right) \right\}
\end{aligned}$$

$$A = -\frac{1}{24}, \quad B = \frac{9}{8}.$$

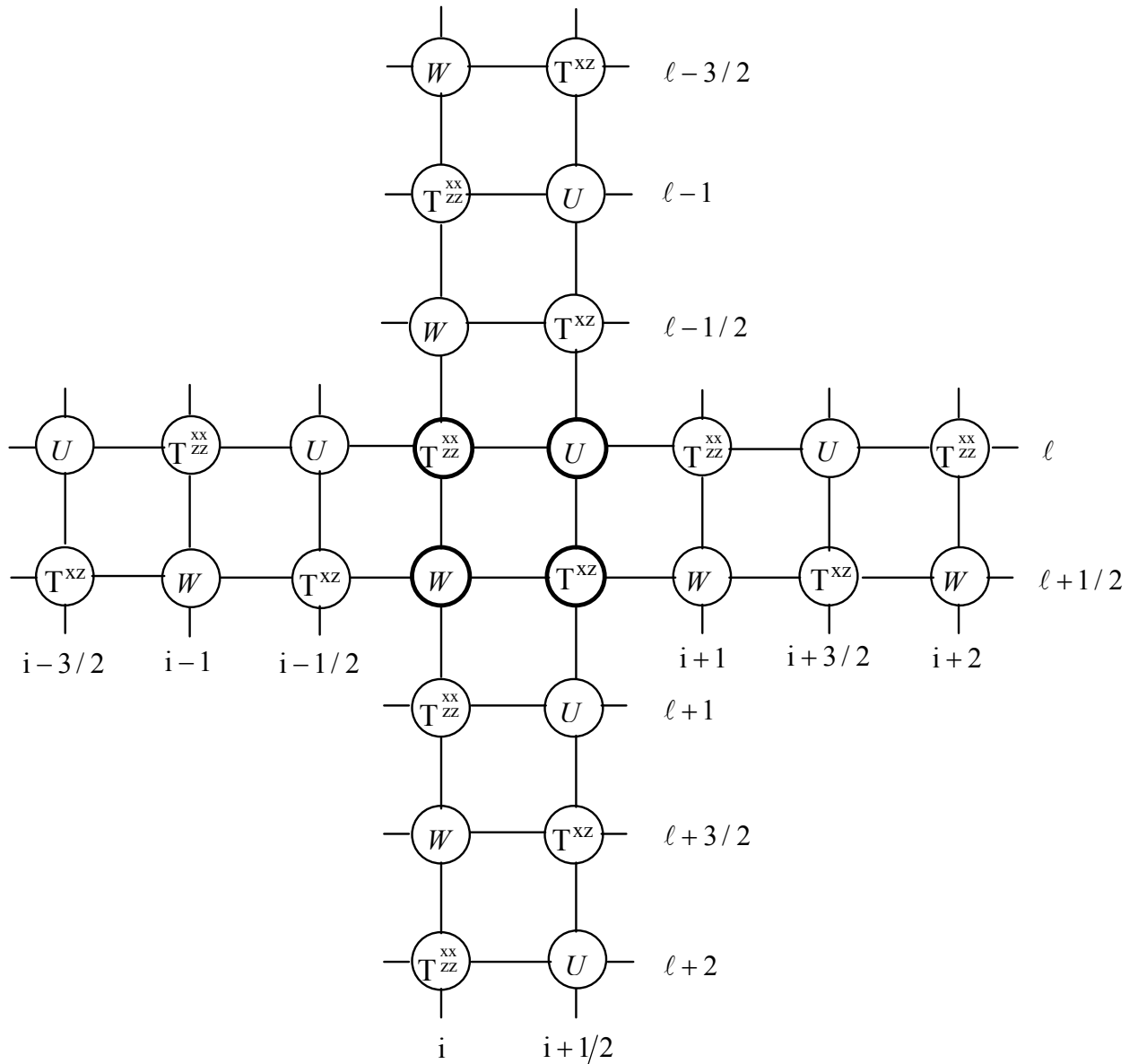


Fig. 5.3.1
Field variables entering the fourth-order velocity-stress finite-difference scheme (5.3.1).

Properties of the fourth-order scheme for the P-SV waves and results of the numerical tests are presented in the paper by Levander (1988).

Similarly as in the case of the displacement-stress scheme, it is easy to obtain a scheme for the 3D case. Graves (1996) presented such a scheme together with a very efficient algorithm of the memory optimization.

6. FINITE-DIFFERENCE SCHEMES FOR INTERIOR POINTS ON IRREGULAR RECTANGULAR GRIDS

Consider a rectangular spatial grid with varying size of grid spacings in both the x- and z- directions (see Fig. 6.1) with $\Delta x_i = x_i - x_{i-1}$ and $\Delta z_\ell = z_\ell - z_{\ell-1}$.

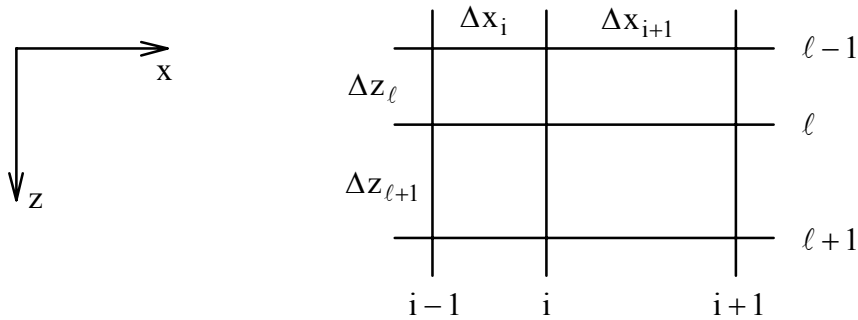


Fig. 6.1
Rectangular grid with varying grid spacings

The rectangular grid with a varying size of the grid spacings was first used by Boore (1970) in the 1D case. Mikumo & Miyatake (1987) used such a grid in the 3D case in a homogeneous medium. Moczo (1989) and Moczo & Bard (1993) applied the grid to the SH case in the laterally inhomogeneous medium.

The above mentioned schemes were based on the displacement formulation. Since the use of such a grid can be useful in the displacement-stress and velocity-stress formulations, we will briefly present an example of the displacement-stress scheme.

6.1 FINITE-DIFFERENCE APPROXIMATIONS ON AN IRREGULAR GRID

Consider for simplicity Taylor's expansion for $\Psi(x + h_+)$ and $\Psi(x - h_-)$:

$$\Psi(x + h_+) = \Psi(x) + h_+ \Psi'(x) + \frac{1}{2} h_+^2 \Psi''(x) + \frac{1}{6} h_+^3 \Psi'''(x) + \dots, \quad (6.1.1)$$

$$\Psi(x - h_-) = \Psi(x) - h_- \Psi'(x) + \frac{1}{2} h_-^2 \Psi''(x) - \frac{1}{6} h_-^3 \Psi'''(x) + \dots. \quad (6.1.2)$$

Subtracting expansion (6.1.2) from (6.1.1) we get

$$\begin{aligned}\Psi(x + h_+) - \Psi(x - h_-) &= (h_+ + h_-)\Psi'(x) + \frac{1}{2}(h_+^2 - h_-^2)\Psi''(x) + \\ &\quad + \frac{1}{6}(h_+^3 + h_-^3)\Psi'''(x) + \dots\end{aligned}$$

and

$$\begin{aligned}\Psi''(x) &= \frac{1}{h_+ + h_-} [\Psi(x + h_+) - \Psi(x - h_-)] - \frac{1}{2}(h_+ - h_-)\Psi''(x) - \\ &\quad - \frac{1}{6}(h_+^2 - h_+h_- + h_-^2)\Psi'''(x) - \dots ,\end{aligned}$$

i. e.,

$$\Psi''(x) = \frac{1}{h_+ + h_-} [\Psi(x + h_+) - \Psi(x - h_-)] + O(h_+ - h_-) ,$$

from which we have an approximation

$$\Psi''(x) \doteq \frac{1}{h_+ + h_-} [\Psi(x + h_+) - \Psi(x - h_-)] . \quad (6.1.3)$$

The approximation is only first-order accurate. The leading term of the approximation error is proportional to $h_+ - h_-$. It is obvious that the smaller the difference in sizes of h_+ and h_- , the better accuracy and the closer to the second-order approximation.

There is an approximation of the first derivative that is second-order accurate and over distance $h_+ + h_-$,

$$\Psi'(x) = \frac{1}{h_+ + h_-} \left\{ \frac{h_-}{h_+} [\Psi(x + h_+) - \Psi(x)] + \frac{h_+}{h_-} [\Psi(x) - \Psi(x - h_-)] \right\} ,$$

however, it also requires the value in the same position in which the derivative is to be approximated, which is not the case on the staggered grid.

In the case of the staggered grid we need to approximate spatial derivatives, e.g., in the x -direction, in two different positions – x_i and $x_{i+1/2}$. As it is illustrated in Fig. 6.1.1, while $x_{i+1/2}$ is at the center of the grid spacing Δx_{i+1} , x_i is not equally distant from grid positions $x_{i-1/2}$ and $x_{i+1/2}$. We will look at the consequences now:

Let $x = x_i$. Then

$$\begin{aligned}h_+ &= \frac{1}{2} \Delta x_{i+1} \quad , \quad h_- = \frac{1}{2} \Delta x_i \quad , \\ h_+ + h_- &= \frac{1}{2} (\Delta x_{i+1} + \Delta x_i) \quad , \quad h_+ - h_- = \frac{1}{2} (\Delta x_{i+1} - \Delta x_i) \quad , \\ \Psi(x) &= \Psi_i \quad , \quad \Psi(x + h_+) = \Psi_{i+1/2} \quad , \quad \Psi(x - h_-) = \Psi_{i-1/2} \quad ,\end{aligned}$$

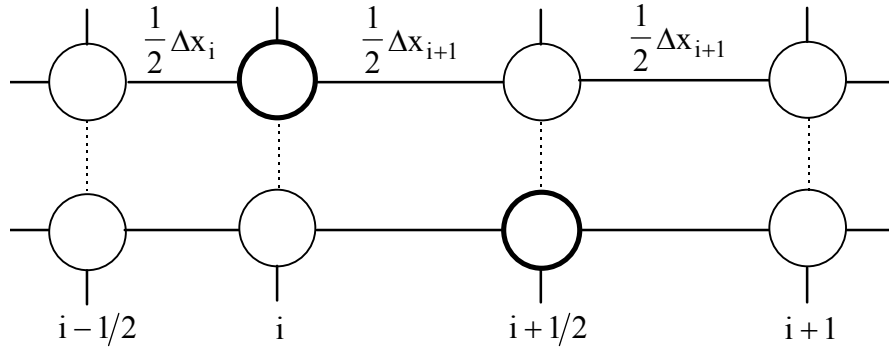


Fig. 6.1.1
Two positions on a staggered grid in which spatial derivatives are to be approximated

and from (6.1.3) we obtain

$$\Psi_x(x_i) = \frac{2}{\Delta x_{i+1} + \Delta x_i} (\Psi_{i+1/2} - \Psi_{i-1/2}) + O(\Delta x_{i+1} - \Delta x_i). \quad (6.1.4)$$

Now, let $x = x_i + \frac{1}{2} \Delta x_{i+1} = x_{i+1/2}$. Then

$$\begin{aligned} h_+ = h_- &= \frac{1}{2} \Delta x_{i+1}, \\ h_+ + h_- &= \Delta x_{i+1}, \quad h_+ - h_- = 0, \\ \Psi(x) &= \Psi_{i+1/2}, \quad \Psi(x+h_+) = \Psi_{i+1}, \quad \Psi(x-h_-) = \Psi_i, \end{aligned}$$

and from (6.1.3) we obtain

$$\Psi_x(x_{i+1/2}) = \frac{1}{\Delta x_{i+1}} (\Psi_{i+1} - \Psi_i) + O(\Delta^2 x_{i+1}). \quad (6.1.5)$$

While $\Psi_x(x_i)$ is approximated by (6.1.4) with the first-order accuracy (the leading term of the approximation error is proportional to $\Delta x_{i+1} - \Delta x_i$), $\Psi_x(x_{i+1/2})$ is approximated by (6.1.5) with the second-order accuracy (the leading term of the approximation error is proportional to $\Delta^2 x_{i+1}$).

It is clear then that in the displacement-stress and velocity-stress schemes on an irregular staggered grid all spatial derivatives are not approximated with the same order of accuracy. We can choose one of two possibilities for each of the spatial derivatives:

x-derivative	2nd-order at $i+1/2$ position	1st-order at i position
1st choice	T^{xz}, U	T^{xx}, T^{zz}, W
2nd choice	T^{xx}, T^{zz}, W	T^{xz}, U
z-derivative	2nd-order at $\ell+1/2$ position	1st-order at ℓ position
1st choice	T^{xz}, W	T^{xx}, T^{zz}, U
2nd choice	T^{xx}, T^{zz}, U	T^{xz}, W

6.2 DISPLACEMENT-STRESS SCHEME ON AN IRREGULAR GRID

Let us apply approximations (6.1.4) and (6.1.5) to equations (2.2.1) on the grid shown in Fig. 6.2.1. We obtain a **displacement-stress finite-difference scheme on the staggered grid with varying grid spacings for the P-SV waves**:

$$\begin{aligned}
 U_{i\ell+1/2}^{m+1} &= 2U_{i\ell+1/2}^m - U_{i\ell+1/2}^{m-1} + (\Delta^2 t / \rho_{i\ell+1/2}) F_{i\ell+1/2}^{x,m} \\
 &+ \frac{\Delta^2 t}{\rho_{i\ell+1/2}} \left\{ \frac{2}{\Delta x_i + \Delta x_{i+1}} \left(T_{i+1/2\ell+1/2}^{xx,m} - T_{i-1/2\ell+1/2}^{xx,m} \right) \right. \\
 &\quad \left. + \frac{1}{\Delta z_{\ell+1}} \left(T_{i\ell+1}^{xz,m} - T_{i\ell}^{xz,m} \right) \right\} \\
 W_{i+1/2\ell}^{m+1} &= 2W_{i+1/2\ell}^m - W_{i+1/2\ell}^{m-1} + (\Delta^2 t / \rho_{i+1/2\ell}) F_{i+1/2\ell}^{z,m} \\
 &+ \frac{\Delta^2 t}{\rho_{i+1/2\ell}} \left\{ \frac{2}{\Delta z_\ell + \Delta z_{\ell+1}} \left(T_{i+1/2\ell+1/2}^{zz,m} - T_{i+1/2\ell-1/2}^{zz,m} \right) \right. \\
 &\quad \left. + \frac{1}{\Delta x_{i+1}} \left(T_{i+1\ell}^{xz,m} - T_{i\ell}^{xz,m} \right) \right\}
 \end{aligned} \tag{6.2.1}$$

$$\begin{aligned}
 T_{i+1/2\ell+1/2}^{xx,m} &= [\lambda + 2\mu]_{i+1/2\ell+1/2} \frac{1}{\Delta x_{i+1}} \left(U_{i+1\ell+1/2}^m - U_{i\ell+1/2}^m \right) \\
 &+ \lambda_{i+1/2\ell+1/2} \frac{1}{\Delta z_{\ell+1}} \left(W_{i+1/2\ell+1}^m - W_{i+1/2\ell}^m \right)
 \end{aligned}$$

$$\begin{aligned}
 T_{i+1/2\ell+1/2}^{zz,m} &= \lambda_{i+1/2\ell+1/2} \frac{1}{\Delta x_{i+1}} \left(U_{i+1\ell+1/2}^m - U_{i\ell+1/2}^m \right) \\
 &+ [\lambda + 2\mu]_{i+1/2\ell+1/2} \frac{1}{\Delta z_{\ell+1}} \left(W_{i+1/2\ell+1}^m - W_{i+1/2\ell}^m \right)
 \end{aligned}$$

$$\begin{aligned}
 T_{i\ell}^{xz,m} &= \mu_{i\ell} \left\{ \frac{2}{\Delta z_\ell + \Delta z_{\ell+1}} \left(U_{i\ell+1/2}^m - U_{i\ell-1/2}^m \right) \right. \\
 &\quad \left. + \frac{2}{\Delta x_i + \Delta x_{i+1}} \left(W_{i+1/2\ell}^m - W_{i-1/2\ell}^m \right) \right\}
 \end{aligned}$$

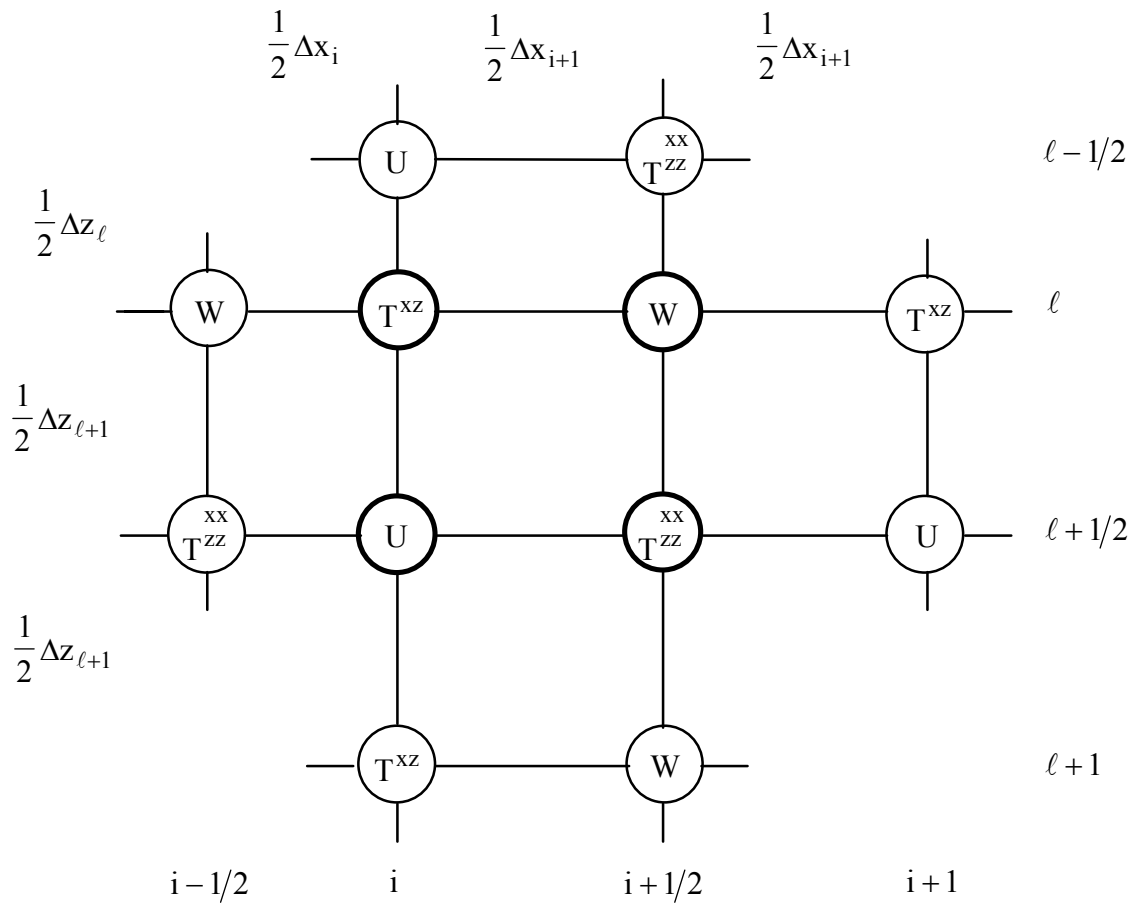


Fig. 6.2.1
Field variables entering the displacement-stress finite-difference scheme (6.2.1).

7. FINITE-DIFFERENCE SCHEMES FOR INTERIOR POINTS ON A COMBINED RECTANGULAR GRID

In many cases a model of a medium comprises near-surface inhomogeneities with lower velocities and a homogeneous bottom part with a higher velocity. If the upper part of the model with a minimum velocity, say β , is covered by a grid with a grid spacing h , then,

according to the sampling criterion, a grid with a larger grid spacing, $h' = h \frac{\beta'}{\beta}$, is suffi-

cient for the bottom part of the medium with velocity β' .

A grid with a varying size of a grid spacing (see Chapter 6) is one possibility to follow the above idea. Here we present a very simple but efficient approach using a combined rectangular grid.

Consider a combined $h \times h$ and $2h \times 2h$ grid as it is shown in Fig. 7.1. We will, furthermore, restrict ourselves to the case of the SH waves and the displacement formulation. As it is clear from Fig. 7.1, there are two types of the grid points at the contact of the grids, say A and B. We can anticipate that the two types require different finite-difference formulae.

Assume now that the $h \times h$ grid covers the upper inhomogeneous part of the medium while the contact of the two grids and the $2h \times 2h$ grid are in the homogeneous medium.

Recall equation (2.3.2) for the SH waves in an inhomogeneous medium,

$$\rho v_{tt} = (\mu v_x)_x + (\mu v_z)_z + f_y$$

and equation (2.4.3) for a homogeneous medium,

$$\rho v_{tt} = \mu v_{xx} + \mu v_{zz} + f_y,$$

which can be written as

$$\rho v_{tt} = \mu (v_{xx} + v_{zz}) + f_y.$$

It is easy to replace the above equations by the displacement finite-difference schemes for the interior grid points of both $h \times h$ and $2h \times 2h$ grids. A finite-difference scheme for the inhomogeneous medium on the $h \times h$ grid can be obtained using a standard second-order approximation (1.1.5) to the second time derivative and using approximations (4.3.6) to spatial derivatives. A finite-difference scheme for a homogeneous medium on the $2h \times 2h$ grid can be obtained applying approximation (1.1.5) to the second time and spatial derivatives. For the inhomogeneous medium and $h \times h$ grid we obtain

$$V_{i\ell}^{m+1} = 2V_{i\ell}^m - V_{i\ell}^{m-1} + \frac{\Delta^2 t}{\rho_{i\ell}} F_{i\ell}^{y,m} + \frac{\Delta^2 t}{\rho_{i\ell}} [L_{xx}(\mu, V) + L_{zz}(\mu, V)] \quad (7.1)$$

$$L_{xx}(\mu, V) = \frac{1}{h^2} [\mu_{i\ell}^x (V_{i+1\ell}^m - V_{i\ell}^m) - \mu_{i-1\ell}^x (V_{i\ell}^m - V_{i-1\ell}^m)] \quad (7.2)$$

$$L_{zz}(\mu, V) = \frac{1}{h^2} [\mu_{i\ell}^z (V_{i\ell+1}^m - V_{i\ell}^m) - \mu_{i\ell-1}^z (V_{i\ell}^m - V_{i\ell-1}^m)]$$

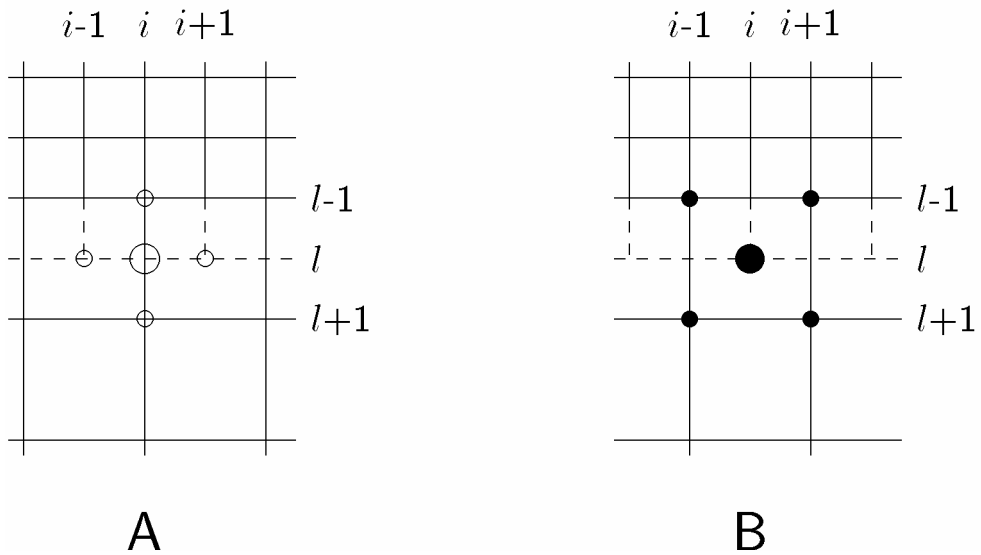
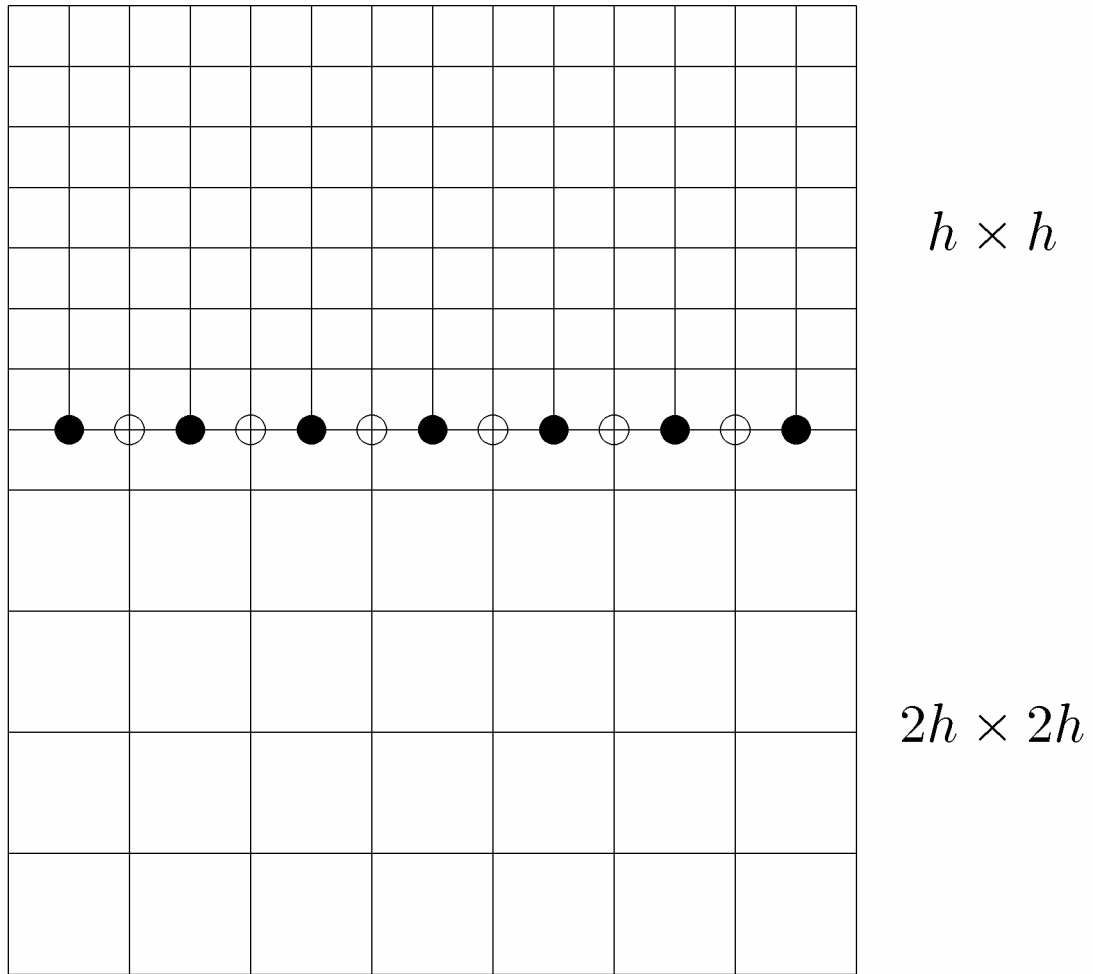


Fig. 7.1
 Combined rectangular grid. There are two types of the grid points at the contact of the $h \times h$ and $2h \times 2h$ grids — A (open circles) and B (full circles).

where $\mu_{i\ell}^x$ and $\mu_{i\ell}^z$ are defined by equations (4.3.4) and (4.3.7).

For the homogeneous medium and the $2h \times 2h$ grid scheme the equation (7.1) can be used with the operators

$$L_{xx}(\mu, V) = \frac{\mu}{4h^2} (V_{i+2\ell}^m - 2V_{i\ell}^m + V_{i-2\ell}^m)$$

and (7.3)

$$L_{zz}(\mu, V) = \frac{\mu}{4h^2} (V_{i\ell+1}^m - 2V_{i\ell}^m + V_{i\ell-1}^m).$$

Note different indexing in the operators which is due to the fact that each even grid column of the finer grid is cut off at the contact of the two grids.

It is clear that for the A-type grid point scheme the equation (7.1) can be used with the operators

$$L_{xx}(\mu, V) = \frac{\mu}{h^2} (V_{i+1\ell}^m - 2V_{i\ell}^m + V_{i-1\ell}^m)$$

and (7.4)

$$L_{zz}(\mu, V) = \frac{\mu}{h^2} (V_{i\ell+1}^m - 2V_{i\ell}^m + V_{i\ell-1}^m).$$

For the B-type grid point we cannot use operators (7.4) since there is no value in the $i\ell + 1$ position available (see Fig. 7.1). We have two possibilities. One is to approximate the missing value by a linear interpolation. This, however, would decrease the order of approximation. The other possibility is to find a second-order approximation of the sum of the two derivatives, i.e., $v_{xx} + v_{zz}$, using four available values at the $i - 1\ell - 1$, $i + 1\ell - 1$, $i - 1\ell + 1$ and $i + 1\ell + 1$ grid points (see Fig. 7.1). Note that we do not mean the sum of two approximations given by the equations (7.4).

From the combination of Taylor's expansions at the four grid points we can easily obtain the second order approximation

$$\begin{aligned} (v_{xx} + v_{zz})|_{i\ell} &= \frac{1}{2h^2} (v_{i+1\ell+1} + v_{i-1\ell+1} + v_{i+1\ell-1} + v_{i-1\ell-1} - 4v_{i\ell}) \\ &\quad - \frac{h^2}{12} (v_{xxxx} + 6v_{xxzz} + v_{zzzz}) + \dots \end{aligned}$$

Then the corresponding operator $L_{xx,zz}(V)$ is

$$L_{xx,zz}(V) = \frac{1}{2h^2} (V_{i+1\ell+1}^m + V_{i-1\ell+1}^m + V_{i+1\ell-1}^m + V_{i-1\ell-1}^m - 4V_{i\ell}^m).$$

Replacing $L_{xx}(\mu, V) + L_{zz}(\mu, V)$ by $\mu L_{xx,zz}(V)$ in scheme (7.1) we obtain the finite-difference scheme for the B-type grid point.

Although we combine the $h \times h$ and $2h \times 2h$ grids, the use of a combined grid is not restricted to the case when the velocity in the bottom homogeneous medium, β' , is twice

or more larger than the minimum velocity in the inhomogeneous medium β . The combined grid can be used even in the case of $1 < \beta'/\beta < 2$. It is just necessary to apply the sampling criterion in the homogeneous basement first in order to determine the grid spacing of the $2h \times 2h$ grid.

A numerical application can be found in Moczo et al. (1996) where the above algorithm enabled to save up to 75% of grid points.

For a more complex case of modeling the P-SV waves by the velocity-stress finite-difference scheme on a combined rectangular grid with a varying size of the grid spacings see Jastram & Tessmer (1994) and Falk et al. (1996).

8. STABILITY CONDITION AND DISPERSION RELATIONS

8.1 STABILITY CONDITION AND DISPERSION RELATIONS FOR THE SECOND-ORDER VELOCITY-STRESS SCHEME FOR THE P-SV WAVES

Stability of the finite-difference schemes can be examined by the von Neumann method, matrix method, discrete perturbation method or energy method. They are explained, e.g., in the mathematical textbooks mentioned in Section 1.1.

Here we restrict ourselves to one example of application of the von Neumann method. The method assumes a harmonic decomposition of the errors at a given time.

Consider the velocity-stress finite-difference scheme (4.2.1) for the P-SV waves. Assume errors in U , W , T^{xx} , T^{zz} and T^{xz} and investigate whether these errors grow with time. Let the errors at $x = i h$, $z = \ell h$ and $t = m \Delta t$ be

$$\begin{aligned} \mathcal{E}(U) &= A E, & \mathcal{E}(T^{xx}) &= C_1 E, \\ \mathcal{E}(W) &= B E, & \mathcal{E}(T^{zz}) &= C_2 E, \\ & & \mathcal{E}(T^{xz}) &= C_3 E \end{aligned} \quad (8.1.1)$$

and
where

$$\begin{aligned} E &= \exp(-i \omega m \Delta t + i k_x i h + i k_z \ell h), \\ k_x &= k \cos \theta, \\ k_z &= k \sin \theta, \end{aligned}$$

θ being an angle of the plane wave with respect to the x-axis and k wavenumber.

The errors satisfy the original finite-difference equations. Therefore, replace U by $\mathcal{E}(U)$, W by $\mathcal{E}(W)$, ... in the scheme (4.2.1). Omit a body force term and indexing material parameters. From the first of equations (4.2.1) we obtain

$$\begin{aligned} & A \exp \left[-i \omega \left(m + \frac{1}{2} \right) \Delta t + i k_x \left(i + \frac{1}{2} \right) h + i k_z \ell h \right] \\ & - A \exp \left[-i \omega \left(m - \frac{1}{2} \right) \Delta t + i k_x \left(i + \frac{1}{2} \right) h + i k_z \ell h \right] \\ = & \frac{\Delta t}{h} \frac{1}{\rho} \left\{ C_1 \exp \left[-i \omega m \Delta t + i k_x (i+1) h + i k_z \ell h \right] \right. \\ & \left. - C_1 \exp \left[-i \omega m \Delta t + i k_x i h + i k_z \ell h \right] \right\} \end{aligned}$$

$$\begin{aligned}
& + C_3 \exp \left[-i \omega m \Delta t + i k_x \left(i + \frac{1}{2} \right) h + i k_z \left(\ell + \frac{1}{2} \right) h \right] \\
& - C_3 \exp \left[-i \omega m \Delta t + i k_x \left(i + \frac{1}{2} \right) h + i k_z \left(\ell - \frac{1}{2} \right) h \right] \} .
\end{aligned}$$

Dividing the above equation by

$$\exp \left[-i \omega m \Delta t + i k_x \left(i + \frac{1}{2} \right) h + i k_z \ell h \right] \quad (8.1.2)$$

we obtain

$$\begin{aligned}
& A \exp \left[-i \omega \frac{1}{2} \Delta t \right] \\
& - A \exp \left[+i \omega \frac{1}{2} \Delta t \right] \\
= & \frac{\Delta t}{h} \frac{1}{\rho} \left\{ C_1 \exp \left[+ i k_x \frac{1}{2} h \right] \right. \\
& - C_1 \exp \left[- i k_x \frac{1}{2} h \right] \\
& + C_3 \exp \left[+ i k_z \frac{1}{2} h \right] \\
& \left. - C_3 \exp \left[- i k_z \frac{1}{2} h \right] \right\} \quad (8.1.3)
\end{aligned}$$

and finally

$$- A \sin \frac{\omega \Delta t}{2} = \frac{\Delta t}{h} \frac{1}{\rho} \left\{ C_1 \sin \frac{k_x h}{2} + C_3 \sin \frac{k_z h}{2} \right\} . \quad (8.1.4)$$

In fact, we could realize, say, the central value (8.1.2) for the first of equations (4.2.1) and write directly equation (8.1.3). We will do this for the remaining equations. From the second of equations (4.2.1) we obtain

$$\begin{aligned}
& B \exp \left[-i \omega \frac{1}{2} \Delta t \right] \\
& - B \exp \left[+i \omega \frac{1}{2} \Delta t \right] \\
= & \frac{\Delta t}{h} \frac{1}{\rho} \left\{ C_2 \exp \left[+ i k_z \frac{1}{2} h \right] \right. \\
& - C_2 \exp \left[- i k_z \frac{1}{2} h \right] \\
& + C_3 \exp \left[+ i k_x \frac{1}{2} h \right] \\
& \left. - C_3 \exp \left[- i k_x \frac{1}{2} h \right] \right\}
\end{aligned}$$

and

$$-B \sin \frac{\omega \Delta t}{2} = \frac{\Delta t}{h} \frac{1}{\rho} \left\{ C_2 \sin \frac{k_z h}{2} + C_3 \sin \frac{k_x h}{2} \right\}. \quad (8.1.5)$$

For the third equation we have

$$\begin{aligned} & C_1 \exp \left[-i\omega \frac{1}{2} \Delta t \right] \\ & -C_1 \exp \left[+i\omega \frac{1}{2} \Delta t \right] \\ = & \frac{\Delta t}{h} \left\{ A \exp \left[+ik_x \frac{1}{2} h \right] \right. \\ & \left. -A \exp \left[-ik_x \frac{1}{2} h \right] \right\} (\lambda + 2\mu) \\ + & \frac{\Delta t}{h} \left\{ B \exp \left[+ik_z \frac{1}{2} h \right] \right. \\ & \left. -B \exp \left[-ik_z \frac{1}{2} h \right] \right\} \lambda \end{aligned}$$

and

$$-C_1 \sin \frac{\omega \Delta t}{2} = \frac{\Delta t}{h} \left\{ (\lambda + 2\mu) A \sin \frac{k_x h}{2} + \lambda B \sin \frac{k_z h}{2} \right\}. \quad (8.1.6)$$

The fourth equation can be written directly according to equation (8.1.6):

$$-C_2 \sin \frac{\omega \Delta t}{2} = \frac{\Delta t}{h} \left\{ \lambda A \sin \frac{k_x h}{2} + (\lambda + 2\mu) B \sin \frac{k_z h}{2} \right\}. \quad (8.1.7)$$

Finally, from the fifth of equations (4.2.1) we obtain

$$\begin{aligned} & C_3 \exp \left[-i\omega \frac{1}{2} \Delta t \right] \\ & -C_3 \exp \left[+i\omega \frac{1}{2} \Delta t \right] \\ = & \frac{\Delta t}{h} \mu \left\{ A \exp \left[+ik_z \frac{1}{2} h \right] \right. \\ & \left. -A \exp \left[-ik_z \frac{1}{2} h \right] \right. \\ & \left. +B \exp \left[+ik_x \frac{1}{2} h \right] \right. \\ & \left. -B \exp \left[-ik_x \frac{1}{2} h \right] \right\} \end{aligned}$$

and

$$-C_3 \sin \frac{\omega \Delta t}{2} = \frac{\Delta t}{h} \mu \left\{ A \sin \frac{k_z h}{2} + B \sin \frac{k_x h}{2} \right\}. \quad (8.1.8)$$

Denote, for simplicity,

$$\frac{\Delta t}{h} = \Delta, \quad \sin \frac{\omega \Delta t}{2} = S, \quad \sin \frac{k_x h}{2} = X, \quad \sin \frac{k_z h}{2} = Z.$$

Then we can write equations (8.1.4) - (8.1.8) as

$$\begin{aligned} -A S &= \Delta \frac{1}{\rho} [C_1 X + C_3 Z] \\ -B S &= \Delta \frac{1}{\rho} [C_2 Z + C_3 X] \\ -C_1 S &= \Delta [(\lambda + 2\mu) A X + \lambda B Z] \\ -C_2 S &= \Delta [\lambda A X + (\lambda + 2\mu) B Z] \\ -C_3 S &= \Delta \mu [A Z + B X]. \end{aligned}$$

Multiplying the first two equations by S, the third one by X, the fourth one by Z, the fifth one by X and Z we obtain

$$\begin{aligned} -A S^2 &= \Delta \frac{1}{\rho} [C_1 X S + C_3 Z S] \\ -B S^2 &= \Delta \frac{1}{\rho} [C_2 Z S + C_3 X S] \\ -C_1 S X &= \Delta [(\lambda + 2\mu) A X^2 + \lambda B X Z] \\ -C_2 S Z &= \Delta [\lambda A X Z + (\lambda + 2\mu) B Z^2] \\ -C_3 S X &= \Delta \mu [A X Z + B X^2] \\ -C_3 S Z &= \Delta \mu [A Z^2 + B X Z]. \end{aligned}$$

Eliminating unknown coefficients C_1 , C_2 and C_3 we obtain

$$\begin{aligned} A S^2 &= \Delta^2 \frac{1}{\rho} [(\lambda + 2\mu) A X^2 + \mu A Z^2 + (\lambda + \mu) B X Z], \\ B S^2 &= \Delta^2 \frac{1}{\rho} [(\lambda + 2\mu) B Z^2 + \mu B X^2 + (\lambda + \mu) A X Z]. \end{aligned}$$

Substituting P-wave and S-wave velocities,

$$\frac{\lambda + 2\mu}{\rho} = \alpha^2, \quad \frac{\mu}{\rho} = \beta^2, \quad \frac{\lambda + \mu}{\rho} = \alpha^2 - \beta^2,$$

we obtain

$$AS^2 = \Delta^2 [\alpha^2 AX^2 + \beta^2 AZ^2 + \alpha^2 BXZ - \beta^2 BXZ],$$

$$BS^2 = \Delta^2 [\alpha^2 BZ^2 + \beta^2 BX^2 + \alpha^2 AXZ - \beta^2 AXZ],$$

and

$$\begin{aligned} A [S^2 - \Delta^2 (\alpha^2 X^2 + \beta^2 Z^2)] + B \Delta^2 [-\alpha^2 XZ + \beta^2 XZ] &= 0, \\ A \Delta^2 [-\alpha^2 XZ + \beta^2 XZ] + B [S^2 - \Delta^2 (\alpha^2 Z^2 + \beta^2 X^2)] &= 0. \end{aligned}$$

Eliminating unknown coefficients A and B we get

$$\begin{aligned} [S^2 - \Delta^2 (\alpha^2 X^2 + \beta^2 Z^2)] [S^2 - \Delta^2 (\alpha^2 Z^2 + \beta^2 X^2)] \\ - \Delta^4 X^2 Z^2 [\beta^2 - \alpha^2] = 0, \end{aligned}$$

$$\begin{aligned} S^4 - S^2 \Delta^2 \alpha^2 Z^2 - S^2 \Delta^2 \beta^2 X^2 - S^2 \Delta^2 \alpha^2 X^2 - S^2 \Delta^2 \beta^2 Z^2 \\ + \Delta^4 (\alpha^4 X^2 Z^2 + \alpha^2 \beta^2 X^4 + \alpha^2 \beta^2 Z^4 + \beta^4 X^2 Z^2) \\ - \Delta^4 X^2 Z^2 (\beta^4 - 2\alpha^2 \beta^2 + \alpha^4) = 0, \end{aligned}$$

$$\begin{aligned} S^4 - S^2 \Delta^2 \alpha^2 (X^2 + Z^2) - S^2 \Delta^2 \beta^2 (X^2 + Z^2) \\ + \Delta^4 \alpha^2 \beta^2 X^4 + \Delta^4 \alpha^2 \beta^2 Z^4 + 2\Delta^4 \alpha^2 \beta^2 X^2 Z^2 = 0, \end{aligned}$$

$$\begin{aligned} S^4 - S^2 \Delta^2 \alpha^2 (X^2 + Z^2) - S^2 \Delta^2 \beta^2 (X^2 + Z^2) \\ + \Delta^4 \alpha^2 \beta^2 (X^2 + Z^2)^2 = 0 \end{aligned}$$

and, finally,

$$[S^2 - \Delta^2 \alpha^2 (X^2 + Z^2)] [S^2 - \Delta^2 \beta^2 (X^2 + Z^2)] = 0.$$

There are two possible solutions of the above equations:

$$S^2 = \Delta^2 \alpha^2 (X^2 + Z^2) \quad \text{corresponds to P-waves}$$

and

$$S^2 = \Delta^2 \beta^2 (X^2 + Z^2) \quad \text{corresponds to S-waves.}$$

Recalling definitions of Δ , S , X and Z we can rewrite the two equations as

$$\sin^2 \frac{\omega \Delta t}{2} = \frac{\Delta^2 t}{h^2} \alpha^2 \left(\sin^2 \frac{k_x h}{2} + \sin^2 \frac{k_z h}{2} \right),$$

$$\sin^2 \frac{\omega \Delta t}{2} = \frac{\Delta^2 t}{h^2} \beta^2 \left(\sin^2 \frac{k_x h}{2} + \sin^2 \frac{k_z h}{2} \right),$$

from which we have

$$\sin \frac{\omega \Delta t}{2} = \pm \frac{\Delta t}{h} \alpha \left(\sin^2 \frac{k_x h}{2} + \sin^2 \frac{k_z h}{2} \right)^{1/2}, \quad (8.1.9)$$

$$\sin \frac{\omega \Delta t}{2} = \pm \frac{\Delta t}{h} \beta \left(\sin^2 \frac{k_x h}{2} + \sin^2 \frac{k_z h}{2} \right)^{1/2}. \quad (8.1.10)$$

Let $\frac{\Delta t}{h} \alpha \sqrt{2} \leq 1$. Then $\left| \sin \frac{\omega \Delta t}{2} \right| \leq 1$. Consequently, ω is real and errors (8.1.1) cannot grow with time. Similarly, let $\frac{\Delta t}{h} \beta \sqrt{2} \leq 1$. Then $\left| \sin \frac{\omega \Delta t}{2} \right| \leq 1$ which means that ω is real. Since $\alpha > \beta$, the condition for the P waves has to be taken as the stability condition. Therefore, the relation

$$\Delta t \leq \frac{h}{\alpha_{\max} \sqrt{2}} \quad (8.1.11)$$

is the stability condition for the velocity-stress scheme (4.2.1), if α_{\max} is a maximum P-wave velocity in a medium. Note that in the case of $\Delta x \neq \Delta z$ (grid spacings in the x- and z-directions, respectively) we would get similarly

$$\Delta t \leq \frac{1}{\alpha_{\max} \left(\frac{1}{\Delta^2 x} + \frac{1}{\Delta^2 z} \right)^{1/2}}. \quad (8.1.12)$$

Both equations (8.1.9) and (8.1.10) can be rewritten (omitting - sign) as

$$\sin \frac{\omega \Delta t}{2} = \frac{\Delta t}{h} c_0 \left(\sin^2 \frac{k_x h}{2} + \sin^2 \frac{k_z h}{2} \right)^{1/2}$$

where c_0 is either α or β . Then

$$\frac{\omega \Delta t}{2} = \arcsin \left[\frac{\Delta t}{h} c_0 \left(\sin^2 \frac{k_x h}{2} + \sin^2 \frac{k_z h}{2} \right)^{1/2} \right].$$

Since the phase velocity c is equal to ω/k , the grid phase velocity will be

$$c^{\text{grid}} = \frac{2}{k \Delta t} \arcsin \left[\frac{\Delta t}{h} c_0 \left(\sin^2 \frac{k_x h}{2} + \sin^2 \frac{k_z h}{2} \right)^{1/2} \right].$$

Divide the above equation by c_0 and using $k = 2\pi/\lambda$ rewrite

$$\frac{2}{c_0 k \Delta t} = \frac{\lambda}{\pi c_0 \Delta t} = \frac{h}{c_0 \Delta t} \frac{1}{\pi h},$$

$$\frac{k_x h}{2} = \pi \frac{h}{\lambda} \cos\theta,$$

$$\frac{k_z h}{2} = \pi \frac{h}{\lambda} \sin\theta.$$

Then

$$\frac{c^{\text{grid}}}{c_0} = \frac{h}{c_0 \Delta t} \frac{1}{\pi h} \arcsin \left\{ \frac{\Delta t}{h} c_0 \left[\sin^2 \left(\pi \frac{h}{\lambda} \cos\theta \right) + \sin^2 \left(\pi \frac{h}{\lambda} \sin\theta \right) \right]^{1/2} \right\}. \quad (8.1.13)$$

We can introduce a stability ratio

$$p = \sqrt{2} \alpha \frac{\Delta t}{h}$$

and write equation (8.1.13) separately for P and S waves:

$$\frac{\alpha^{\text{grid}}}{\alpha} = \frac{\sqrt{2} \lambda}{\pi p h} \arcsin \left\{ \frac{p}{\sqrt{2}} \left[\sin^2 \left(\pi \frac{h}{\lambda} \cos\theta \right) + \sin^2 \left(\pi \frac{h}{\lambda} \sin\theta \right) \right]^{1/2} \right\}$$

and

$$\frac{\beta^{\text{grid}}}{\beta} = \frac{\sqrt{2} \alpha \lambda}{\pi p \beta h} \arcsin \left\{ \frac{\beta}{\alpha} \frac{p}{\sqrt{2}} \left[\sin^2 \left(\pi \frac{h}{\lambda} \cos\theta \right) + \sin^2 \left(\pi \frac{h}{\lambda} \sin\theta \right) \right]^{1/2} \right\}. \quad (8.1.14)$$

The above equations are grid dispersion relations for the velocity-stress finite-difference scheme (4.2.1). Note an important fact that the grid dispersion of the S-waves does depend on the α/β ratio (i. e., also on **Poisson's ratio** $\nu = \frac{2 - \alpha^2/\beta^2}{2(1 - \alpha^2/\beta^2)}$) while the grid dispersion of the P-waves does not.

The grid dispersion is illustrated in Fig. 8.1.1.

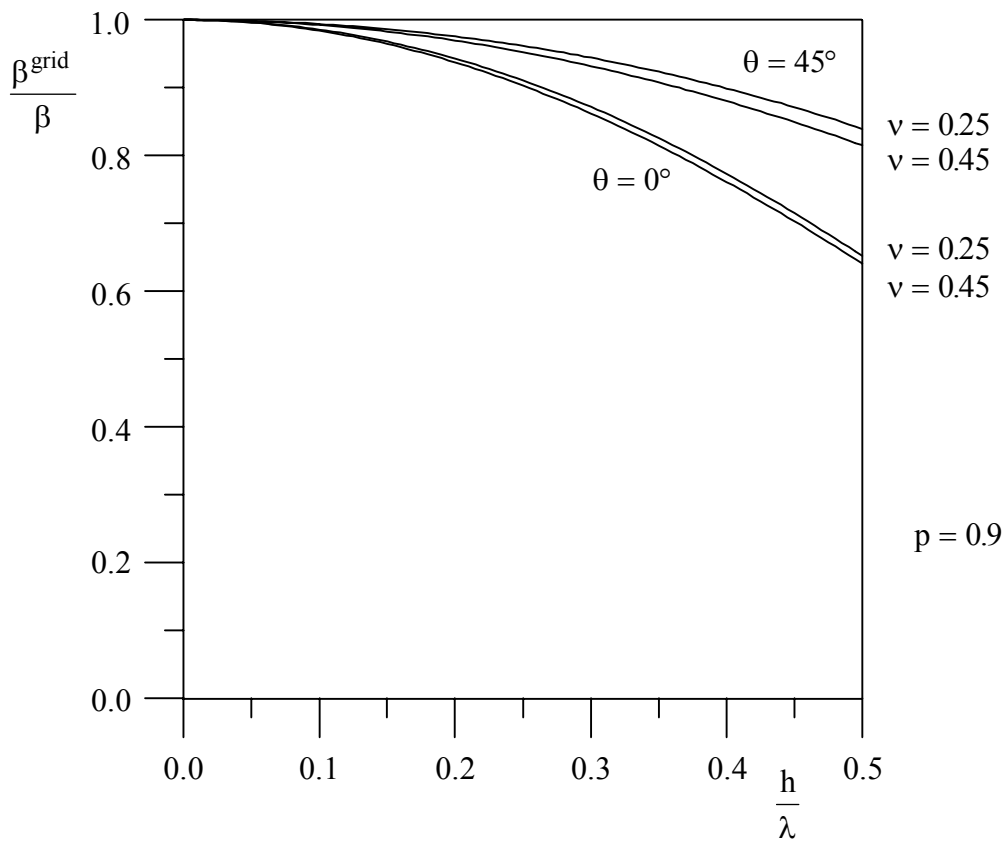
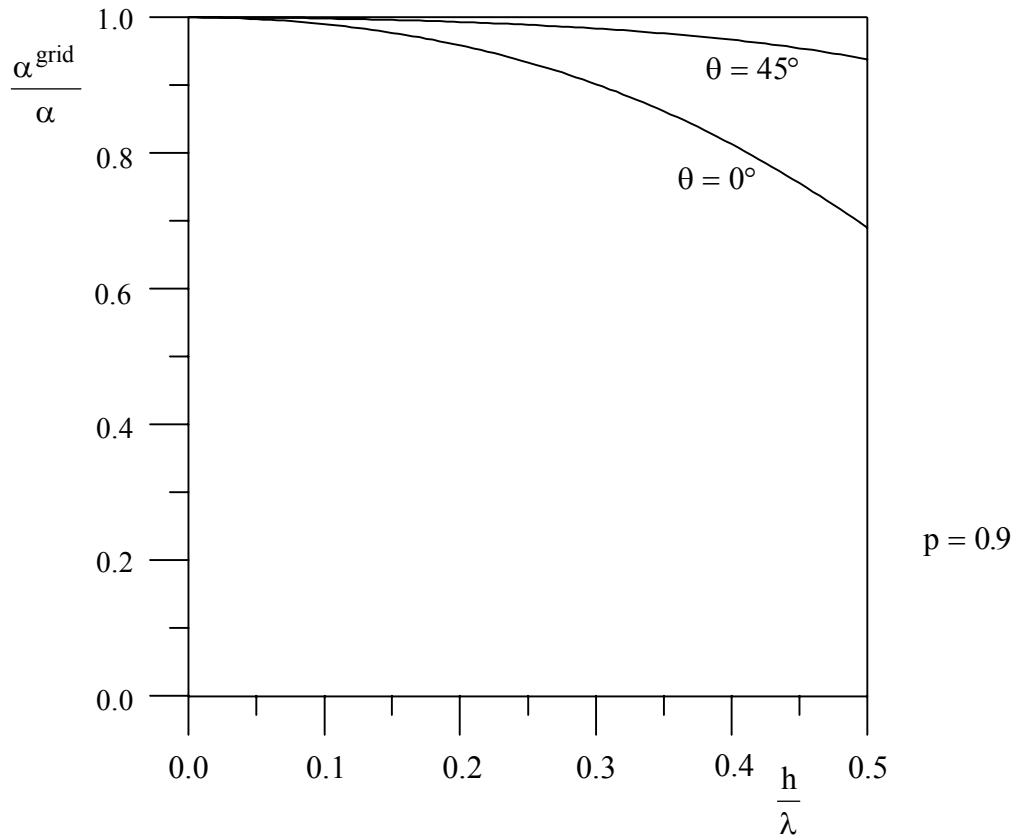


Fig. 8.1.1
Grid dispersion of the P- and S- waves in the velocity-stress finite-difference scheme (4.2.1)

8.2 STABILITY CONDITIONS FOR THE FINITE-DIFFERENCE SCHEMES

Second-Order Schemes

- conventional grid (displacement formulation)

$$\text{SH} \quad \Delta t < \frac{1}{\sqrt{2}} \frac{h}{\beta}$$

$$\text{P-SV, 3D} \quad \Delta t < h(\beta^2 + \alpha^2)^{-\frac{1}{2}}$$

- staggered grid (displacement-stress and velocity-stress formulations)

$$\text{SH} \quad \Delta t < \frac{1}{\sqrt{2}} \frac{h}{\beta}$$

$$\text{P-SV} \quad \Delta t < \frac{1}{\sqrt{2}} \frac{h}{\alpha}$$

$$\text{3D} \quad \Delta t < \frac{1}{\sqrt{3}} \frac{h}{\alpha}$$

Fourth-Order Schemes

- staggered grid (displacement-stress and velocity-stress formulations)

$$\text{P-SV} \quad \Delta t < \frac{6}{7\sqrt{2}} \frac{h}{\alpha}$$

$$\text{3D} \quad \Delta t < \frac{6}{7\sqrt{3}} \frac{h}{\alpha}$$

α – maximum P-wave velocity in a medium

β – maximum S-wave velocity in a medium

h – grid spacing; $h = \Delta x = \Delta y = \Delta z$

9. APPROXIMATION OF TRACTION-FREE SURFACE

9.1 TRACTION-FREE CONDITION

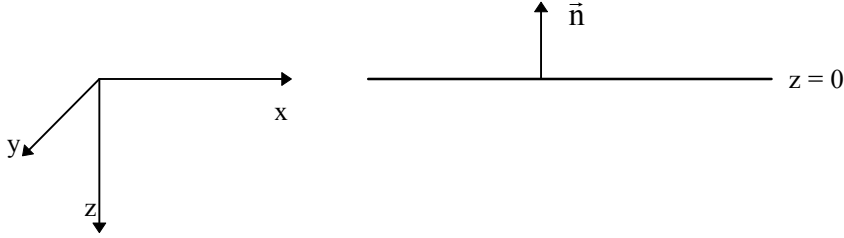


Fig. 9.1.1

Consider a horizontal surface at $z=0$ shown in Fig. 9.1.1. Let \bar{n} be a unit normal to the surface. Then $\bar{n} = \bar{n}(0, 0, -1)$. Furthermore, consider the surface as a traction-free surface, i.e.,

$$\vec{T}(\bar{n}) = 0.$$

Since

$$T_i = \tau_{ji} n_j$$

we have

$$\tau_{31} = 0, \quad \tau_{32} = 0, \quad \tau_{33} = 0,$$

or

$$\tau_{zx} = 0, \quad \tau_{zy} = 0, \quad \tau_{zz} = 0.$$

Consider for simplicity again only the P-SV case. Then

$$\tau_{zx} = \mu (u_z + w_x) = 0 \quad (9.1.1a)$$

and

$$\tau_{zz} = \lambda (u_x + w_z) + 2\mu w_z = 0 \quad (9.1.1b)$$

which we can write as

$$\tau_{zx} = 0 : \quad u_z = -w_x \quad \text{or} \quad u_z = -w_x \quad (9.1.2a)$$

and

$$\tau_{zz} = 0 : \quad w_z = -\frac{\lambda}{\lambda+2\mu} u_x \quad \text{or} \quad w_z = -\frac{\lambda}{\lambda+2\mu} u_x. \quad (9.1.2b)$$

9.2 APPROXIMATION OF THE FREE SURFACE IN THE VELOCITY-STRESS FORMULATION

Consider the second-order velocity-stress finite-difference scheme (4.2.1). Localize the free surface so that T_{i0}^{xx} , T_{i0}^{zz} and $U_{i+1/20}$ are located on the free surface as it is shown in Fig. 9.2.1.

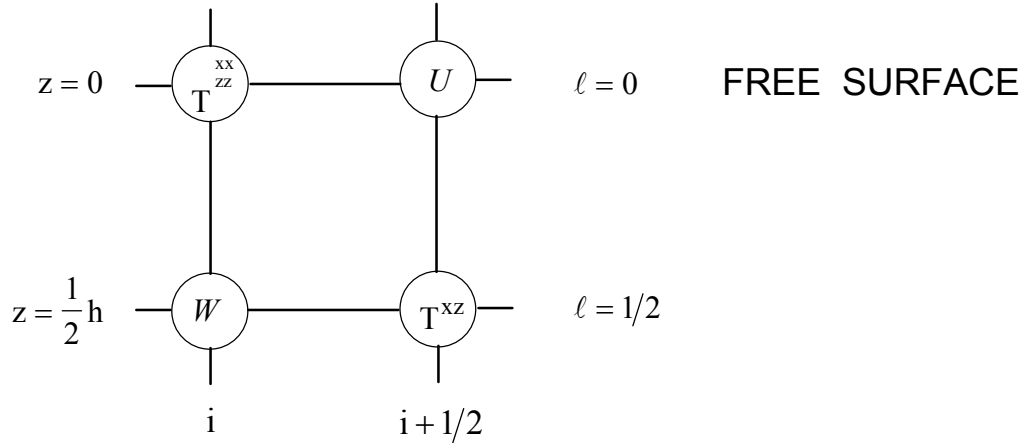


Fig. 9.2.1

We have to update U, T^{xx}, W and T^{xz} , and, at the same time to assure that $T^{zz} = 0$ and $T^{xz} = 0$ on the free surface.

Recall equations (2.2.3) omitting the body force term:

$$\rho u_t = \tau_{xx,x} + \tau_{xz,z} \quad (a)$$

$$\rho w_t = \tau_{xz,x} + \tau_{zz,z} \quad (b)$$

$$\tau_{xx,t} = [\lambda + 2\mu] u_x + \lambda w_z \quad (c)$$

$$\tau_{zz,t} = \lambda u_x + [\lambda + 2\mu] w_z \quad (d)$$

$$\tau_{xz,t} = \mu (u_z + w_x) \quad (e)$$

There is no problem with the x-derivatives in equations (a - e). What we have to look at is approximation of the z-derivatives.

In equation (c) we can replace w_z by $-\lambda / (\lambda + 2\mu) u_x$ according to equation (9.1.2b) and solve for T_{i0}^{xx} .

Since $\tau_{zz} = 0$ on the free surface, we do not need equation (d). We simply prescribe $T_{i0}^{zz} = 0$ for all time levels.

In equation (a) we need to find an approximation to $\tau_{xz,z}$. We will extend the grid above $z=0$ (i.e., $\ell=0$) and image τ_{xz} as an odd function with respect to $z=0$ (Levander, 1988). Then obviously $\tau_{xz} = 0$ at $z=0$. Then

$$T_{i+1/2 -1/2}^{xz} = -T_{i+1/2 1/2}^{xz}$$

and

$$\tau_{xz,z}|_{z=0} \doteq \frac{2}{h} T_{i+1/2 1/2}^{xz}.$$

There is no problem to approximate equations (b) and (e) since both W and T^{xz} are localized half grid spacing below the free surface.

To make a summary, the scheme to update T^{xx} , T^{zz} and U on the free surface is

$$\begin{aligned} U_{i+1/2 0}^{m+1/2} &= U_{i+1/2 0}^{m-1/2} + \frac{\Delta t}{h} \frac{1}{\rho_{i+1/2 0}} (T_{i+1 0}^{xx,m} - T_{i 0}^{xx,m} + 2 T_{i+1/2 1/2}^{xz,m}) \\ T_{i 0}^{xx,m+1} &= T_{i 0}^{xx,m} + \frac{\Delta t}{h} \frac{4\mu(\lambda + \mu)}{\lambda + 2\mu} \Big|_{i 0} (U_{i+1/2 0}^{m+1/2} - U_{i-1/2 0}^{m+1/2}) \\ T_{i 0}^{zz,m+1} &= 0. \end{aligned}$$

The equations for updating $W_{i 1/2}^{m+1/2}$ and $T_{i+1/2 1/2}^{xz,m+1}$ are the same as those in the scheme (4.2.1).

The problem is more complicated in the case of the fourth-order scheme (5.3.1) since the grid is longer in both x- and z-directions (see Fig. 5.3.1).

Now we will consider updating T^{xx} , T^{zz} and U on the free surface. As in the previous case there is no problem with T^{xx} and T^{zz} : we can use equation (9.1.2b) to replace w_z in equation (c) to solve for $T_{i 0}^{xx}$, and, instead of solving equation (d), we simply prescribe $T_{i 0}^{zz} = 0$.

In order to update U , we need two T^{xz} values above the free surface – $T_{i+1/2 -1/2}^{xz}$ and $T_{i+1/2 -3/2}^{xz}$. As in the previous case we can image τ_{xz} as an odd function with respect to $z=0$. Then $\tau_{xz} = 0$ at $z=0$ and

$$T_{i+1/2 -1/2}^{xz} = -T_{i+1/2 1/2}^{xz}, \quad T_{i+1/2 -3/2}^{xz} = -T_{i+1/2 3/2}^{xz}. \quad (9.2.2)$$

Look now at updating W and T^{xz} at $z=h/2$, i.e., $\ell=1/2$. If we image τ_{zz} as an odd function with respect to $z=0$, we have $\tau_{zz} = 0$ at $z=0$,

$$T_{i-1}^{zz} = -T_{i 1}^{zz}$$

and we can solve equation (d) for $W_{i 1/2}$.

In order to solve equation (e) for $T_{i+1/2-1/2}^{xz}$, we need $U_{i+1/2-1}$. We have several possibilities to approximate $U_{i+1/2-1}$. Since we image τ_{xz} as an odd function with respect to $z=0$,

$$\tau_{xz}\Big|_{z=-1/2} = -\tau_{xz}\Big|_{z=1/2}$$

and

$$(u_z + w_x)\Big|_{z=-1/2} = -(u_z + w_x)\Big|_{z=1/2}$$

from which we get

$$U_{i+1/2-1} = U_{i+1/2+1} + W_{i+1+1/2} - W_{i+1/2} + W_{i+1-1/2} - W_{i-1/2}. \quad (9.2.3)$$

From equation (9.1.2b) we have

$$w_z\Big|_{z_0} = -\frac{\lambda}{\lambda+2\mu} u_x\Big|_{z_0}$$

which gives

$$W_{i+1/2} - W_{i-1/2} = -\frac{\lambda}{\lambda+2\mu}\Big|_{i_0} (U_{i+1/2+0} - U_{i-1/2+0})$$

and consequently

$$W_{i-1/2} = W_{i+1/2} + \frac{\lambda}{\lambda+2\mu}\Big|_{i_0} (U_{i+1/2+0} - U_{i-1/2+0}) \quad (9.2.4a)$$

and

$$W_{i+1-1/2} = W_{i+1+1/2} + \frac{\lambda}{\lambda+2\mu}\Big|_{i+1_0} (U_{i+3/2+0} - U_{i+1/2+0}). \quad (9.2.4b)$$

Substituting $W_{i-1/2}$ and $W_{i+1-1/2}$ from equations (9.2.4) into equation (9.2.3) we finally obtain

$$\begin{aligned} U_{i+1/2-1} &= U_{i+1/2+1} + 2W_{i+1+1/2} - 2W_{i+1/2} \\ &+ \frac{\lambda}{\lambda+2\mu}\Big|_{i+1_0} (U_{i+3/2+0} - U_{i+1/2+0}) \\ &- \frac{\lambda}{\lambda+2\mu}\Big|_{i_0} (U_{i+1/2+0} - U_{i-1/2+0}). \end{aligned} \quad (9.2.5)$$

Another possibility is to put simply $U = 0$ everywhere above the free surface (Robertsson, 1996).

Now we will consider at updating T^{xx}, T^{zz} and U at $z = h$, i.e., $\ell = 1$.

In order to solve equations (c) and (d) for T_{i1}^{xx} and T_{i1}^{zz} , we need $W_{i-1/2}$. This is given by equation (9.2.4a).

Another possibility is to put $W = 0$ everywhere above the free surface.

In order to solve equation (a) for $U_{i+1/2 1}$ we need $T_{i+1/2 -1/2}^{xz}$. This is given by equation (9.2.2).

To make a summary, here is the scheme:

$$\begin{aligned}
U_{i+1/2 0}^{m+1/2} &= U_{i+1/2 0}^{m-1/2} \\
&+ \frac{\Delta t}{h} \frac{1}{\rho_{i+1/2 0}} \left\{ A \left(T_{i+2 0}^{xx,m} - T_{i-1 0}^{xx,m} + 2 T_{i+1/2 3/2}^{xz,m} \right) \right. \\
&\quad \left. + B \left(T_{i+1 0}^{xx,m} - T_{i 0}^{xx,m} + 2 T_{i+1/2 1/2}^{xz,m} \right) \right\} \\
W_{i 1/2}^{m+1/2} &= W_{i 1/2}^{m-1/2} \\
&+ \frac{\Delta t}{h} \frac{1}{\rho_{i 1/2}} \left\{ A \left(T_{i+3/2 1/2}^{xz,m} - T_{i-3/2 1/2}^{xz,m} + T_{i 2}^{zz,m} + T_{i 1}^{zz,m} \right) \right. \\
&\quad \left. + B \left(T_{i+1/2 1/2}^{xz,m} - T_{i-1/2 1/2}^{xz,m} + T_{i 1}^{zz,m} - T_{i 0}^{zz,m} \right) \right\} \\
T_{i 0}^{xx,m+1} &= T_{i 0}^{xx,m} \\
&+ \frac{\Delta t}{h} \left\{ \frac{4\mu(\lambda+\mu)}{\lambda+2\mu} \Big|_{i 0} \left[A \left(U_{i+3/2 0}^{m+1/2} - U_{i-3/2 0}^{m+1/2} \right) \right. \right. \\
&\quad \left. \left. + B \left(U_{i+1/2 0}^{m+1/2} - U_{i-1/2 0}^{m+1/2} \right) \right] \right\} \\
T_{i 0}^{zz,m+1} &= 0 \\
T_{i+1/2 1/2}^{xz,m+1} &= T_{i+1/2 1/2}^{xz,m} \\
&+ \frac{\Delta t}{h} \mu_{i+1/2 1/2} \left\{ A \left[W_{i+2 1/2}^{m+1/2} - W_{i-1 1/2}^{m+1/2} \right. \right. \\
&\quad \left. \left. + U_{i+1/2 2}^{m+1/2} - U_{i+1/2 1}^{m+1/2} - 2W_{i+1 1/2}^{m+1/2} + 2W_{i 1/2}^{m+1/2} \right] \right\}
\end{aligned}$$

$$\begin{aligned}
& - \frac{\lambda}{\lambda + 2\mu} \Big|_{i+1,0} (U_{i+3/2,0}^{m+1/2} - U_{i+1/2,0}^{m+1/2}) \\
& + \frac{\lambda}{\lambda + 2\mu} \Big|_{i,0} (U_{i+1/2,0}^{m+1/2} - U_{i-1/2,0}^{m+1/2})] \\
& + \mathbf{B} \left(U_{i+1/2,1}^{m+1/2} - U_{i+1/2,0}^{m+1/2} + W_{i+1/2}^{m+1/2} - W_{i/2}^{m+1/2} \right) \}
\end{aligned}$$

or

$$\begin{aligned}
T_{i+1/2,1/2}^{xz,m+1} &= T_{i+1/2,1/2}^{xz,m} \\
& + \frac{\Delta t}{h} \mu_{i+1/2,1/2} \{ \mathbf{A} \left(U_{i+1/2,2}^{m+1/2} + W_{i+2,1/2}^{m+1/2} - W_{i-1,1/2}^{m+1/2} \right) \\
& + \mathbf{B} \left(U_{i+1/2,1}^{m+1/2} - U_{i+1/2,0}^{m+1/2} + W_{i+1/2}^{m+1/2} - W_{i/2}^{m+1/2} \right) \}
\end{aligned}$$

$$\begin{aligned}
T_{i,1}^{xx,m+1} &= T_{i,1}^{xx,m} \\
& + \frac{\Delta t}{h} \{ (\lambda + 2\mu)_{i,1} [\mathbf{A} \left(U_{i+3/2,1}^{m+1/2} - U_{i-3/2,1}^{m+1/2} \right) \\
& + \mathbf{B} \left(U_{i+1/2,1}^{m+1/2} - U_{i-1/2,1}^{m+1/2} \right)] \\
& + \lambda_{i,1} [\mathbf{A} \left(W_{i,5/2}^{m+1/2} - W_{i,1/2}^{m+1/2} - \frac{\lambda}{\lambda + 2\mu} \Big|_{i,0} \left(U_{i+1/2,0}^{m+1/2} - U_{i-1/2,0}^{m+1/2} \right) \right) \\
& + \mathbf{B} \left(W_{i,3/2}^{m+1/2} - W_{i,1/2}^{m+1/2} \right)]
\end{aligned}$$

or

$$\begin{aligned}
T_{i,1}^{xx,m+1} &= T_{i,1}^{xx,m} \\
& + \frac{\Delta t}{h} \{ (\lambda + 2\mu)_{i,1} [\mathbf{A} \left(U_{i+3/2,1}^{m+1/2} - U_{i-3/2,1}^{m+1/2} \right) + \mathbf{B} \left(U_{i+1/2,1}^{m+1/2} - U_{i-1/2,1}^{m+1/2} \right)] \\
& + \lambda_{i,1} [\mathbf{A} \left(W_{i,5/2}^{m+1/2} + \mathbf{B} \left(W_{i,3/2}^{m+1/2} - W_{i,1/2}^{m+1/2} \right) \right)] \}
\end{aligned}$$

Equations for $T_{i,1}^{zz,m+1}$ are the same as for $T_{i,1}^{xx,m+1}$ except that $(\lambda + 2\mu)_{i,1}$ and $\lambda_{i,1}$ are interchanged.

$$\begin{aligned}
U_{i+1/2,1}^{m+1/2} &= U_{i+1/2,1}^{m-1/2} \\
&+ \frac{\Delta t}{h} \frac{1}{\rho_{i+1/2,1}} \left\{ A \left(T_{i+2,1}^{xx,m} - T_{i-1,1}^{xx,m} + T_{i+1/2,5/2}^{xz,m} + T_{i+1/2,1/2}^{xz,m} \right) \right. \\
&\quad \left. + B \left(T_{i+1,1}^{xx,m} - T_{i,1}^{xx,m} + T_{i+1/2,3/2}^{xz,m} - T_{i+1/2,1/2}^{xz,m} \right) \right\} . \\
A &= -\frac{1}{24}, \quad B = \frac{9}{8} .
\end{aligned}$$

9.3 APPROXIMATION OF THE FREE SURFACE IN THE DISPLACEMENT FORMULATION

In this section we will present the approach suggested by Zahradník (1995b). Numerical tests by Zahradník & Priolo (1995) and Moczo et al. (1997) showed that the scheme simulates the flat free surface very accurately.

It can be shown by theoretical investigation of the consistency of the displacement scheme (4.3.13) on the horizontal free surface that application of the so-called **vacuum formalism** (the interior scheme is applied at the grid points on the surface while $\mu=0$ and $\lambda=0$ are assumed above the surface) applied to the scheme leads to violation of the traction-free condition. A term violating the condition comes from the approximation of the $(\lambda w_z)_x$ derivative. Therefore, another approximation of the mixed derivatives should be found.

Consider again equations (4.3.8),

$$\Phi = a\Psi_x \quad , \quad \Phi_z = (a\Psi_x)_z . \quad (9.3.1)$$

Instead of (4.3.9) we will approximate the Φ_z derivative as an arithmetic average of approximations in two different x-positions (see Fig. 9.3.1)

$$\Phi_z|_{i\ell} \doteq \frac{1}{2} \left[\frac{1}{h} \left(\Phi_{i+1/2, \ell+1/2} - \Phi_{i+1/2, \ell-1/2} \right) + \frac{1}{h} \left(\Phi_{i-1/2, \ell+1/2} - \Phi_{i-1/2, \ell-1/2} \right) \right] \quad (9.3.2)$$

From (9.3.1) we have

$$\frac{\Phi}{a} = \Psi_x . \quad (9.3.3)$$

Integration of equation (9.3.3)

$$\int_{z_\ell}^{z_{\ell+1}} \frac{\Phi(x_{i+1/2}, z)}{a(x_{i+1/2}, z)} dz = \int_{z_\ell}^{z_{\ell+1}} \Psi_x(x_{i+1/2}, z) dz ,$$

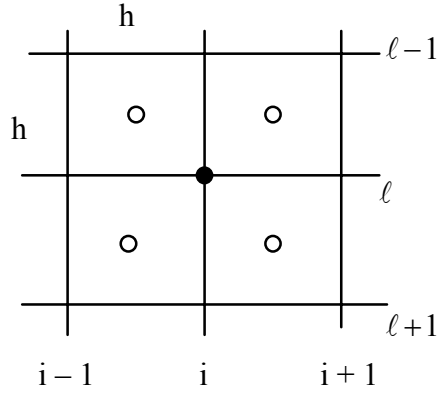


Fig. 9.3.1
Illustration of approximation (9.3.2)

leads to

$$\Phi_{i+1/2 \ell+1/2} \doteq a_{i+1/2 \ell}^z \Psi_x \Big|_{i+1/2 \ell+1/2} \quad (9.3.4a)$$

where

$$a_{i+1/2 \ell}^z = h \left[\int_{z_\ell}^{z_{\ell+1}} \frac{dz}{a(x_{i+1/2}, z)} \right]^{-1}.$$

Similarly, we obtain

$$\Phi_{i+1/2 \ell-1/2} \doteq a_{i+1/2 \ell-1}^z \Psi_x \Big|_{i+1/2 \ell-1/2}, \quad (9.3.4b)$$

$$\Phi_{i-1/2 \ell+1/2} \doteq a_{i-1/2 \ell}^z \Psi_x \Big|_{i-1/2 \ell+1/2}, \quad (9.3.4c)$$

and

$$\Phi_{i-1/2 \ell-1/2} \doteq a_{i-1/2 \ell-1}^z \Psi_x \Big|_{i-1/2 \ell-1/2}. \quad (9.3.4d)$$

Approximate the x-derivative in equation (9.3.4a):

$$\Psi_x \Big|_{i+1/2 \ell+1/2} \doteq \frac{1}{h} \left(\Psi_{i+1 \ell+1/2} - \Psi_{i \ell+1/2} \right).$$

Approximate both values of Ψ in $z_{\ell+1/2}$ positions as arithmetic averages of the Ψ values in z_ℓ and $z_{\ell+1}$ positions:

$$\Psi_{i+1 \ell+1/2} \doteq \frac{1}{2} \left(\Psi_{i+1 \ell} + \Psi_{i+1 \ell+1} \right),$$

$$\Psi_{i \ell+1/2} \doteq \frac{1}{2} \left(\Psi_{i \ell} + \Psi_{i \ell+1} \right).$$

Then we obtain

$$\Psi_x \Big|_{i+1/2 \ell+1/2} \doteq \frac{1}{2h} \left(\Psi_{i+1 \ell} + \Psi_{i+1 \ell+1} - \Psi_{i \ell} - \Psi_{i \ell+1} \right). \quad (9.3.5a)$$

Similarly,

$$\Psi_x \Big|_{i+1/2 \ell-1/2} \doteq \frac{1}{2h} \left(\Psi_{i+1 \ell} + \Psi_{i+1 \ell-1} - \Psi_{i \ell} - \Psi_{i \ell-1} \right), \quad (9.3.5b)$$

$$\Psi_x \Big|_{i-1/2 \ell+1/2} \doteq \frac{1}{2h} \left(\Psi_{i \ell+1} + \Psi_{i \ell} - \Psi_{i-1 \ell+1} - \Psi_{i-1 \ell} \right), \quad (9.3.5c)$$

and

$$\Psi_x \Big|_{i-1/2 \ell-1/2} \doteq \frac{1}{2h} \left(\Psi_{i \ell} + \Psi_{i \ell-1} - \Psi_{i-1 \ell} - \Psi_{i-1 \ell-1} \right). \quad (9.3.5d)$$

Substituting approximations (9.3.5), (9.3.4) and (9.3.2) into (9.3.1) we obtain

$$\begin{aligned} (a\Psi_x)_{z|_i \ell} \doteq & \frac{1}{4h^2} \left[a_{i+1/2 \ell}^z \left(\Psi_{i+1 \ell} + \Psi_{i+1 \ell+1} - \Psi_{i \ell} - \Psi_{i \ell+1} \right) \right. \\ & - a_{i+1/2 \ell-1}^z \left(\Psi_{i+1 \ell} + \Psi_{i+1 \ell-1} - \Psi_{i \ell} - \Psi_{i \ell-1} \right) \\ & + a_{i-1/2 \ell}^z \left(\Psi_{i \ell+1} + \Psi_{i \ell} - \Psi_{i-1 \ell+1} - \Psi_{i-1 \ell} \right) \\ & \left. - a_{i-1/2 \ell-1}^z \left(\Psi_{i \ell} + \Psi_{i \ell-1} - \Psi_{i-1 \ell} - \Psi_{i-1 \ell-1} \right) \right]. \end{aligned} \quad (9.3.6)$$

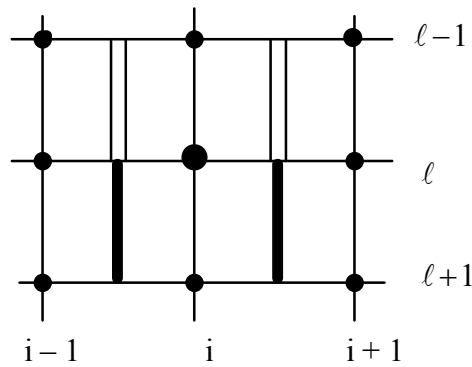


Fig. 9.3.2

Illustration of approximation (9.3.6). Vertical lines in positions $i-1/2$ and $i+1/2$ indicate effective material parameters

Localize now the free surface at $z=z_\ell=z_0$. Apply the so-called vacuum formalism, i.e., put $a=0$ for $z < z_\ell$. Then we obtain from (9.3.6)

$$\begin{aligned}
\left(a\Psi_x \right)_{z|_{i\ell}} \doteq & \frac{1}{4h^2} \left[a_{i+1/2\ell}^z \left(\Psi_{i+1\ell} + \Psi_{i+1\ell+1} - \Psi_{i\ell} - \Psi_{i\ell+1} \right) \right. \\
& \left. + a_{i-1/2\ell}^z \left(\Psi_{i\ell+1} + \Psi_{i\ell} - \Psi_{i-1\ell+1} - \Psi_{i-1\ell} \right) \right].
\end{aligned} \tag{9.3.7}$$

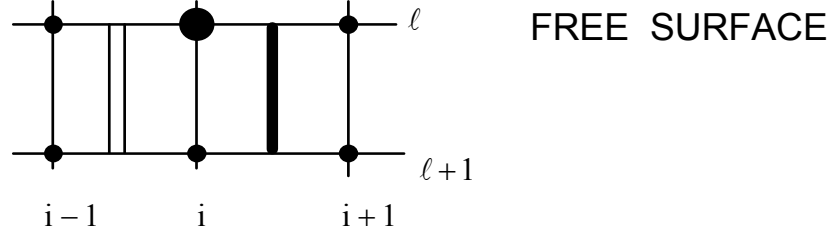


Fig. 9.3.3
Illustration of approximation (9.3.7). Vertical lines in positions $i-1/2$ and $i+1/2$ indicate effective material parameters

Applying now the $x \rightarrow z$, $z \rightarrow x$, $i \rightarrow \ell$, $\ell \rightarrow i$ substitutions in formula (9.3.6) we obtain an approximation

$$\begin{aligned}
\left(a\Psi_z \right)_{x|_{i\ell}} \doteq & \frac{1}{4h^2} \left[a_i^{x\ell+1/2} \left(\Psi_{i\ell+1} + \Psi_{i+1\ell+1} - \Psi_{i\ell} - \Psi_{i+1\ell} \right) \right. \\
& - a_{i-1\ell+1/2}^x \left(\Psi_{i\ell+1} + \Psi_{i-1\ell+1} - \Psi_{i\ell} - \Psi_{i-1\ell} \right) \\
& + a_i^{x\ell-1/2} \left(\Psi_{i+1\ell} + \Psi_{i\ell} - \Psi_{i+1\ell-1} - \Psi_{i\ell-1} \right) \\
& \left. - a_{i-1\ell-1/2}^z \left(\Psi_{i\ell} + \Psi_{i-1\ell} - \Psi_{i\ell-1} - \Psi_{i-1\ell-1} \right) \right].
\end{aligned} \tag{9.3.8}$$

Localizing again the free surface at $z = z_\ell = z_0$ and applying the vacuum formalism we get from (9.3.8)

$$\begin{aligned}
\left(a\Psi_z \right)_{x|_{i\ell}} \doteq & \frac{1}{4h^2} \left[a_i^{x\ell+1/2} \left(\Psi_{i\ell+1} + \Psi_{i+1\ell+1} - \Psi_{i\ell} - \Psi_{i+1\ell} \right) \right. \\
& \left. - a_{i-1\ell+1/2}^x \left(\Psi_{i\ell+1} + \Psi_{i-1\ell+1} - \Psi_{i\ell} - \Psi_{i-1\ell} \right) \right].
\end{aligned} \tag{9.3.9}$$

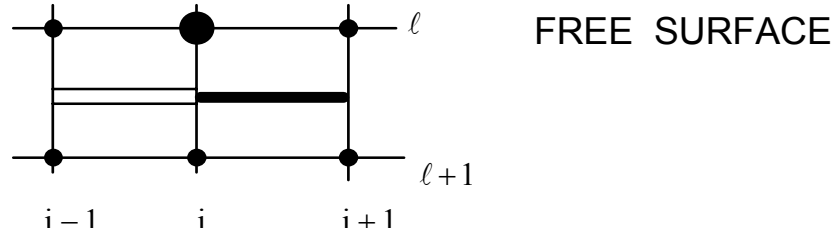


Fig. 9.3.4
Illustration of approximation (9.3.9)

To make a summary, the displacement finite-difference scheme for the P-SV waves for the grid points on the free surface is the same as scheme (4.3.13) for the interior grid points with the following exceptions:

1. $\ell = 0$,
2. only half values of the $a_{i\ell}^x$ and $a_{i-1\ell}^x$ parameters should be considered,
3. the L_{zz} , L_{zx} and L_{xz} operators are

$$L_{zz}(a, \Psi) = \frac{1}{h^2} a_{i\ell}^z \left(\Psi_{i\ell+1}^m - \Psi_{i\ell}^m \right),$$

$$L_{zx}(a, \Psi) = \frac{1}{4h^2} \left\{ a_{i\ell+1/2}^x \left(\Psi_{i\ell+1}^m + \Psi_{i+1\ell+1}^m - \Psi_{i\ell}^m - \Psi_{i+1\ell}^m \right) - a_{i-1\ell+1/2}^x \left(\Psi_{i\ell+1}^m + \Psi_{i-1\ell+1}^m - \Psi_{i\ell}^m - \Psi_{i-1\ell}^m \right) \right\} \quad (9.3.10)$$

and

$$L_{xz}(a, \Psi) = \frac{1}{4h^2} \left\{ a_{i-1/2\ell}^z \left(\Psi_{i\ell}^m + \Psi_{i\ell+1}^m - \Psi_{i-1\ell}^m - \Psi_{i-1\ell+1}^m \right) + a_{i+1/2\ell}^z \left(\Psi_{i+1\ell}^m + \Psi_{i+1\ell+1}^m - \Psi_{i\ell}^m - \Psi_{i\ell+1}^m \right) \right\}.$$

While a reasonably accurate and stable modeling of the flat free surface can be achieved by several finite-difference techniques, an implementation of the free-surface topography is not a trivial problem. This is especially true about the displacement formulation. The more complex geometry of the free surface, the lower accuracy and more limitations on the physical parameters of the medium in order to keep the free-surface approximation stable.

Due to the explicit presence of the stress-tensor components in the equations of motion the implementation of the traction-free condition is easier in the displacement-stress and velocity-stress formulations. The techniques of Pitarka & Irikura (1996), Ohminato & Chouet (1997) and Hestholm & Ruud (in press) are examples. Ohminato & Chouet's (1997) choice of positions of the stress-tensor components in the grid might be better than that usually used and assumed in Section 9.2.

For a concise review of modeling the free-surface topography in the finite-difference method see Moczo et al. (1997) and Robertsson (1996).

The problem of implementing conditions on boundaries of complex geometric shapes is an inherent problem of the finite-difference method. Moczo et al. (1997) overcome the problem by combining the finite-element and finite-difference methods.

10. SIMULATION OF SEISMIC SOURCE

10.1 SIMULATION OF A POINT SOURCE WITH ARBITRARY FOCAL MECHANISM USING A BODY-FORCE TERM

Before we start with the finite-difference approximations of the body-force term in the equation of motion, we will briefly review basic relations.

The **representation theorem** reads

$$u_n(\vec{x}, t) = \iint_{\Sigma} m_{pq} * G_{np,q} d\Sigma$$

where m_{pq} is the **moment-density tensor**

$$m_{pq}(\vec{\xi}, t) = c_{pqrs}(\vec{\xi}) [u_r(\vec{\xi}, t)] v_s(\vec{\xi})$$

where $\vec{\xi}$ specifies a position on a **fault surface** Σ , c_{pqrs} is a **tensor of elastic moduli**, $[\vec{u}]$ is a **slip vector** and \vec{v} is a fault normal. $G_{np,q}$ is a derivative of the **Green's tensor**. $G_{np,q}$ is physically an equivalent of having a single couple with an arm in the q-direction and forces in the p-direction on a fault surface Σ at $\vec{\xi}$. $m_{pq} * G_{np,q}$ is a displacement at \vec{x} due to couples at $\vec{\xi}$ and m_{pq} is the strength of the (p,q) couple.

In the point-source approximation surface Σ can be considered as a system of couples located at a point:

$$u_n(\vec{x}, t) = \left(\iint_{\Sigma} m_{pq} d\Sigma \right) * G_{np,q} .$$

The **moment tensor** M_{pq} is defined as

$$M_{pq} = \iint_{\Sigma} m_{pq} d\Sigma .$$

Then

$$u_n(\vec{x}, t) = M_{pq} * G_{np,q}$$

where M_{pq} is the strength of the resulting (p,q) couple at the point.

In the case of a tangential slip ($\vec{v} \cdot \vec{n} = 0$; $[\vec{u}] = \Delta u \vec{n}$, see Fig.10.1.1 for explanation) in an isotropic medium the moment-density tensor takes a simple form

$$m_{pq} = \mu (v_p[u_q] + v_q[u_p])$$

or

$$m_{pq} = \mu \Delta u (v_p n_q + v_q n_p) .$$

Then the moment tensor is

$$M_{pq} = \iint_{\Sigma} \mu \Delta u (v_p n_q + v_q n_p) d\Sigma .$$

Assuming a homogeneous medium in the source region or average μ we get

$$M_{pq} = \mu (v_p n_q + v_q n_p) \iint_{\Sigma} \Delta u(\vec{\xi}, t) d\Sigma .$$

The integral can be approximated:

$$\iint_{\Sigma} \Delta u(\vec{\xi}, t) d\Sigma \doteq \overline{\Delta u}(t) \iint_{\Sigma} d\Sigma = \overline{\Delta u}(t) A = \overline{\Delta u} s(t) A$$

where $s(t) = \frac{\overline{\Delta u}(t)}{\overline{\Delta u}}$ and $\overline{\Delta u} = \overline{\Delta u}(t \rightarrow \infty)$.

Then the moment tensor reads

$$M_{pq} = \mu A \overline{\Delta u} s(t) (v_p n_q + v_q n_p) .$$

The **scalar seismic moment** M_0 is defined as

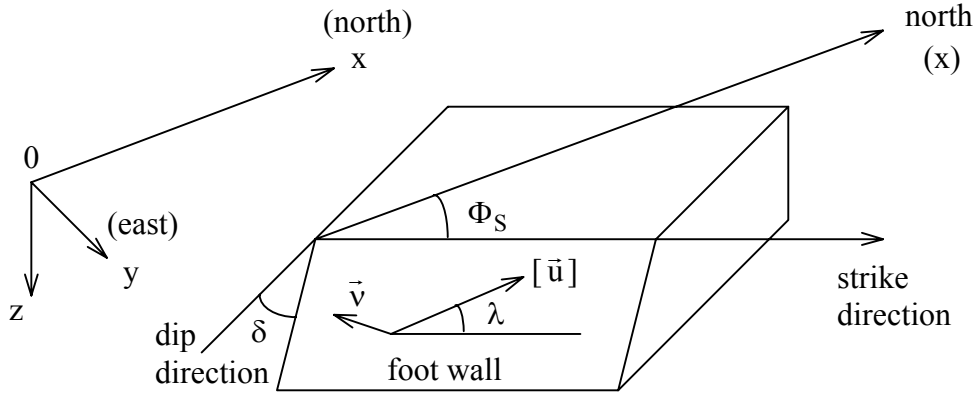
$$M_0 = \mu A \overline{\Delta u} .$$

Then for the tangential slip

$$M_{pq} = M_0 (v_p n_q + v_q n_p) s(t) . \quad (10.1.1)$$

In the coordinate system shown in Fig. 10.1.1 the components of the fault normal vector \vec{v} and vector \vec{n} are:

$$\begin{aligned} n_x &= \cos\lambda \cos\Phi_S + \cos\delta \sin\lambda \sin\Phi_S \\ n_y &= \cos\lambda \sin\Phi_S - \cos\delta \sin\lambda \cos\Phi_S \\ n_z &= -\sin\lambda \sin\delta \\ v_x &= -\sin\delta \sin\Phi_S \\ v_y &= \sin\delta \cos\Phi_S \\ v_z &= -\cos\delta \end{aligned} \quad (10.1.2)$$



Φ_S	strike	\vec{v}	fault normal
δ	dip	$[\vec{u}] = \Delta u \vec{n}$	
λ	rake	slip $[\vec{u}]$ taken as the movement of the hanging wall relative to the foot wall	

Fig. 10.1.1
Definition of the fault-orientation parameters and the coordinate system

From (10.1.1) and (10.1.2) follows

$$\begin{aligned}
 M_{xx}(t) &= -M_0 (\sin \delta \cos \lambda \sin 2\Phi_S + \sin 2\delta \sin \lambda \sin^2 \Phi_S) s(t) , \\
 M_{xy}(t) &= M_0 (\sin \delta \cos \lambda \cos 2\Phi_S + \frac{1}{2} \sin 2\delta \sin \lambda \sin 2\Phi_S) s(t) , \\
 M_{xz}(t) &= -M_0 (\cos \delta \cos \lambda \cos \Phi_S + \cos 2\delta \sin \lambda \sin \Phi_S) s(t) , \\
 M_{yy}(t) &= M_0 (\sin \delta \cos \lambda \sin 2\Phi_S - \sin 2\delta \sin \lambda \cos^2 \Phi_S) s(t) , \\
 M_{yz}(t) &= -M_0 (\cos \delta \cos \lambda \sin \Phi_S - \cos 2\delta \sin \lambda \cos \Phi_S) s(t) , \\
 M_{zz}(t) &= M_0 \sin 2\delta \sin \lambda s(t) .
 \end{aligned} \tag{10.1.3}$$

Due to the symmetry of the moment tensor

$$M_{xy} = M_{yx} , \quad M_{xz} = M_{zx} , \quad M_{yz} = M_{zy} .$$

We want to simulate a point dislocation source in the finite-difference scheme. This means a simulation of a system of the force-couples (p,q) with a strength M_{pq} acting at a grid point. A body-force term in the equation of motion provides such a possibility. Frankel (1993) proposed such an approach and used it in the displacement formulation on a conventional grid. Graves (1996) adapted the approach in the velocity-stress formulation on a staggered grid.

Consider, e.g., an (y,x) couple acting at a grid point (i_s, k_s, l_s) ; see Fig. 10.1.2.

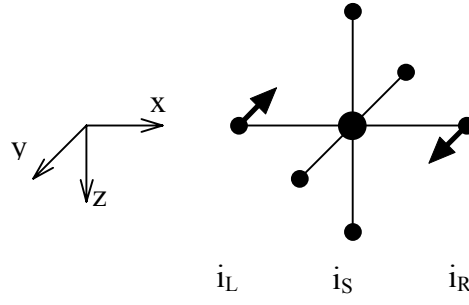


Fig. 10.1.2
Illustration of simulation of the (y,x) couple on the conventional grid

Then the corresponding body-force term in the equation of motion, i.e., f_y can be approximated as

$$f_y \doteq \frac{1}{h^3} \frac{1}{2h} M_{yx}(t) (\delta_{ii_R} \delta_{kk_R} \delta_{\ell\ell_R} - \delta_{ii_L} \delta_{kk_L} \delta_{\ell\ell_L})$$

where $2h$ is the arm length and $1/h^3$ normalizes the force to the unit volume.

Generally, assuming that the body-force couples act at the grid point $ik\ell$, for a conventional (i.e., not staggered) grid we get

$$\begin{aligned}
 F_{i+1k\ell}^x &= -F_{i-1k\ell}^x = \frac{1}{2h^4} M_{xx}(t) , \\
 F_{i+1k\ell}^y &= -F_{i-1k\ell}^y = \frac{1}{2h^4} M_{yx}(t) , \\
 F_{i+1k\ell}^z &= -F_{i-1k\ell}^z = \frac{1}{2h^4} M_{zx}(t) , \\
 F_{ik+1\ell}^x &= -F_{ik-1\ell}^x = \frac{1}{2h^4} M_{xy}(t) , \\
 F_{ik+1\ell}^y &= -F_{ik-1\ell}^y = \frac{1}{2h^4} M_{yy}(t) , \\
 F_{ik+1\ell}^z &= -F_{ik-1\ell}^z = \frac{1}{2h^4} M_{zy}(t) , \\
 F_{ik\ell+1}^x &= -F_{ik\ell-1}^x = \frac{1}{2h^4} M_{xz}(t) , \\
 F_{ik\ell+1}^y &= -F_{ik\ell-1}^y = \frac{1}{2h^4} M_{yz}(t) , \\
 F_{ik\ell+1}^z &= -F_{ik\ell-1}^z = \frac{1}{2h^4} M_{zz}(t) .
 \end{aligned} \tag{10.1.4}$$

In the case of a tangential slip $M_{pq}(t)$ is given by relation (10.1.1) or (10.1.3).

Simulation of the source on a staggered grid is slightly more complicated. This is because each displacement (or particle velocity) component is located in different position in the grid. Let us illustrate this in the x-z plane in the P-SV case. Assume the body-force couples acting at the grid point $i+1/2 \ell+1/2$ where T^{xx} and T^{zz} are located. Consider the x-component of the body-force term. Since this term is present in the equation for the u component we can apply it only in the grid positions where U is located.

Force couples having forces in the x-direction contribute to the f_x term. Consider first an (x,x) couple. This can be simulated at $i \ell+1/2$ and $i+1 \ell+1/2$ grid points; see Fig. 10.1.3.

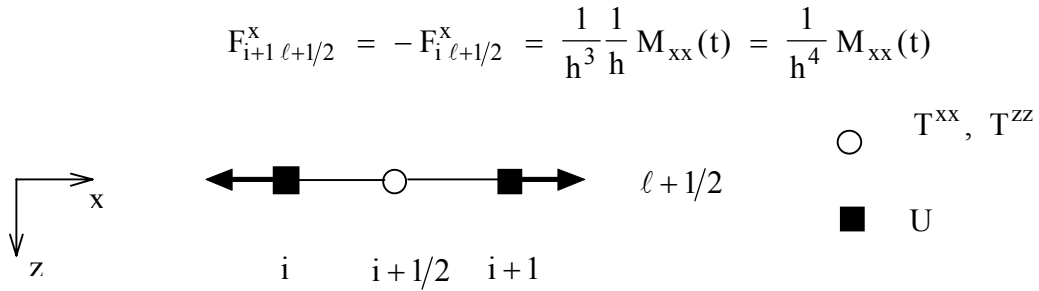


Fig. 10.1.3
Illustration of simulation of the (x,x) couple on the staggered grid

Consider now an (x,z) couple. We cannot simulate it at grid points $i+1/2 \ell+1$ and $i+1/2 \ell$, (i.e., analogously as in the case of a conventional grid) since U is not located at these grid points. We can consider, however, one couple along grid line $i+1$ and one couple along grid line i , i.e.,

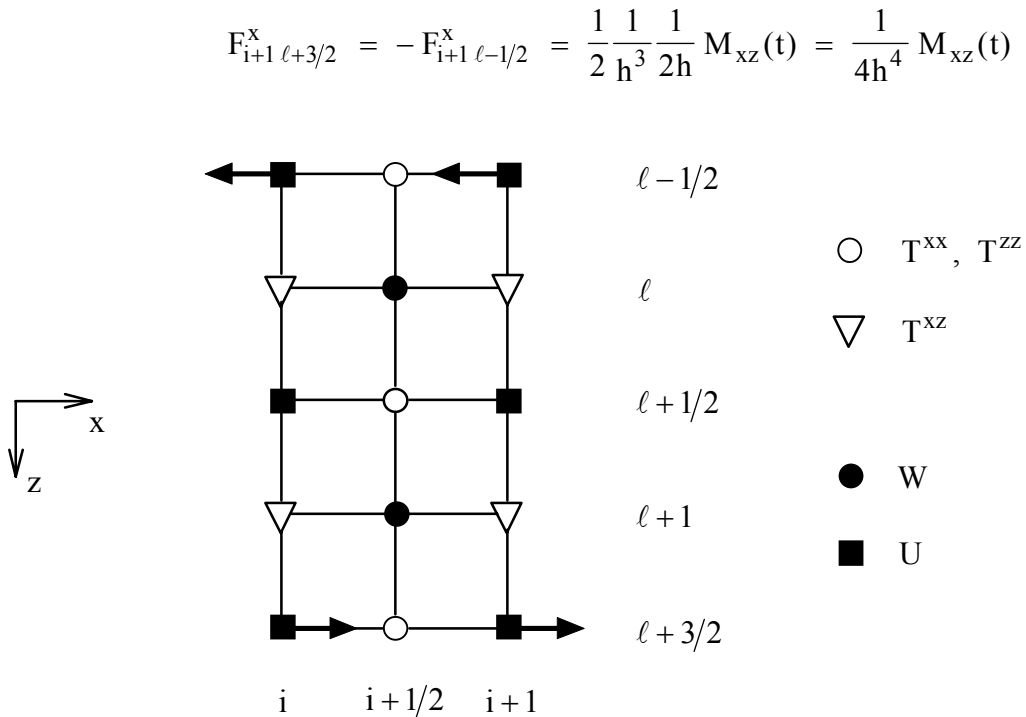


Fig. 10.1.4
Illustration of simulation of the (x,z) couple on the staggered grid

and

$$F_i^x \ell+3/2 = -F_i^x \ell-1/2 = \frac{1}{2} \frac{1}{h^3} \frac{1}{2h} M_{xz}(t) = \frac{1}{4h^4} M_{xz}(t)$$

(see Fig. 10.1.4) and take an average of the two couples.

Generally, assuming the body-force couples acting at the grid point $i+1/2 \ k+1/2 \ \ell+1/2$, for a staggered grid with T^{xx} , T^{yy} and T^{zz} located at the grid point $i+1/2 \ k+1/2 \ \ell+1/2$, we get

$$\begin{aligned}
F_{i+1}^x \ k+1/2 \ \ell+1/2 &= -F_i^x \ k+1/2 \ \ell+1/2 = \frac{1}{h^4} M_{xx}(t) \\
F_{i+1}^x \ k+3/2 \ \ell+1/2 &= -F_{i+1}^x \ k-1/2 \ \ell+1/2 = \frac{1}{4h^4} M_{xy}(t) \\
F_i^x \ k+3/2 \ \ell+1/2 &= -F_i^x \ k-1/2 \ \ell+1/2 = \frac{1}{4h^4} M_{xy}(t) \\
F_{i+1}^x \ k+1/2 \ \ell+3/2 &= -F_{i+1}^x \ k+1/2 \ \ell-1/2 = \frac{1}{4h^4} M_{xz}(t) \\
F_i^x \ k+1/2 \ \ell+3/2 &= -F_i^x \ k+1/2 \ \ell-1/2 = \frac{1}{4h^4} M_{xz}(t) \\
\\
F_{i+1/2 \ k+1}^y \ \ell+1/2 &= -F_{i+1/2 \ k}^y \ \ell+1/2 = \frac{1}{h^4} M_{yy}(t) \\
F_{i+3/2 \ k+1}^y \ \ell+1/2 &= -F_{i-1/2 \ k+1}^y \ \ell+1/2 = \frac{1}{4h^4} M_{yx}(t) \\
F_{i+3/2 \ k}^y \ \ell+1/2 &= -F_{i-1/2 \ k}^y \ \ell+1/2 = \frac{1}{4h^4} M_{yx}(t) \quad (10.1.5) \\
F_{i+1/2 \ k+1}^y \ \ell+3/2 &= -F_{i+1/2 \ k+1}^y \ \ell-1/2 = \frac{1}{4h^4} M_{yz}(t) \\
F_{i+1/2 \ k}^y \ \ell+3/2 &= -F_{i+1/2 \ k}^y \ \ell-1/2 = \frac{1}{4h^4} M_{yz}(t) \\
\\
F_{i+1/2 \ k+1/2 \ \ell+1}^z &= -F_{i+1/2 \ k+1/2 \ \ell}^z = \frac{1}{h^4} M_{zz}(t) \\
F_{i+3/2 \ k+1/2 \ \ell+1}^z &= -F_{i-1/2 \ k+1/2 \ \ell+1}^z = \frac{1}{4h^4} M_{zx}(t) \\
F_{i+3/2 \ k+1/2 \ \ell}^z &= -F_{i-1/2 \ k+1/2 \ \ell}^z = \frac{1}{4h^4} M_{zx}(t) \\
F_{i+1/2 \ k+3/2 \ \ell+1}^z &= -F_{i+1/2 \ k-1/2 \ \ell+1}^z = \frac{1}{4h^4} M_{zy}(t) \\
F_{i+1/2 \ k+3/2 \ \ell}^z &= -F_{i+1/2 \ k-1/2 \ \ell}^z = \frac{1}{4h^4} M_{zy}(t)
\end{aligned}$$

Equations (10.1.5) can be rewritten replacing actual-position indices by indices corresponding to the finite-difference cells (see Section 4.1):

$$\begin{aligned}
F_{i+1\ k\ \ell}^x &= -F_{i\ k\ \ell}^x = \frac{1}{h^4} M_{xx}(t) \\
F_{i+1\ k+1\ \ell}^x &= -F_{i+1\ k-1\ \ell}^x = \frac{1}{4h^4} M_{xy}(t) \\
F_{i\ k+1\ \ell}^x &= -F_{i\ k-1\ \ell}^x = \frac{1}{4h^4} M_{xy}(t) \\
F_{i+1\ k\ \ell+1}^x &= -F_{i+1\ k\ \ell-1}^x = \frac{1}{4h^4} M_{xz}(t) \\
F_{i\ k\ \ell+1}^x &= -F_{i\ k\ \ell-1}^x = \frac{1}{4h^4} M_{xz}(t) \\
\\
F_{i\ k+1\ \ell}^y &= -F_{i\ k\ \ell}^y = \frac{1}{h^4} M_{yy}(t) \\
F_{i+1\ k+1\ \ell}^y &= -F_{i-1\ k+1\ \ell}^y = \frac{1}{4h^4} M_{yx}(t) \\
F_{i+1\ k\ \ell}^y &= -F_{i-1\ k\ \ell}^y = \frac{1}{4h^4} M_{yx}(t) \\
F_{i\ k+1\ \ell+1}^y &= -F_{i\ k+1\ \ell-1}^y = \frac{1}{4h^4} M_{yz}(t) \\
F_{i\ k\ \ell+1}^y &= -F_{i\ k\ \ell-1}^y = \frac{1}{4h^4} M_{yz}(t) \\
\\
F_{i\ k\ \ell+1}^z &= -F_{i\ k\ \ell}^z = \frac{1}{h^4} M_{zz}(t) \\
F_{i+1\ k\ \ell+1}^z &= -F_{i-1\ k\ \ell+1}^z = \frac{1}{4h^4} M_{zx}(t) \\
F_{i+1\ k\ \ell}^z &= -F_{i-1\ k\ \ell}^z = \frac{1}{4h^4} M_{zx}(t) \\
F_{i\ k+1\ \ell+1}^z &= -F_{i\ k-1\ \ell+1}^z = \frac{1}{4h^4} M_{zy}(t) \\
F_{i\ k+1\ \ell}^z &= -F_{i\ k-1\ \ell}^z = \frac{1}{4h^4} M_{zy}(t)
\end{aligned} \tag{10.1.6}$$

Equations (10.1.6) with the finite-difference cell indices are ready for programming.

In the case of the source acting at the grid point $ik\ell$ in the staggered grid with T^{xx} , T^{yy} and T^{zz} located at the grid point $ik\ell$ we would obtain

$$\begin{aligned}
F_{i+1/2 \ k \ \ell}^x &= -F_{i-1/2 \ k \ \ell}^x = \frac{1}{h^4} M_{xx}(t) \\
F_{i+1/2 \ k+1 \ \ell}^x &= -F_{i+1/2 \ k-1 \ \ell}^x = \frac{1}{4h^4} M_{xy}(t) \\
F_{i-1/2 \ k+1 \ \ell}^x &= -F_{i-1/2 \ k-1 \ \ell-1/2}^x = \frac{1}{4h^4} M_{xy}(t) \\
F_{i+1/2 \ k \ \ell+1}^x &= -F_{i+1/2 \ k \ \ell-1}^x = \frac{1}{4h^4} M_{xz}(t) \\
F_{i-1/2 \ k \ \ell+1}^x &= -F_{i-1/2 \ k \ \ell-1}^x = \frac{1}{4h^4} M_{xz}(t) \\
\\
F_i^y \ k+1/2 \ \ell &= -F_i^y \ k-1/2 \ \ell = \frac{1}{h^4} M_{yy}(t) \\
F_{i+1}^y \ k+1/2 \ \ell &= -F_{i-1}^y \ k+1/2 \ \ell = \frac{1}{4h^4} M_{yx}(t) \\
F_{i+1}^y \ k-1/2 \ \ell &= -F_{i-1}^y \ k-1/2 \ \ell = \frac{1}{4h^4} M_{yx}(t) \quad (10.1.7) \\
F_i^y \ k+1/2 \ \ell+1 &= -F_i^y \ k+1/2 \ \ell-1 = \frac{1}{4h^4} M_{yz}(t) \\
F_i^y \ k-1/2 \ \ell+1 &= -F_i^y \ k-1/2 \ \ell-1 = \frac{1}{4h^4} M_{yz}(t) \\
\\
F_i^z \ k \ \ell+1/2 &= -F_i^z \ k \ \ell-1/2 = \frac{1}{h^4} M_{zz}(t) \\
F_{i+1}^z \ k \ \ell+1/2 &= -F_{i-1}^z \ k \ \ell+1/2 = \frac{1}{4h^4} M_{zx}(t) \\
F_{i+1}^z \ k \ \ell-1/2 &= -F_{i-1}^z \ k \ \ell-1/2 = \frac{1}{4h^4} M_{zx}(t) \\
F_i^z \ k+1 \ \ell+1/2 &= -F_i^z \ k-1 \ \ell+1/2 = \frac{1}{4h^4} M_{zy}(t) \\
F_i^z \ k+1 \ \ell-1/2 &= -F_i^z \ k-1 \ \ell-1/2 = \frac{1}{4h^4} M_{zy}(t)
\end{aligned}$$

For alternative approaches to the implementation of the source see, for example, Yomogida & Etgen (1993), Coutant et al. (1995), and Olsen et al. (1995).

10.2 DECOMPOSITION OF THE WAVEFIELD

Let \vec{S} be a displacement due to a source. Then the **total displacement** \vec{U} is

$$\vec{U} = \vec{S} + \vec{U}_R \quad (10.2.1)$$

where \bar{U}_R is a displacement corresponding to the **residual** (or **scattered**) wavefield.

Consider now rectangles (or squares) **a** and **b** on a conventional rectangular grid (see Fig. 10.2.1). Let us assume the source located inside rectangle **b**.

Using decomposition (10.2.1) we can compute the total wavefield outside rectangle **b** without introducing source term in the finite-difference scheme used inside rectangle **b** or prescribing displacement at the grid points inside rectangle **b**. \bar{U}_R inside and on rectangle **b** can be computed by the finite-difference scheme (a second-order scheme is assumed; a fourth-order scheme would require more rectangles). \bar{U}_R on rectangle **a** is computed as

$$\bar{U}_R(\mathbf{a}) = \bar{U}(\mathbf{a}) - \bar{S}(\mathbf{a}) . \quad (10.2.2)$$

\bar{U} on rectangle **b** is computed as

$$\bar{U}(\mathbf{b}) = \bar{S}(\mathbf{b}) + \bar{U}_R(\mathbf{b}) . \quad (10.2.3)$$

\bar{U} outside rectangle **b** (i. e., starting on rectangle **a**) is computed by the finite-difference scheme.

Such an indirect wavefield excitation was proposed by Alterman & Karal (1968). It was applied later by Vidale & Helmberger (1987) in the fourth-order modeling.

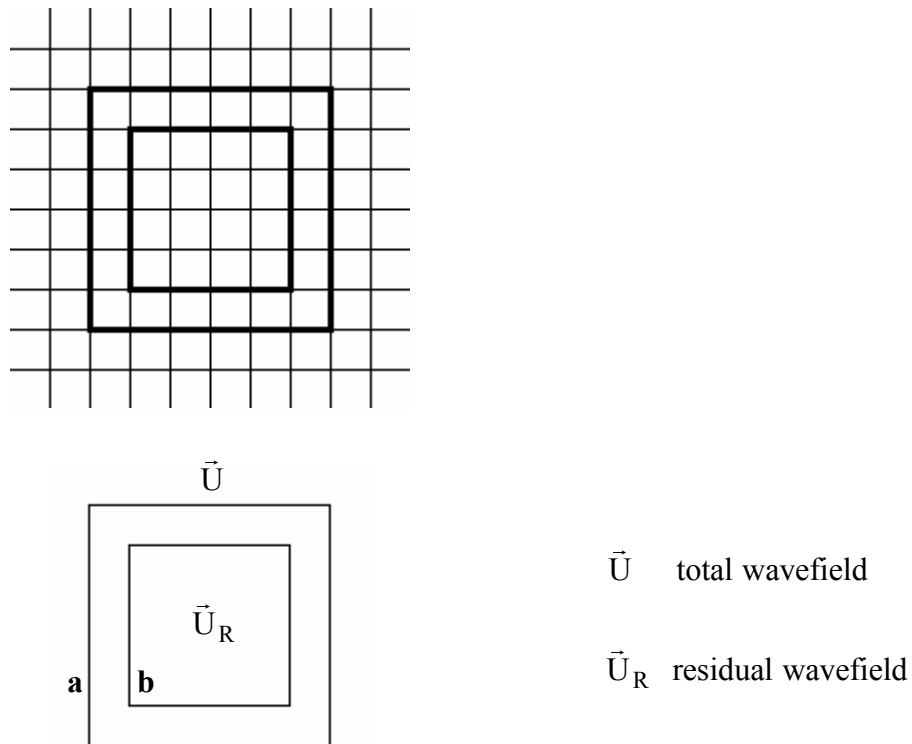


Fig. 10.2.1
Excitation rectangles **a** and **b**

A special case when only two, the so-called excitation lines are used for a wavefield excitation (e.g., Moczo, 1989) is illustrated in Fig. 10.2.2.

In this case \bar{U}_R on line **b** and below line **b** is computed by the finite-difference scheme. \bar{U}_R on line **a** is computed according to equation (10.2.2). \bar{U} on line **b** is computed according to equation (10.2.3). \bar{U} on line **a** and above line **a** is computed by the finite-difference scheme.

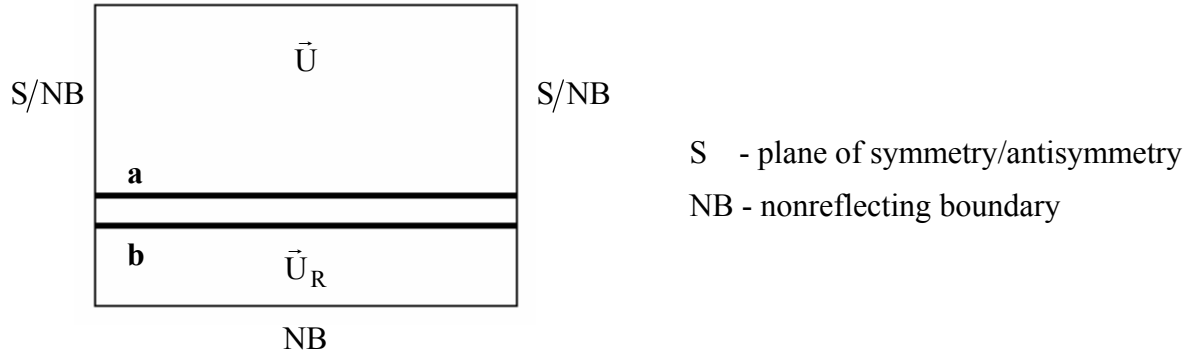


Fig. 10.2.2
Excitation lines **a** and **b**

A third example of an indirect wavefield excitation is a part of the two-step hybrid computation (Zahradník, 1995a, Zahradník & Moczo, 1996, Moczo et al., 1997) as it is illustrated in Fig. 10.2.3.

In the 1st step, the wavefield is recorded along lines **a** and **b**. This wavefield, \bar{U}_K , consists of the wavefield radiated from the source (incident wavefield) and also of that reflected from the free surface (this is important).

In the 2nd step

- \bar{U}_R on rectangle **b** and inside the region bounded by rectangle **b**, nonreflecting (NB) boundaries and free surface (including) is computed by the finite-difference scheme,
- \bar{U}_R on rectangle **a** is computed as

$$\bar{U}_R(\mathbf{a}) = \bar{U}(\mathbf{a}) - \bar{U}_K(\mathbf{a}), \quad (10.2.4)$$

- \bar{U} on rectangle **b** is computed as

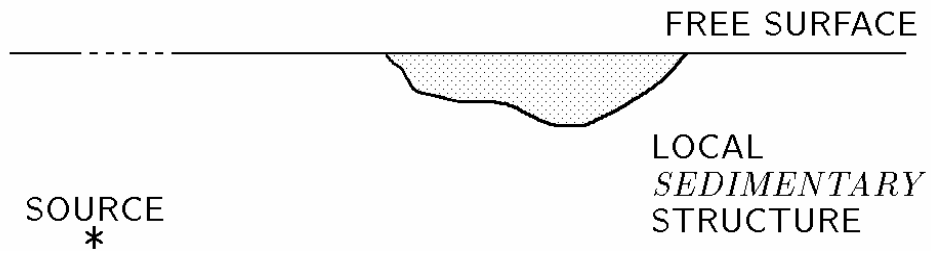
$$\bar{U}(\mathbf{b}) = \bar{U}_K(\mathbf{b}) + \bar{U}_R(\mathbf{b}), \quad (10.2.5)$$

- \bar{U} on rectangle **a**, inside the region bounded by **a** and the free surface (including) is computed by the finite-difference scheme.

The use of the discrete-wavenumber method is not necessary - the source radiation and background wave propagation can be computed by any suitable method.

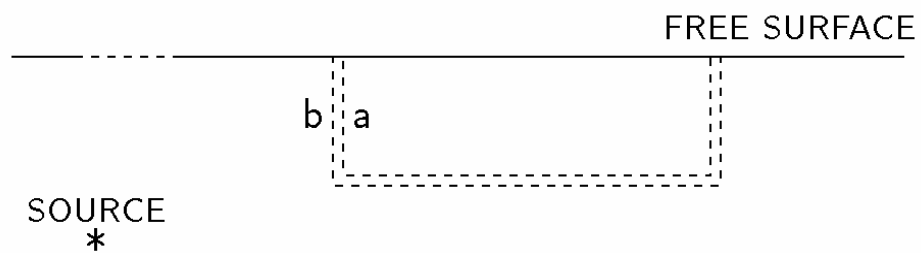
For the indirect excitation at two vertical grid lines see Fähr (1992) and Fähr et al. (1993).

PROBLEM CONFIGURATION



TWO-STEP SOLUTION

1st STEP: DW COMPUTATION



2nd STEP: FD COMPUTATION

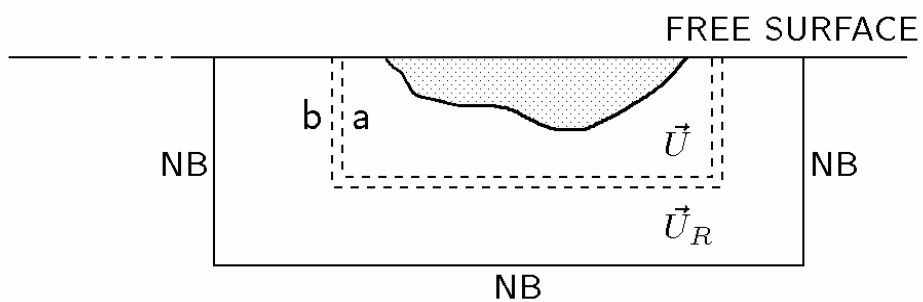


Fig. 10.2.3

Scheme of the hybrid discrete-wavenumber – finite-difference method. DW – discrete wavenumber method, FD – finite-difference method.

11. SIMULATION OF NONREFLECTING BOUNDARIES

The spatial finite-difference grid is bounded by artificial boundaries. In an ideal case these boundaries should be perfectly transparent for any wave impinging on the boundary. Generally we only can approximate transparency. Many different techniques were developed to simulate the so-called absorbing or nonreflecting boundaries. We will briefly mention some of them.

11.1 ARTIFICIAL DAMPING ZONE

A simple technique to simulate nonreflecting boundary condition was suggested by Cerjan et al. (1985). In their approach a useful part of a spatial grid is surrounded by a boundary zone A as it is shown in Fig. 11.1.1. The zone is defined by a number of grid lines N and the attenuating function A(i).

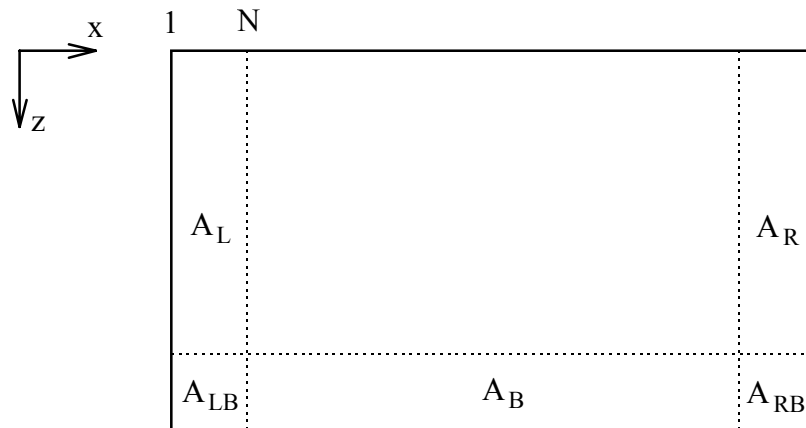


Fig. 11.1.1
Artificial damping zone A consisting of a strip of N grid lines

Displacement values or particle-velocity values corresponding to both the updated and previous time levels are reduced (multiplied by A(i)) after each time step.

Cerjan et al. (1985) used function A defined, for example, for the left boundary zone as

$$A_L(i) = \exp\left[-(c(N-i))^2\right] ; \quad 1 \leq i \leq N ,$$

$$A_L(i) = 1 ; \quad i > N .$$

Requiring that

$$A_L(1) = A_0 \quad \text{and} \quad A_L(N) = 1.0$$

coefficient c is determined as

$$c = \frac{1}{N-1} (-\ln A_0)^{1/2} .$$

Virieux suggested the function

$$A(x) = A_0 + \frac{1}{2} (1 - A_0) \left[1 - \cos \left(\frac{\pi (x-1)}{A_w - 1} \right) \right] ; \quad 1 \leq x \leq A_w ,$$

$$A(x) = 1 \quad ; \quad x > A_w .$$

Its first derivative at $x = A_w$ is continuous. The function for a discrete argument is

$$A_L(i) = A_0 + \frac{1}{2} (1 - A_0) \left[1 - \cos \left(\frac{\pi (i-1)}{N-1} \right) \right] ; \quad 1 \leq i \leq N ,$$

$$A_L(i) = 1 \quad ; \quad i > N .$$

Usually $N \geq 20$ is necessary and A_0 should not be smaller than 0.92. It is recommended to properly adjust values of N and A_0 for the problem under consideration.

In the corner zone, e. g., A_{LB} , the attenuating function is given by a product $A_L(i)A_B(\ell)$, where ℓ is a discrete argument in the $-z$ -direction.

The artificial damping zone can be combined with some finite-difference scheme that is applied at the boundary grid lines ($i = 1$ in the case of the left boundary) and approximately simulates a nonreflecting boundary.

11.2 SHOCK ABSORBER ZONE

Sochacki et al. (1987) suggested a different type of the boundary zone to simulate nonreflecting boundaries. It is based on inclusion of a damping term in the equation of motion. Consider, for example, the equation for the u component of displacement

$$u_{tt} + 2A u_t = \frac{1}{\rho} \square$$

where A is a damping function and \square represents the right-hand side of the equation of motion. Then we can obtain the finite-difference scheme which can be symbolically written as

$$U^{m+1} = \frac{1}{1 + \Delta t A} \left[2U^m - (1 - \Delta t A)U^{m-1} + \frac{\Delta^2 t}{\rho} \square_{\Delta} \right]$$

where \square_{Δ} represents the finite-difference approximation of \square .

An example for the right-bottom corner zone (shown in Fig. 11.2.1) can be

$$A_{RB}(x, z) = \left[\frac{(x - x_0)(z - z_0)}{h^2} \right]^C ; \quad \begin{array}{l} x_0 < x \leq x_R \\ z_0 < z \leq z_B \end{array}$$

$$C = \frac{\ln A_0}{\ln ab - 2 \ln h} ,$$

h being a grid spacing. Similarly as in the case of the artificial damping zone, it is necessary to properly adjust parameters a , b and A_0 for the problem under consideration.

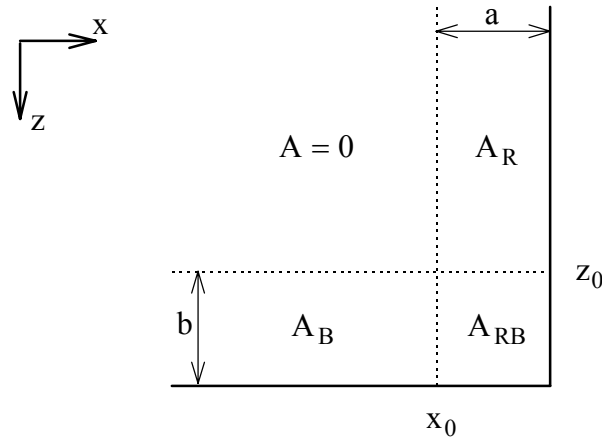


Fig. 11.2.1
Illustration of the shock absorber zone for the right-bottom corner

For a different type of the absorbing boundary zone based on two additional damping terms in the equation of motion see Korn & Stöckl (1982).

11.3 APPROXIMATE ABSORBING BOUNDARY CONDITIONS

One possible approach is to apply a paraxial (one-way) wave equation at the artificial grid boundary since such an equation only permits energy propagation in a limited range of angles. An example of the first-order paraxial equation can be the equation for the SH-wave propagating in the x -direction,

$$\frac{1}{\beta} v_t + v_x = 0 .$$

An example of the second-order approximation is

$$\frac{1}{\beta} v_{tt} + v_{tx} - \frac{\beta}{2} v_{zz} = 0 .$$

Paraxial equations can be replaced by the finite-difference schemes which are then applied at the boundary. This approach was first used by Clayton & Engquist (1977) and then by, for example, Fuyuki & Matsumoto (1980), Emerman & Stephen (1983) and Stacey (1988).

Emerman & Stephen (1983) showed that the Clayton & Engquist's condition is unstable for $\beta/\alpha < 0.46$. Stacey (1988) showed stability of his condition for $\alpha/\beta < 2.2$. Emerman & Stephen (1983) suggested a modification of the Clayton & Engquist (1977) condition which is stable for any $\beta/\alpha > 0$.

Another approach is based on minimizing the coefficient of reflection at the artificial boundary such as in Reynolds (1978) and Peng & Toksöz (1994, 1995).

Higdon (1991) developed an approximation of the absorbing boundary condition that is based on the composition of simple first-order differential operators. Each operator gives perfect absorption for a plane wave impinging on the boundary at certain velocity and angle of incidence. An example of the finite-difference scheme simulating the boundary condition can be obtained by approximating the operator

$$\left[\left(\cos\theta_P \frac{\partial}{\partial t} - \alpha \frac{\partial}{\partial x} \right) \right] \left[\left(\cos\theta_S \frac{\partial}{\partial t} - \beta \frac{\partial}{\partial x} \right) \right]$$

applied to each component of displacement. Here, θ_P and α (θ_S and β) are angle of incidence of the P-wave and the P-wave velocity (angle of incidence of the S-wave and the S-wave velocity), respectively.

We will finish with a unified representation of several boundary conditions. Consider, e. g., the left boundary. A displacement value $U_{1k\ell}^{m+1}$ can be updated according to the formula

$$\begin{aligned} U_{1k\ell}^{m+1} = & A_{01} U_{2k\ell}^{m+1} + A_{02} U_{3k\ell}^{m+1} \\ & + A_{10} U_{1k\ell}^m + A_{11} U_{2k\ell}^m + A_{12} U_{3k\ell}^m \\ & + A_{20} U_{1k\ell}^{m-1} + A_{21} U_{2k\ell}^{m-1} + A_{22} U_{3k\ell}^{m-1} \end{aligned} \quad (11.3.1)$$

where the coefficients A_{pq} ; $p, q \in \{0,1,2\}$ are given in Tab. 11.3.1.

In the table, Δt is the time step, h is the grid spacing, c is the velocity and

$$q_{ix} = \frac{b(a_i + v) - v}{(a_i + v)(1 - b)} ,$$

$$q_{it} = \frac{b(a_i + v) - a_i}{(a_i + v)(1 - b)} ,$$

$$q_{ixt} = \frac{b}{b - 1}$$

where $v = \alpha \Delta t/h$, α being the P-wave velocity, $i \in \{1,2\}$, and b is a weighting coefficient. Parameters a_i are the positive dimensionless constants.

	Clayton & Engquist (A1) 1977	Reynolds 1978	Emerman & Stephen 1983	Higdon 1991
A_{00}	0	0	0	0
A_{01}	0	0	$\frac{\Delta t - h/c}{\Delta t + h/c}$	$-(q_{1x} + q_{2x})$
A_{02}	0	0	0	$-q_{1x} q_{2x}$
A_{10}	$1 - \frac{c \Delta t}{h}$	$1 - \frac{c \Delta t}{h}$	$\frac{2h/c}{\Delta t + h/c}$	$-(q_{1t} + q_{2t})$
A_{11}	$\frac{c \Delta t}{h}$	$1 + \frac{c \Delta t}{h}$	$\frac{2h/c}{\Delta t + h/c}$	$-(q_{1x} q_{2t} + q_{1t} q_{2x} + q_{1xt} + q_{2xt})$
A_{12}	0	0	0	$-(q_{1x} q_{2xt} + q_{2x} q_{1xt})$
A_{20}	0	0	$\frac{\Delta t - h/c}{\Delta t + h/c}$	$-q_{1t} q_{2t}$
A_{21}	0	$-1 - \frac{c \Delta t}{h}$	-1	$-(q_{1t} q_{2xt} + q_{2t} q_{1xt})$
A_{22}	0	$\frac{c \Delta t}{h}$	0	$-q_{1xt} q_{2xt}$

Tab. 11.3.1
Coefficients of the absorbing boundary conditions (11.3.1)

The boundary condition developed by Peng & Toksöz (1994, 1995) is represented in the form (11.3.1); however, the formulae for the A_{pq} coefficients are rather lengthy.

The boundary condition (11.3.1) can be applied to different components of the displacement or particle velocity with different values of parameters.

An interesting approach to making use of the boundary conditions developed for the P-SV case in the 3D modeling was suggested by Chang & McMechan (1989).

Numerical experience with different types of the absorbing boundary conditions indicates that there is no best absorbing boundary condition which would be universally (i. e., in all wavefield configurations) both sufficiently accurate and stable. A user of the finite-difference method is recommended to be able to use several different techniques.

12. CONCLUDING REMARKS

The finite-difference method is the most popular and widely used numerical method for modeling seismic wave propagation and earthquake ground motion. There are several reasons for this. The method is relatively simple. It is applicable to complex media. The finite-difference scheme is relatively easy to implement in computer codes.

It is also important that the finite-difference method is considerably simpler than the finite-element method and mainly it requires less computer time and memory than the finite-element method.

The advantages of the finite-difference method with respect to the finite-element method are reasons why the finite-difference method has been recently used for the three-dimensional simulations of seismic ground motion due to major earthquakes in California and Japan.

At the same time each user of the finite-difference method should be aware of the major problems of the method when applied to complex media (e.g., laterally inhomogeneous media with irregular nonplanar interfaces between layers and blocks, and, possibly, also with free-surface topography). It is not trivial to model nonplanar internal material discontinuities and, mainly, free-surface topography in a sufficiently accurate and stable manner. Implementation of conditions on boundaries of complex shapes is a general and inherent problem of the finite-difference method. (Satisfying boundary conditions is much easier for the finite-element method.)

Another important aspect of applying the finite-difference method to realistic problems is a limitation imposed by available computer memory and power. Memory optimization algorithms and sophisticated programming are necessary for such applications.

The existing finite-difference schemes differ from each other by accuracy, stability and computational efficiency. There is no best scheme which would be the most accurate, stable and efficient in all seismic wave propagation and ground motion problems. A seismologist should not only choose a scheme which is the most appropriate for the problem to be solved but also check the accuracy of a particular numerical computation. It is important to keep in mind that when not properly treated the finite-difference method can give noticeably inaccurate results. On the other hand, when properly treated, the finite-difference method is a very strong tool in modeling seismic wave propagation and earthquake ground motion.

REFERENCES

This is a list of selected, mostly recent papers which are directly related to the presented material and contribute methodologically to the application of the finite-difference method to seismic wave propagation problems.

PART A : INTRODUCTION

1. Solving Partial Differential Equations by the Finite-Difference Method

1.1 Introduction to the Finite-Difference Method

Forsythe, G.E. and W.R. Wasow, 1960. Finite Difference Methods for Partial Differential Equations. J. Wiley & Sons, New York.

Isaacson, E. and H.B. Keller, 1966. Analysis of Numerical Methods. J. Wiley & Sons, New York.

Richtmyer, R.D. and K.W. Morton, 1967. Difference Methods for Initial Value Problems. J. Wiley & Sons, New York; (reprinted by Kreiger, New York, 1994).

Mitchell, A.R. and D.F. Griffiths, 1980. The Finite Difference Method in Partial Differential Equations. J. Wiley & Sons, New York.

Morton, K.W. and D.F. Mayers, 1994. Numerical Solution of Partial Differential Equations. Cambridge University Press.

1.2 Example: Case of the One-Dimensional Wave Equation

Aki, K. and P.G. Richards, 1980. Quantitative Seismology. Theory and Methods, Vol. II. W.H.Freeman & Co., San Francisco

PART B : APPLICATION OF THE FINITE-DIFFERENCE METHOD TO THE EQUATION OF MOTION IN A PERFECTLY ELASTIC MEDIUM

2. Equation of Motion

Aki, K. and P.G. Richards, 1980. Quantitative Seismology. Theory and Methods, Vol. I. W.H.Freeman & Co., San Francisco.

3. Heterogeneous Formulation of the Equation of Motion and Heterogeneous Finite-Difference Schemes

Zahradník, J., P. Moczo and F. Hron, 1993. Testing four elastic finite-difference schemes for behaviour at discontinuities. *Bull. Seism. Soc. Am.*, 83, 107-129.

Zahradník, J. and E. Priolo, 1995. Heterogeneous formulations of elastodynamic equations and finite-difference schemes. *Geophys. J. Int.*, 120, 663-676.

4. Finite-Difference Schemes for Interior Points on Regular Grids

4.1 Displacement-Stress Scheme on a Staggered Grid

Luo, Y. and G. Schuster, 1990. Parsimonious staggered grid finite-differencing of the wave equation. *Geophys. Res. Lett.*, 17, 155-158.

Ohminato, T. and B.A. Chouet, 1997. A free-surface boundary condition for including 3D topography in the finite-difference method. *Bull. Seism. Soc. Am.*, 87, 494-515.

4.2 Velocity-Stress Scheme on a Staggered Grid

Madariaga, R., 1976. Dynamics of an expanding circular fault. *Bull. Seism. Soc. Am.*, 67, 163-182.

Virieux, J. and R. Madariaga, 1982. Dynamic faulting studied by a finite difference method. *Bull. Seism. Soc. Am.*, 72, 345-369.

Virieux, J., 1984. SH-wave propagation in heterogeneous media: velocity-stress finite-difference method. *Geophysics*, 49, 1933-1957.

Virieux, J., 1986. P-SV wave propagation in heterogeneous media: velocity-stress finite-difference method. *Geophysics*, 51, 889-901.

Levander, A.R., 1988. Fourth-order finite-difference P-SV seismograms. *Geophysics*, 53, 1425-1436.

Graves, R.W., 1996. Simulating seismic wave propagation in 3D elastic media using staggered-grid finite differences. *Bull. Seism. Soc. Am.*, 86, 1091-1106.

4.3 Displacement Scheme on a Conventional Grid

Alterman, Z. and F.C. Karal, 1968. Propagation of elastic waves in layered media by finite-difference methods. *Bull. Seism. Soc. Am.*, 58, 367-398.

Kelly, K.R., R.W. Ward, S. Treitel and R.M. Alford, 1976. Synthetic seismograms: a finite-difference approach. *Geophysics*, 41, 2-27.

Kummer, B. and A. Behle, 1982. Second-order finite-difference modeling of SH-wave propagation in laterally inhomogeneous media. *Bull. Seism. Soc. Am.*, 72, 793-808.

Kummer, B., A. Behle and F. Dorau, 1987. Hybrid modeling of elastic-wave propagation in two-dimensional laterally inhomogeneous media. *Geophysics*, 52, 765-771.

Zahradnik, J., 1995b. Simple elastic finite-difference scheme. *Bull. Seism. Soc. Am.*, 85, 1879-1887.

Zahradnik, J. and E. Priolo, 1995. Heterogeneous formulations of elastodynamic equations and finite-difference schemes. *Geophys. J. Int.*, 120, 663-676.

Moczo, P., E. Bystrický, J. Kristek, J.M. Carcione and M. Bouchon, 1997. Hybrid modeling of P-SV seismic motion at inhomogeneous viscoelastic topographic structures. *Bull. Seism. Soc. Am.*, 87, 1305-1323.

5. Fourth-Order Finite-Difference Schemes for Interior Grid Points

5.1 Fourth-Order Finite-Difference Approximations

Dablain, M.A., 1986. The application of high-order differencing to the scalar wave equation. *Geophysics*, 51, 54-66.

Yomogida, K. and J.T. Etgen, 1993. 3-D wave propagation in the Los Angeles basin for the Whittier-Narrows earthquake. *Bull. Seism. Soc. Am.*, 83, 1325-1344.

5.3 Velocity-Stress Scheme on a Staggered Grid

Levander, A.R., 1988. Fourth-order finite-difference P-SV seismograms. *Geophysics*, 53, 1425-1436.

Graves, R.W., 1996. Simulating seismic wave propagation in 3D elastic media using staggered-grid finite differences. *Bull. Seism. Soc. Am.*, 86, 1091-1106.

6. Finite-Difference Schemes for Interior Points on Irregular Rectangular Grids

Boore, D.M., 1970. Love waves in nonuniform waveguides: finite difference calculations. *J. Geophys. Res.*, 75, 1512-1527.

Mikumo, T. and T. Miyatake, 1987. Numerical modeling of realistic fault rupture processes. In: *Seismic strong motion synthetics*, B.A. Bolt, ed., Academic Press, 91-151.

Moczo, P., 1989. Finite-difference technique for SH-waves in 2-D media using irregular grids - application to the seismic response problem. *Geophys. J. Int.*, 99, 321-329.

Moczo, P. and P.-Y. Bard, 1993. Wave diffraction, amplification and differential motion near strong lateral discontinuities. *Bull. Seism. Soc. Am.*, 83, 85-106.

7. Finite-Difference Schemes for Interior Points on a Combined Rectangular Grid

Jastram, C. and E. Tessmer, 1994. Elastic modelling on a grid with vertically varying spacing. *Geophysical Prospecting*, 42, 357-370.

Falk, J., E. Tessmer and D. Gajewski, 1996. Tube wave modelling by the finite-differences method with varying grid spacing. *Pageoph*, 148, 77-93.

Moczo, P., P. Labák, J. Kristek and F. Hron, 1996. Amplification and differential motion due to an antiplane 2D resonance in the sediment valleys embedded in a layer over the halfspace. *Bull. Seism. Soc. Am.*, 86, 1434-1446.

8. Stability Condition and Dispersion Relations

Virieux, J., 1986. P-SV wave propagation in heterogeneous media: velocity-stress finite-difference method. *Geophysics*, 51, 889-901.

Levander, A.R., 1988. Fourth-order finite-difference P-SV seismograms. *Geophysics*, 53, 1425-1436.

9. Approximation of Traction-Free Surface

Moczo, P., E. Bystrický, J. Kristek, J.M. Carcione and M. Bouchon, 1997. Hybrid modeling of P-SV seismic motion at inhomogeneous viscoelastic topographic structures. *Bull. Seism. Soc. Am.*, 87, 1305-1323.

Ohminato, T. and B.A. Chouet, 1997. A free-surface boundary condition for including 3D topography in the finite-difference method. *Bull. Seism. Soc. Am.*, 87, 494-515.

9.2 Approximation of the Free Surface in the Velocity-Stress Formulation

Levander, A.R., 1988. Fourth-order finite-difference P-SV seismograms. *Geophysics*, 53, 1425-1436.

Graves, R.W., 1996. Simulating seismic wave propagation in 3D elastic media using staggered-grid finite differences. *Bull. Seism. Soc. Am.*, 86, 1091-1106.

Pitarka, A. and K. Irikura, 1996. Modeling 3D surface topography by finite-difference method: Kobe-JMA station site, Japan, case study. *Geophys. Res. Lett.*, 23, 2729-2732.

Robertsson, J.O.A., 1996. A numerical free-surface condition for elastic/viscoelastic finite-difference modeling in the presence of topography. *Geophysics*, 61, 1921-1934.

Hestholm, S. and B. Ruud, in press. 3-D finite difference elastic wave modeling including surface topography. *Geophysics*.

9.3 Approximation of the Free Surface in the Displacement Formulation

Zahradník, J., P. Moczo and F. Hron, 1993. Testing four elastic finite-difference schemes for behaviour at discontinuities. *Bull. Seism. Soc. Am.*, 83, 107-129.

Zahradník, J., 1995b. Simple elastic finite-difference scheme. *Bull. Seism. Soc. Am.*, 85, 1879-1887.

Zahradník, J. and E. Priolo, 1995. Heterogeneous formulations of elastodynamic equations and finite-difference schemes. *Geophys. J. Int.*, 120, 663-676.

Moczo, P., E. Bystrický, J. Kristek, J.M. Carcione and M. Bouchon, 1997. Hybrid modeling of P-SV seismic motion at inhomogeneous viscoelastic topographic structures. *Bull. Seism. Soc. Am.*, 87, 1305-1323.

10. Simulation of Seismic Source

10.1 Simulation of a Point Source with Arbitrary Focal Mechanism Using a Body-Force Term

Aboudi, J., 1971. Numerical simulation of seismic sources. *Geophysics*, 36, 810-821.

Frankel, A., 1993. Three-dimensional simulations of ground motions in the San Bernardino Valley, California, for hypothetical earthquakes on the San Andreas fault. *Bull. Seism. Soc. Am.*, 83, 1020-1041.

Yomogida, K. and J.T. Etgen, 1993. 3-D wave propagation in the Los Angeles basin for the Whittier-Narrows earthquake. *Bull. Seism. Soc. Am.*, 83, 1325-1344.

Coutant, O., J. Virieux and A. Zollo, 1995. Numerical source implementation in a 2D finite difference scheme for wave propagation. *Bull. Seism. Soc. Am.*, 85, 1507-1512.

Olsen, K.B., R.J. Archuleta and J.R. Matarese, 1995. Magnitude 7.75 earthquake on the San Andreas fault: three-dimensional ground motion in Los Angeles. *Science*, 270, 1628-1632.

Graves, R.W., 1996. Simulating seismic wave propagation in 3D elastic media using staggered-grid finite differences. *Bull. Seism. Soc. Am.*, 86, 1091-1106.

10.2 Decomposition of the Wavefield

Alterman, Z. and F.C. Karal, 1968. Propagation of elastic waves in layered media by finite-difference methods. *Bull. Seism. Soc. Am.*, 58, 367-398.

Vidale, J.E. and D.V. Helmberger, 1987. Path effects in strong motion seismology. In: *Seismic strong motion synthetics*, B.A. Bolt, ed., Academic Press, 267-319.

Moczó, P., 1989. Finite-difference technique for SH-waves in 2-D media using irregular grids - application to the seismic response problem. *Geophys. J. Int.*, 99, 321-329.

Fäh, D., 1992. A hybrid technique for the estimation of strong ground motion in sedimentary basins. Diss. ETH Nr. 9767, Swiss Federal Institute of Technology, Zurich.

Fäh, D., P. Suhadolc and G.F. Panza, 1993. Variability of seismic ground motion in complex media: the case of a sedimentary basin in the Friuli (Italy) area. *J. Applied Geophysics*, 30, 131-148.

Zahradnik, J., 1995a. Comment on 'A hybrid method for estimation of ground motion in sedimentary basins: Quantitative modeling for Mexico City' by D. Fäh, P. Suhadolc, St. Mueller and G.F. Panza. *Bull. Seism. Soc. Am.*, 85, 1268-1270.

Zahradník, J. and P. Moczo, 1996. Hybrid seismic modeling based on discrete-wavenumber and finite-difference methods. *Pure and Applied Geophysics*, 148, 21-38.

Moczo, P., E. Bystrický, J. Kristek, J.M. Carcione and M. Bouchon, 1997. Hybrid modeling of P-SV seismic motion at inhomogeneous viscoelastic topographic structures. *Bull. Seism. Soc. Am.*, 87, 1305-1323.

11. Simulation of Nonreflecting Boundaries

Clayton, R. and B. Engquist, 1977. Absorbing boundary conditions for acoustic and elastic wave equations. *Bull. Seism. Soc. Am.*, 67, 1529-1540.

Reynolds, A.C., 1978. Boundary conditions for the numerical solution of wave propagation problems. *Geophysics*, 43, 1099-1110.

Fuyuki, M. and Y. Matsumoto, 1980. Finite difference analysis of Rayleigh wave scattering at a trench. *Bull. Seism. Soc. Am.*, 70, 2051-2069.

Korn, M. & H. Stöckl, 1982. Reflection and transmission of Love channel waves at coal seam discontinuities computed with a finite difference method. *J. Geophys.*, 50, 171-176.

Emerman, S.H. and R.A. Stephen, 1983. Comment on "Absorbing boundary conditions for acoustic and elastic wave equations," by R. Clayton and B. Engquist. *Bull. Seism. Soc. Am.*, 73, 661-665.

Cerjan, C., D. Kosloff, R. Kosloff and M. Reshef, 1985. A nonreflecting boundary condition for discrete acoustic and elastic wave equations. *Geophysics*, 50, 705-708.

Sochacki, J., R. Kubichek, J. George, W.R. Fletcher and S. Smithson, 1987. Absorbing boundary conditions and surface waves. *Geophysics*, 52, 60-71.

Stacey, R., 1988. Improved transparent boundary formulations for the elastic-wave equation. *Bull. Seism. Soc. Am.*, 78, 2089-2097.

Chang, W.-F. and G.A. McMechan, 1989. Absorbing boundary conditions for 3-D acoustic and elastic finite-difference calculations. *Bull. Seism. Soc. Am.*, 79, 211-218.

Higdon, R.L., 1991. Absorbing boundary conditions for elastic waves. *Geophysics*, 56, 231-241.

Peng, C. and M.N. Toksöz, 1994. An optimal absorbing boundary condition for finite difference modeling of acoustic and elastic wave propagation. *J. Acoust. Soc. Am.*, 95, 733-745.

Peng, C. and M.N. Toksöz, 1995. An optimal absorbing boundary condition for elastic wave modeling. *Geophysics*, 60, 296-301.

Recommended Reading

Alford, R.M., K.R. Kelly and D. Boore, 1974. Accuracy of finite-difference modeling of the acoustic wave equation. *Geophysics*, 39, 834-842.

Marfurt, K.J., 1984. Accuracy of finite-difference and finite-element modeling of the scalar and elastic wave equations. *Geophysics*, 49, 533-549.

Fornberg, B., 1988. Generation of finite difference formulas on arbitrary spaced grids. *Math. Computation*, 51, 699-706.

Stephen, R.A., 1988. A review of finite difference methods for seismo-acoustics problems at the seafloor. *Rev. Geophys.*, 26, 445-458.

Muir, F., J. Dellinger, J. Etgen and D. Nichols, 1992. Modeling elastic fields across irregular boundaries. *Geophysics*, 57, 1189-1193.

Cunha, C.A., 1993. Elastic modeling in discontinuous media. *Geophysics*, 59, 1840-1851.

Klimeš, L., 1996. Accuracy of elastic finite differences in smooth media. *Pure and Applied Geophysics*, 148, 39-76.